TIME DOMAIN IMPULSE ANTENNA STUDY

Dr. Morris Handelsman

University of Vermont

Approved for public release;
distribution unlimited.

FOREWORD

This Final Report, covering the period 1 September 1971 to 29 February 1972, was accomplished by the University of Vermont, Electrical Engineering Department, Burlington, Vermont, under contract F30602-71-C-0278, Job Order Number 45060000, for Rome Air Development Center, Griffiss Air Force Base, New York. Mr. John A. Potenza (OCTA) was the RADC Project Engineer.

This report has been reviewed by the Information Office (OI) and is releasable to the National Technical Information Service (NTIS).

This technical report has been reviewed and is approved.

John Potenza

Approved: JOHN POTENZA
Project Engineer
Antenna Section

Approved: JAMES L. RYNNING
Colonel, USAF
Chief, Surveillance and
Control Division

FOR THE COMMANDER: Fred I Diamond

FRED I. DIAMOND
Acting Chief, Plans Office

ABSTRACT

This final report contains the results of an investigation to use the concepts of radiation from accelerating charges to develop the radiation characteristics of pulse-excited antennas in the time domain. The transition to antennas is accomplished through derivation of a radiation equation involving the time-derivative of the antenna currents. For sinusoidal time variation this equation reproduces well-known results for a number of common antennas. For pulse-excited linear antennas, the radiation equation produces a result derived previously by retarded potential and other methods. Numerical comparison with a published frequency-domain analysis of a pulsed dipole shows reasonable agreement except for angles close to the end-fire direction. Further work on this point is required. For a pulsed loop, comparison with a published time-domain analysis using the Sommerfeld radiation equation for a small dipole shows that both approaches lead to the same final equation. Concerning transient aperture antennas an analysis by Chernousov is described, wherein equivalent surface currents replace the aperture fields. The Chernousov aperture results are shown to be expressable in terms of equivalent surface accelerating charges, and for one-dimension to reduce to results derived previously by Cheng and Tseng. It is concluded that while the accelerated charge approach provides a direct physical explanation of and an analytic basis for study of impulse antenna radiation in the time domain, more work is needed to establish its merits relative to other time-domain methods.

EVALUATION

1. Over the past few years there has been an active and increasing interest in the behavior of antennas when excited by short time duration impulsive like signals and fields. Moreover, it is evident that conventional cw concepts and theories are inadequate for describing and analyzing impulsive antenna performance. The intent of the work reported on herein was to examine basic underlying time domain principles and concepts useful for understanding and analyzing the basic radiation properties of short pulse antennas.

2. This report presents the results of a six month research effort to develop the concepts of accelerating charges as the underlying and basic radiation mechanism for impulse antennas. It has been shown that radiation can be conveniently formulated in the time domain by the time derivative of current or accelerated charges over differential elements. Appropriate expressions were derived from basic principles for linear and small loop antennas which resulted in direct physical explanations of impulsive antenna radiation. Although these same results can be obtained by other time domain representations, the accelerated charge formulation provides physical interpretation and insight into the radiation mechanism for these type antennas.

3. A promising method for analyzing high gain aperture antennas was also identified and discussed. Although not developed fully, the method was shown to reduce, giving results to previously obtained for a one dimensional case.

4. Based upon the work performed under this preliminary short term effort, it is concluded that the accelerated charge concepts provide a valid analytic basis for impulse radiation. However, before significant advantages over other approaches can be demonstrated, additional effort will have to be expended to extend the scope and detail of the work completed herein. Future work has been identified and discussed in the report.

John Potenza

JOHN POTENZA
Project Engineer
Antenna Section

TABLE OF CONTENTS

Section Page

1 INTRODUCTION 1

1.1 General 1
1.2 Purpose of Program 1
1.3 Contents of This Report 1
1.4 Program Organization 2

2 THE NATURE OF RADIATION FROM ACCELERATING CHARGES 3

2.1 Introduction 3
2.2 The Fields of Moving Charges 5
2.3 The Radiation Fields 6
2.4 Linear Antennas 7
2.5 How Radiation Waves Are Produced By An Accelerating Charge 14

3 RESPONSE OF A WIRE ANTENNA TO PULSE EXCITATION AND RADIATION IN THE BROADSIDE DIRECTION 22

3.1 Traveling Pulse on Wire Antenna; The Source of Radiation 22
3.2 Radiation Normal to a Wire Antenna 26

4 RADIATION OF A PULSE-EXCITED LINEAR WIRE ANTENNA IN ANY DIRECTION 41

4.1 Derivation of Equations 41
4.2 Radiation Due to Step-Function Excitation 50
4.3 Radiation Due to Pulse Excitation; Comparison with a Frequency-Domain Analysis 59
4.4 Discussion of Pulsed Wire-Antenna Radiation, Especially at Small Values of θ 70

5 RADIATION FROM LOOP ANTENNAS 81

5.1 Introduction 81
5.2 Sinusoidal Time-Varying Excitation 81
5.3 Pulse Excitation 85

TABLE OF CONTENTS (continued)

Section Page

6 TRANSIENT RADIATION FROM APERTURE ANTENNAS 90

6.1 Introduction 90
6.2 Review of Chernousov Paper (Ref. 37) 91
6.3 Accelerated-Charge Viewpoint 94
6.4 Planar In-Phase Aperture 96
6.5 Some Additional Results 97

7 CONCLUSIONS AND RECOMMENDATIONS 99

8 REFERENCES 103

Appendixes

I LIENARD-WIECHERT POTENTIALS 107

1. Scalar and Vector Potentials 107
2. Lienard-Wiechert Potentials 111

II THE FIELDS OF MOVING CHARGES 117

1. Equations for the Fields 117
2. Discussion of the Fields 126
3. Radiation Fields for the Low-Velocity Case 127

III WAVE PROPAGATION ON TRANSMISSION LINES AND LINEAR ANTENNAS 129

1. Traveling Waves on Lossless Transmission Lines 129
2. Traveling Waves with Sinusoidal Time Variation on Lossy Lines 130
3. Wave Travel of Step-Functions and Pulses on Lossy Lines 131
4. Velocity of Propagation Along a Thin Wire Antenna 132
5. Some Characteristics of Wave Propagation Along a Thin-Wire Line 134
6. Surface Charges 137

TABLE OF CONTENTS (continued)

Appendixes Page

IV DRIFT VELOCITY OF ELECTRONS IN CONDUCTORS 141

1. Free Electron Theory of Metals 141
2. Relaxation Times 141
3. Equations for Drift Velocity of Electrons 143
4. Estimation of Electron Drift Velocities in Conductors 148

V DERIVATION OF THE RADIATION FIELDS OF AN ELECTRIC DIPOLE USING MOVING CHARGES 154

VI SOME RESULTS OF DELTA FUNCTION INTEGRALS 163

VII ILLUSTRATIONS OF USE OF EQUATION (74) FOR SOME STANDARD ANTENNAS WITH SINUSOIDAL TIME-VARYING EXCITATION 165

1. Traveling-Wave Antenna 165
2. Half-Wave Length Dipole 166
3. Linear Antenna with Arbitrary Current Distribution I(Z,t) 167

LIST OF ILLUSTRATIONS

Figure		Page
1	Charge q at retarded position $\bar{X}'(t')$.	4
2	Linear antenna	8
3	Radiation patterns of accelerating charges.	10
4	Electric dipole or current element.	11
5	Virtual position of charge moving at constant velocity along straight line.	15
6	Radiation due to an accelerated charge	19
7	Traveling current pulse on straight wire.	23
8	Leading edge of traveling trapezoidal pulse shown at time t_0.	23
9	Monopole over ground plane	28
10	Radiation field of monopole.	29
11	Radiation from leading edge of pulse.	29
12	Initial radiated field when entire pulse is on monopole.	31
13	Cancellation of radiation from leading and trailing edges.	31
14	Pulse after reflection at tip.	33
15	Reinforcement of radiation from edges during reflection from tip.	33
16	Reflected pulse traveling back to base of monopole.	35
17	Radiation field after first reflection.	35
18	Incident and reflected waves at base.	37

LIST OF ILLUSTRATIONS (continued)

Figure		Page
19	Radiation field subsequent to reflection from base.	37
20	Second reflection from tip.	38
21	Radiated waveform subsequent to second reflection from tip.	38
22	Second reflection from base.	40
23	Radiated waveform subsequent to second reflection from base.	40
24	Linear antenna geometry.	42
25	Leading edge detail.	48
26	Finite-slope function $I(z',t')$ at fixed time t'.	48
27	Step function as a limiting process.	52
28	Geometry for traveling step function.	52
29	Radiation $H_\phi(4\pi r/I_0)$ due to step and impulse functions on a dipole, no reflection at input.	60
30	Radiation $H_\phi(4\pi r/I_0)$ at $\theta = 90^\circ$ due to step and impulse functions on a dipole, no reflection at input.	61
31	Radiation $H_\phi(4\pi r/I_0)$ due to step function on a dipole.	62
32(a)	Radiation waveforms for $\theta = 90^\circ, 70^\circ$.	66
32(b)	Radiation waveforms for $\theta = 60^\circ, 45^\circ$.	67
32(c)	Radiation waveforms for $\theta = 20^\circ$.	68
33	Line integral of H for semi-infinite wire.	73
34	Line integral of H for semi-infinite cone.	73

LIST OF ILLUSTRATIONS (continued)

Figure		Page
35	Currents and wavefronts for current wave on semi-infinite wire.	75
36	Wavefronts in far-field of finite-length antenna.	76
37	Loop geometry.	83
38	Aperture antenna.	92
39	Charge e moving on path $\bar{r}'(t')$.	110
40	Chain of dipoles and current, charge and local $\bar{E}$ field distributions.	138
41	Surface charges at a bend in a conductor carrying current.	140

TABLE OF ABBREVIATIONS AND SYMBOLS

English symbols

$\bar{A}$	vector magnetic potential, weber per meter
A	area, square meter
A_o	dipole moment amplitude, farad-meter
$\bar{a}$	vector acceleration, meter per square second
a	acceleration meter per square second
a	radius of round wire, meter
$\hat{a}_z, \hat{a}_r, \hat{a}_\theta, \hat{a}_\phi$	unit vectors in direction of increasing Z, r, θ and ϕ respectively
$\bar{B}$	magnetic flux density, tesla
b	constant of proportionality of frictional resistance, newton-second per meter
C	transmission line distributed capacitance, farad per meter
c	velocity of light
$\bar{D}$	electric flux density, coulomb per square meter
d	diameter of round wire, meter
$\bar{E}$	electric field intensity, volt per meter
e	charge on particle or electron, coulomb
f	frequency, hertz
$f(\ )$	general function
$f(t')$	special function defined by Eq. (I-32)
G	transmission line shunt conductance, mho per meter

$\bar{g}$	current density, ampere per square meter
g( )	general function
$\bar{H}$	magnetic field intensity, ampere per meter
h	length of antenna, meter
I,i	current, ampere
I_o	current amplitude or constant value, ampere
$\bar{J}$	current density, ampere per square meter
J_o	amplitude of current density, also constant value, ampere per square meter
$\bar{J}_s$	linear current density, ampere per meter
j	square root of minus one
k	defined by Eq. (III-10)
L	derivative of $f(t')$, defined by Eq. (I-40)
l	distance along transmission line, meter
$\bar{l}$	vector denoting charge separation, meter
M	mass of electron, kilogram
N	number of free electrons per cubic meter
$\hat{n}$	unit vector from source point P' to field point P
n_o	number of free electrons per unit length of wire
$\bar{p}$	dipole moment, farad-meter
q	charge, coulomb
$\bar{R},\bar{r}$	vector from source point P' to field point P, meter
$\bar{r}$	general position vector from origin, meter

$\bar{r}'$	position vector to points on prescribed path of motion, meter
R	transmission line series resistance, ohm per meter
R_o	transmission line characteristic resistance, ohm
R_L	transmission line load resistance, ohm
$\bar{r}_v$	virtual present position of moving charge; see Eq. (41).
$\bar{S}$	cross-sectional area of wire, square meter
S	defined by Eq. (I-49)
T	duration of flat portion of trapezoidal pulse, second
t	time at field point, second
t'	time at source point, second
t_f	mean free time of electron, second
t_r, t_R	pulse rise time, second
$\bar{U}$	velocity, meter per second
U	unit step function
$\bar{v}$	velocity, meter per second
$\bar{V}_d$	electron drift velocity, meter per second
X_1, X_2, X_3	coordinates of position vector $\bar{X}$ of field point, meter
X'_1, X'_2, X'_3	coordinates of position vector $\bar{X}'$ of source point, meter
X,Y,Z	cartesian coordinates, meter
Z_o	characteristic impedance, ohm

Greek symbols

alpha	α	transmission line attenuation constant, neper per meter
beta	$\bar{\beta}$	particle velocity divided by velocity of light
beta	β	transmission line propagation constant, radian per meter
gamma	γ	transmission line complex propagation constant
gamma	Γ_c	current reflection coefficient
delta	δ	skin depth, meter
delta	Δ	incremental change
epsilon	ϵ	permittivity, farad per meter
theta	θ	polar angle in spherical coordinates; also angle between particle path and direction to field point, radian
lamda	λ	wavelength, meter
mu	μ	permeability, henry per meter
pi	π	3.1416...
rho	ρ	charge density, coulomb per cubic meter
sigma	σ	conductivity, mho per meter
sigma	σ_0	conductivity at zero frequency
tau	τ	pulse duration, second
tau	τ_1	relaxation time, given by Eq. (IV-5), second
tau	Υ	defined by Eq. (IV-25)
phi	ϕ	azimuthal angle in spherical coordinates, radian

phi Φ	scalar potential, volt
psi ψ	general function
omega ω	radian frequency $2\pi f$, radian per second

Mathematical symbols

∇	delt
$\nabla \times$	curl
$\nabla \cdot$	divergence
∇	gradient
$[\;\;]_{ret}$	evaluate at retarded time
Re ( )	real part of ( )
sinc	function defined after Eq. (IV-35)
$\lvert\;\;\rvert$	magnitude
$\dot{(\;)}$	derivative with respect to time
$(\;)'$	differentiation with respect to argument of ( )
$\sum$	summation

Subscripts

o	ϵ_o, μ_o = free-space permittivity and permeability, respectively
a	radiation fields due to acceleration

Superscripts

$(\bar{\;})$	vector quantity

Abbreviations

d.c.	direct current

SECTION 1

INTRODUCTION

1.1 GENERAL

This final technical report covers work performed from 1 Sept. 1971 to 29 Feb. 1972 under USAF Contract No. F30602-71-C-0278/PMRA, entitled Time Domain Impulse Antenna Study, for the Rome Air Development Center, Research and Technology Division, Air Force Systems Command, Griffiss Air Force Base, New York, by Dr. Morris Handelsman, Electrical Engineering Department, College of Technology, University of Vermont, Burlington, Vt.

1.2 PURPOSE OF PROGRAM

The purpose of this program is to investigate, develop, and apply the concept of radiation from accelerating charges to antenna systems excited by impulsive signals or fields. Thus the purpose is to develop in the time domain, an approach to the understanding of the behaviour of impulse-excited antennas, through the radiation characteristics of the accelerated charges on such antennas.

1.3 CONTENTS OF THIS REPORT

In this final report, Section 2 discusses the nature of radiation from accelerating charges. Sections 3 and 4 discuss the radiation from a pulse-excited linear wire antenna in a direction normal to the wire, and in any direction, respectively. Section 5 discusses radiation from pulse excited loop antennas. Section 6 discusses transient radiation from aperture antennas. Section 7 contains conculsions and recommendations. Section 8 lists references. Seven appendices contain discussions and results considered basic and pertinent to the understanding of radiation from antennas through the mechanism of accelerated charges as follows: I. Lienard-Wiechert Potentials, II. The Fields of Moving Charges, III. Wave Propagation on Transmission Lines and Linear Antennas, IV. Drift Velocity of Electrons in Conductors, V. Derivation of the Radiation Fields of an Electric Dipole Using Moving Charges, VI. Some Results of Delta Function Integrals, and VII. Illustrations of Use of Equation (74) for Some Standard Antennas with Sinusoidal Time-Varying Excitation.

1.4 PROGRAM ORGANIZATION

The person who performed this work is Dr. Morris Handelsman of the Electrical Engineering Department, College of Technology, University of Vermont. Acknowledgements are gratefully made to Mr. Hugh C. Maddocks and Mr. Albert E. Ruehli, Ph.D. candidates, for discussions on the Lienard-Wiechert potentials of the Hertzian dipole, and the frequency spectrum of pulses, respectively.

SECTION 2

THE NATURE OF RADIATION FROM ACCELERATING CHARGES

2.1 INTRODUCTION

Given the position $\bar{x}'(t')$ of a moving charge q at all times t', as shown in Fig. 1, the fields at an observation point $P(\bar{x}, t)$ may be found through the Lienard-Wiechert potentials. These potentials, developed in detail in Appendix I, are in MKS units,

$$\Phi(\bar{x}, t) = \frac{q}{4\pi\varepsilon_0}\left[\frac{1}{s}\right]_{ret} \tag{1}$$

$$\bar{A}(\bar{x}, t) = \frac{\mu_0 q}{4\pi}\left[\frac{\bar{v}}{s}\right]_{ret} \tag{2}$$

where

$$s \equiv r - \frac{\bar{r}\cdot\bar{v}}{c} = r - \bar{r}\cdot\bar{\beta} = r(1-\beta\cos\theta) \tag{3}$$

velocity $\bar{v} = d\bar{x}'/dt'$ (4)

$$\bar{\beta} \equiv \bar{v}/c \tag{5}$$

and $[\;]_{ret}$ means that the quantity inside the brackets is to be evaluated at the retarded time

$$t' = t - r/c \tag{6}$$

Thus t' is the time at which a signal is emitted at $\bar{x}'$ so as to arrive at $\bar{x}$ at time t.

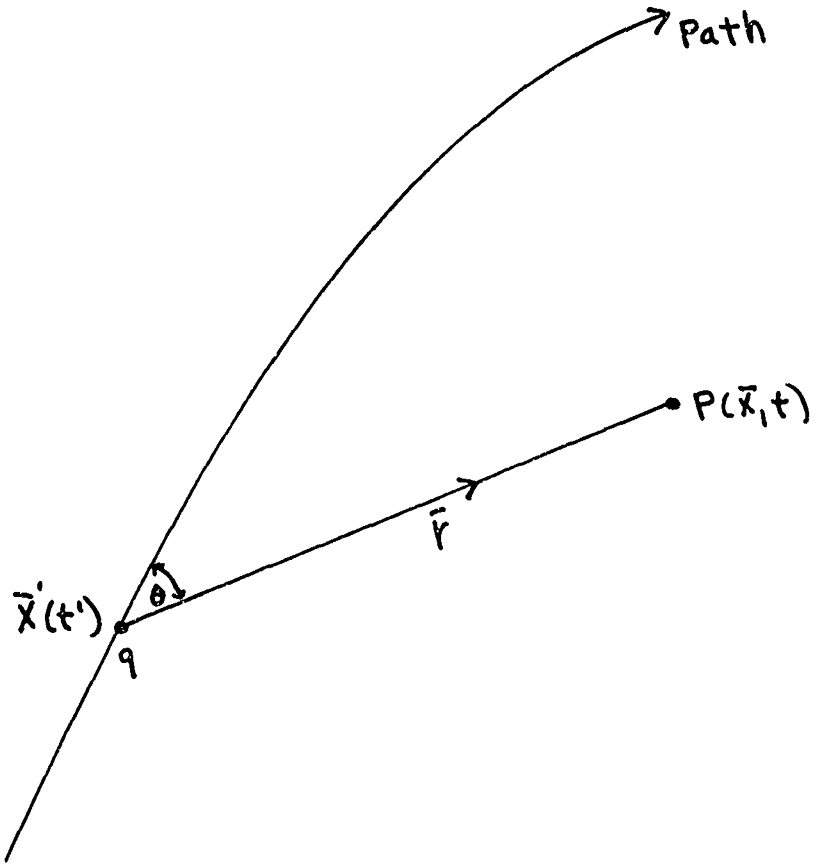

FIG. 1 Charge q at retarded position $\vec{x}'(t')$.

2.2 THE FIELDS OF MOVING CHARGES

The fields $\bar{B}$ and $\bar{E}$ are given by

$$\bar{B} = \nabla \times \bar{A} \tag{7}$$

$$\bar{E} = -\nabla \Phi - \frac{\partial \bar{A}}{\partial t} \tag{8}$$

This results in the following equation for the fields (for details see Appendix II):

$$\bar{E} = \frac{q}{4\pi\varepsilon_0}\left[\frac{1}{s^3}(\bar{r}-\bar{\beta}r)(1-\beta^2) + \frac{1}{c^2 s^3}\left\{\bar{r}\times\left[(\bar{r}-\bar{\beta}r)\times\bar{a}\right]\right\}\right]_{ret} \tag{9}$$

$$\bar{B} = \frac{q}{4\pi\varepsilon_0}\left[\frac{\bar{\beta}\times\bar{r}}{c s^3}(1-\beta^2) + \frac{\bar{r}}{c^3 s^3 r}\times\left\{\bar{r}\times\left[(\bar{r}-\bar{\beta}r)\times\bar{a}\right]\right\}\right]_{ret.} \tag{10}$$

Here $\bar{a}$ = acceleration of the charge $= d\bar{v}/dt'$.

For a stationary charge, Eq. (3) shows that $s = r$, while $\bar{\beta}$ and $\bar{a}$ are zero. The $\bar{E}$ field then becomes the static Coulomb field

$$\bar{E} = \frac{q\hat{a}_r}{4\pi\varepsilon_0 r^2} \tag{11}$$

where $\hat{a}_r$ = unit vector in $\bar{r}$ direction, while $\bar{B} = 0$. For a charge moving with uniform velocity without acceleration, $\bar{\beta} =$ constant and $\bar{a} = 0$. The $\bar{E}$ and $\bar{B}$ fields vary as $1/r^2$, and are non-radiation fields (quasistatic or induction fields).

2.3 THE RADIATION FIELDS

When the charge has acceleration $\bar{a}$, the last terms in Eqs. (9,10) are the radiation fields, vary as $1/r$, and depend upon $\bar{a}$. These radiation fields, denoted by subscript a for acceleration, are

$$\bar{E}_a = \frac{q}{4\pi\varepsilon_o c^2}\left[\frac{\bar{r}\times\{(\bar{r}-\bar{\beta}r)\times\bar{a}\}}{s^3}\right]_{ret} \tag{12}$$

$$\bar{B}_a = \frac{q}{4\pi\varepsilon_o c^3}\left[\frac{\bar{r}\times\{\bar{r}\times[(\bar{r}-\bar{\beta}r)\times\bar{a}]\}}{s^3 r}\right]_{ret} \tag{13}$$

Inspection of Eqs. (12,13) shows that

$$\bar{B}_a = \frac{1}{c}\,\hat{a}_r \times \bar{E}_a \tag{14}$$

Hence

$$\bar{H}_a = \frac{1}{\mu_o}\bar{B}_a = \sqrt{\varepsilon_o/\mu_o}\;\hat{a}_r \times \bar{E}_a \tag{15}$$

That is, $\bar{E}_a$, $\bar{H}_a$, and $\hat{a}_r$ (the retarded position unit vector) are mutually perpendicular, and the ratio of $|E_a|$ to $|H_a|$ is

$$|E_a/H_a| = \sqrt{\mu_o/\varepsilon_o}\ \text{ohms} \tag{16}$$

which are all familiar relationships to the antenna engineer.

2.4 LINEAR ANTENNAS

For a linear antenna extending along the Z-axis, as shown in Fig. 2, velocity $\bar{v}$ and acceleration $\bar{a}$ are colinear. Then, in Eq. (12),

$$(\bar{r}-\bar{\beta} r)\times\bar{a} = \bar{r}\times\bar{a} \tag{17}$$

Hence, omitting the $[\;\;]_{ret}$ notation,

$$\bar{E}_a = \frac{q}{4\pi\varepsilon_0}\,\frac{\bar{r}\times(\bar{r}\times\bar{a})}{c^2 s^3}$$

$$\bar{E}_a = \frac{q}{4\pi\varepsilon_0 c^2}\,\frac{\hat{a}_r\times(\hat{a}_r\times\bar{a})}{r(1-\beta\cos\theta)^3} \tag{18}$$

$$\bar{H}_a = \frac{\hat{a}_r\times\bar{E}_a}{\sqrt{\mu_0/\varepsilon_0}} \tag{19}$$

Using $\bar{a}=a\,\hat{a}_z$,

$$\hat{a}_r\times(\hat{a}_r\times\bar{a}) = a\sin\theta\,\hat{a}_\theta \tag{20}$$

where $\hat{a}_\theta$ is the unit vector in the increasing θ direction, using spherical coordinates. Then

$$E_\theta = \frac{qa\sin\theta}{4\pi\varepsilon_0 c^2 r(1-\beta\cos\theta)^3} \tag{21}$$

$$H_\phi = E_\theta\,/\sqrt{\mu_0/\varepsilon_0} \tag{22}$$

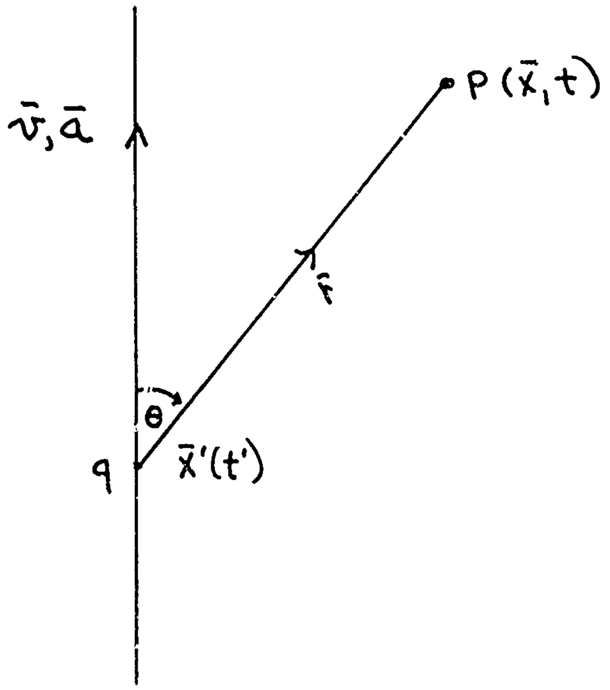

FIG. 2 Linear antenna.

The radiation patterns which result from Eqs. (21,22) are shown in Fig. 3. For low velocity particles, which is the usual case for charges (electrons) moving in conductors (see Appendix IV) for detailed discussion on the drift velocity of electrons in conductors), $\beta \ll 1$, and

$$E_\theta = \left[\frac{qa \sin\theta}{4\pi\varepsilon_0 c^2 r} \right]_{ret} \qquad (\beta \ll 1) \qquad (23)$$

This is the "figure eight" pattern, shown in Fig. 3(a), which varies as $\sin\theta$, again familiar to the antenna engineer. For relativistic speeds $\beta \to 1$, Eq. (21) shows that there is a "forward" bunching, as indicated in Fig. 3(b). The direction of maximum intensity is now tipped forward.

The $\overline{H}$ field is

$$H_\phi = \left[\frac{qa \sin\theta}{4\pi c r} \right]_{ret} \qquad (\beta \ll 1) \qquad (24)$$

To illustrate an application of Eq. (24) consider the radiation field of an electric dipole or current element of length h , extending along the Z-axis, with a current distribution along h which is constant except at the ends where the current is zero. See Fig. 4. Let the current vary sinusoidally in time. This case is examined in more detail in Appendix V. The sinusoidal case is examined initially principally because the $\overline{H}$ fields for this case, using conventional theory, are well-known.

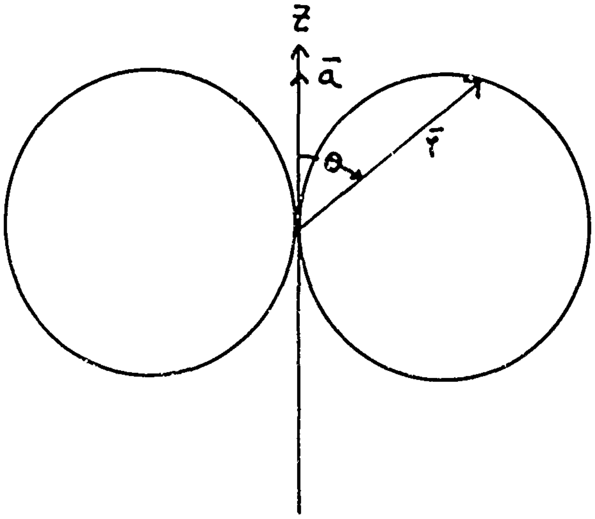

(a) Velocity v<< c

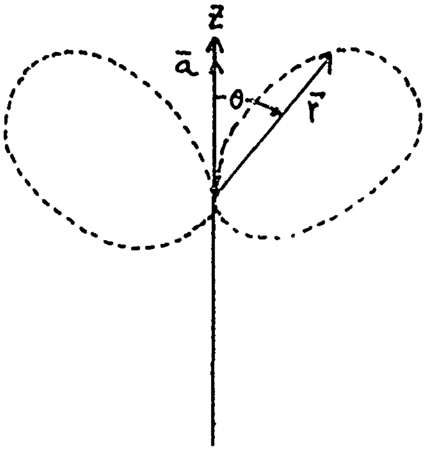

(b) Velocity v approaching c

FIG. 3 Radiation patterns of accelerating charges.

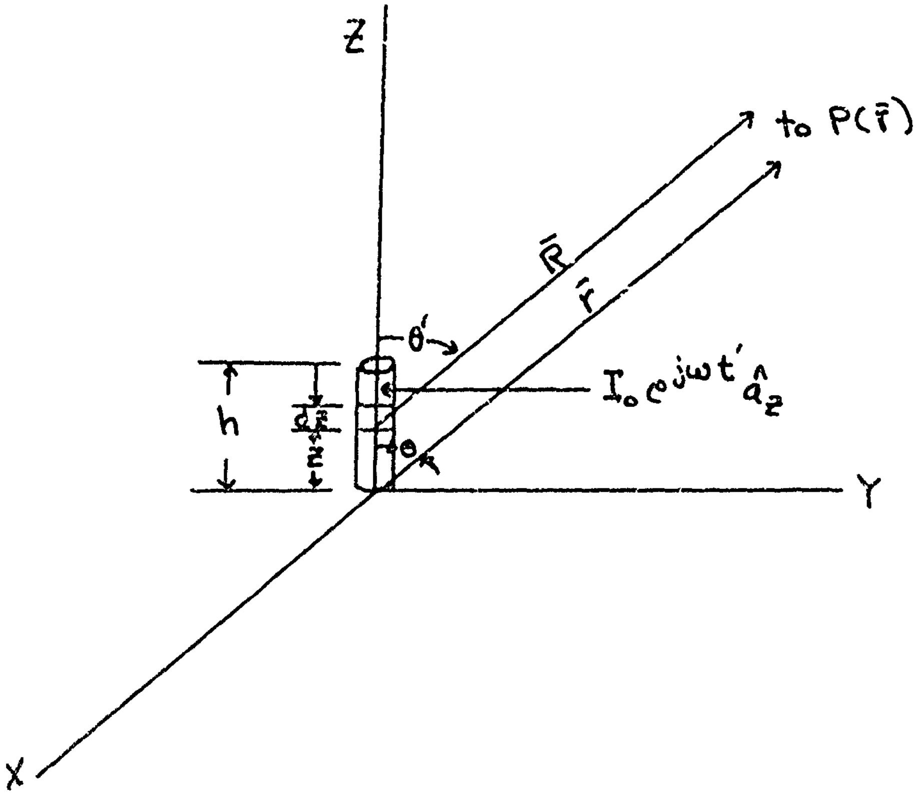

FIG. 4 Electric dipole or current element.

The $\bar{H}$ field for h small compared to wavelength λ, is (Ref. 20, p. 498; Ref. 21, p. 93)

$$\bar{H} = \frac{jkI_0 h \sin\theta}{4\pi r} e^{-jkr} e^{j\omega t} \hat{a}_\phi \tag{25}$$

where $k \equiv \omega/c = 2\pi/\lambda$, and the current by definition, is

$$\bar{I} = I_0 e^{j\omega t'} \hat{a}_z \tag{26}$$

The charge dq in a differential length dz at $(0, 0, z)$ on the radiator is

$$dq = \rho A\, dz \tag{27}$$

where ρ is the moving (electron) charge density in coulombs per cubic meter, and A is the appropriate cross-sectional area. This charge moves through distance dz in time dt', so the current is

$$\bar{I} = \frac{\partial q}{\partial t'} \hat{a}_z = \rho A \frac{\partial z}{\partial t'} \hat{a}_z = \rho A \bar{v} \tag{28}$$

where $\bar{v} = (\partial z/\partial t')\hat{a}_z$ is the velocity of the charge. The current density (amperes per square meter) $\bar{J}$ is

$$\bar{J} = \bar{I}/A = \rho \bar{v} \tag{29}$$

Assuming ρ is essentially constant in $0 < z < h$ (see Appendix III for discussion), then the acceleration $\bar{a}$ is

$$\bar{a} = \frac{\partial \bar{v}}{\partial t'} = \frac{1}{\rho A} \frac{\partial \bar{I}}{\partial t'} \tag{30}$$

From Eq. (26),

$$\frac{\partial \bar{I}}{\partial t'} = j\omega I_o e^{j\omega t'} \quad (31)$$

Replacing q in Eq. (24) by the above dq, then the term (qa) in Eq. (24) becomes, using Eqs. (27,30,31),

$$qa = \frac{\partial I(z,t')}{\partial t'} dz = j\omega I_o dz e^{j\omega t'} \quad (32)$$

The retarded value of (qa) is found by using Eq. (6) for t', so that

$$e^{j\omega t'} = e^{j\omega(t-R/c)} = e^{-jkR} e^{j\omega t} \quad (33)$$

Since dq is at distance R from P at time t', the r in the denominator of Eq. (24) becomes R. Thus dH_ϕ due to dq is

$$dH_\phi(\bar{r},t) = \frac{j\omega I_o e^{j\omega t}}{4\pi c} \frac{e^{-jkR} \sin\theta'}{R} dz \quad (34)$$

and

$$H_\phi(\bar{r},t) = \frac{j\omega I_o e^{j\omega t}}{4\pi c} \int_0^h \frac{e^{-jkR} \sin\theta'}{R} dz \quad (35)$$

For the radiation field (far-field distances)

$$\begin{aligned} \theta' &\approx \theta \\ R &\approx r - z\cos\theta \end{aligned} \quad (36)$$

Using $h \ll \lambda$, the integral in Eq. (35) reduces to

$$\int_0^h \frac{e^{-jkR}\sin\theta'}{R}\,dz = h\,\frac{e^{-jkr}}{r}\sin\theta \qquad (37)$$

Hence the field calculated from Eq. (24) becomes

$$H_\phi(\bar{r},t) = \frac{jkI_o h}{4\pi r}\sin\theta\, e^{-jkr} e^{j\omega t} \qquad (38)$$

which agrees with Eq. (25).

2.5 HOW RADIATION WAVES ARE PRODUCED BY AN ACCELERATING CHARGE

It is possible to derive the radiation equation Eq. (23) using a graphical construction and simple analysis (Ref. 23, pp. 60-63 or Ref. 24, pp. 334-340). This derivation may be of help in understanding how the radiation field of an accelerating charge arises, and is presented here. The charge q is taken to move on a straight line. Three preliminary points are made first, in the paragraphs below.

First it is noted that the term ($\bar{r}-\bar{\beta}r$) appears twice in Eq. (9) and therefore deserves interpretation. Remembering that $\bar{r}$ is the retarded position of the charge, let $\bar{r}_v$ be the "virtual" present position (at time t) of q, i.e., the position it would occupy at time t if the acceleration $\bar{a}$ is zero. In Fig. 5 the time of propagation from the retarded position Q_o

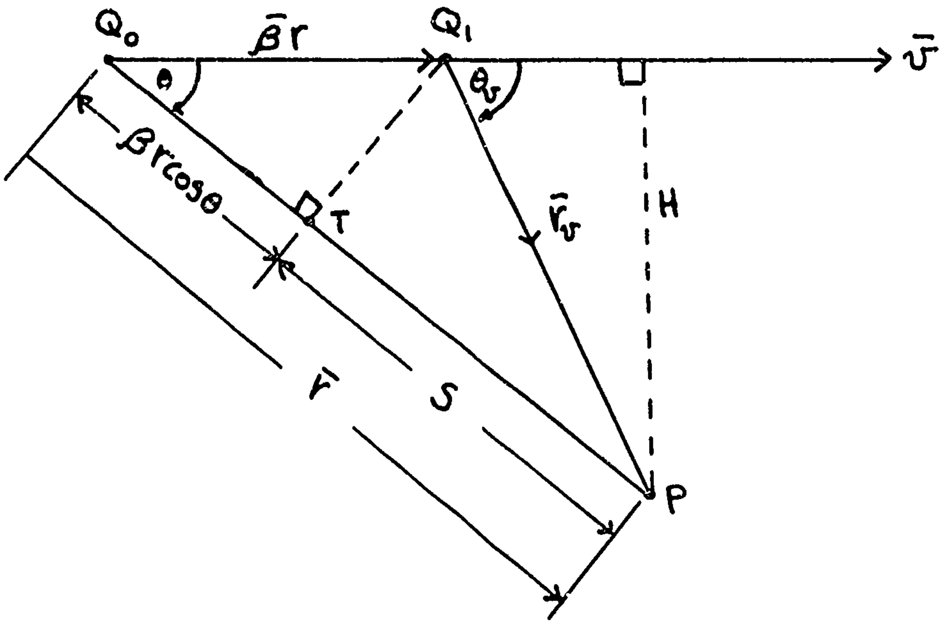

FIG. 5 Virtual position of charge moving at constant velocity along straight line.

where the charge is at time $t-r/c$ to the observation point P is simply

$$t = r/c \tag{39}$$

During this time t , the charge is moving with constant velocity $\bar{v} = \bar{\beta}c$, and zero acceleration, along the line, so it reaches the point Q_1, at the same time that the energy which left from Q_o reaches P.

Hence

$$\overline{Q_oQ_1} = \bar{v}t = \bar{\beta}r \tag{40}$$

It is seen that

$$\bar{r}_v = \bar{r} - \bar{\beta}r \tag{41}$$

Thus the term ($\bar{r}-\bar{\beta}r$) is the virtual present position.

Second, the quantity S in Eq. (3) can be identified on Fig. 5. Since

$$\bar{r}\cdot\bar{\beta} = (\beta r)\cos\theta \tag{42}$$

then ($\bar{r}\cdot\bar{\beta}$) is the projection of the vector $\bar{\beta}r$ on $\bar{r}$, i.e., the segment $\overline{Q_oT}$ of the line $\bar{r} = \overline{Q_oP}$. Then from (Eq. (3), it follows that

$$S = r - \bar{r}\cdot\bar{\beta} = \overline{TP} \tag{43}$$

Further, S can be written in terms of r_v and θ_v , the virtual position and angle, respectively, of the charge at Q_1 . Thus in the right triangle Q_1TP,

$$S^2 = r_v^2 - \beta^2 r^2 \sin^2\theta$$

But the perpendicular H from P to the line of motion is

$$H = r\sin\theta = r_v \sin\theta_v \tag{44}$$

Hence

$$r^2\sin^2\theta = r_v^2 \sin^2\theta_v \tag{45}$$

and

$$S = r_v(1-\beta^2\sin^2\theta_v)^{1/2} \tag{46}$$

Third, the first term in Eq. (9), designated as $\bar{E}_1$, can now be written, using (Eqs. (41,46), as

$$\bar{E}_1 = \left[\frac{q}{4\pi\varepsilon_0}\,\frac{\hat{a}_{r_v}}{r_v^2}\right]\left[\frac{1-\beta^2}{(1-\beta^2\sin^2\theta_v)^{3/2}}\right] \tag{47}$$

where $\hat{a}_{r_v}$ is the unit vector along $\bar{r}_v$, pointing from the present position of q to P. It is seen that $\bar{E}_1$, which is the total field of a charge moving at constant velocity, since acceleration $\bar{a}$ is zero, is identical to the Coulomb field of a stationary charge, given by the quantity in the first brackets of Eq. (47), modified by the quantity in the second brackets, which is a function of the velocity. Eq. (47) agrees with Ref. 25 (p. 254). For low velocity particles, where $\beta \ll 1$, the quantity in the second brackets is essentially unity. Hence the important result: The field of a charge moving at a low constant velocity is essentially the ordinary Coulomb field associated with a stationary charge. Thus, as put in Ref. 24 (p. 337), for a charge moving with constant velocity, the lines of force diverging radially from the charge move with the charge, acting as if they were rigid wires attached to the charge.

Now the effects of acceleration can be ascertained. Following Ref. 24 (pp. 334-340), let point charge q move along a line as shown in Fig. 6, with constant velocity $v \ll c$, arriving at point 0 at time t_0. During a time interval Δt, let q be accelerated to velocity $v+\Delta v$, reaching point O_1, at time $t_0+\Delta t$, after which it moves at the new constant velocity. As established above, the $\bar{E}$ lines move with q as long as it does not accelerate. The effects of any disturbance such as the short period of acceleration are assumed to propagate outward at the speed of light c, which is reasonable. Draw a sphere S_0 around 0 of radius

$$r_0 = c(t-t_0) \tag{48}$$

where $t>t_0$. Any signal traveling at velocity c reaching any point in the region outside S_0 at time t must have left q at a time before t_0. Thus the $\bar{E}$ lines outside S_0 are the same as those of the charge moving with the original constant velocity v. Therefore, by the third point established above, the $\bar{E}$ lines outside S_0 are essentially the same as those of charge

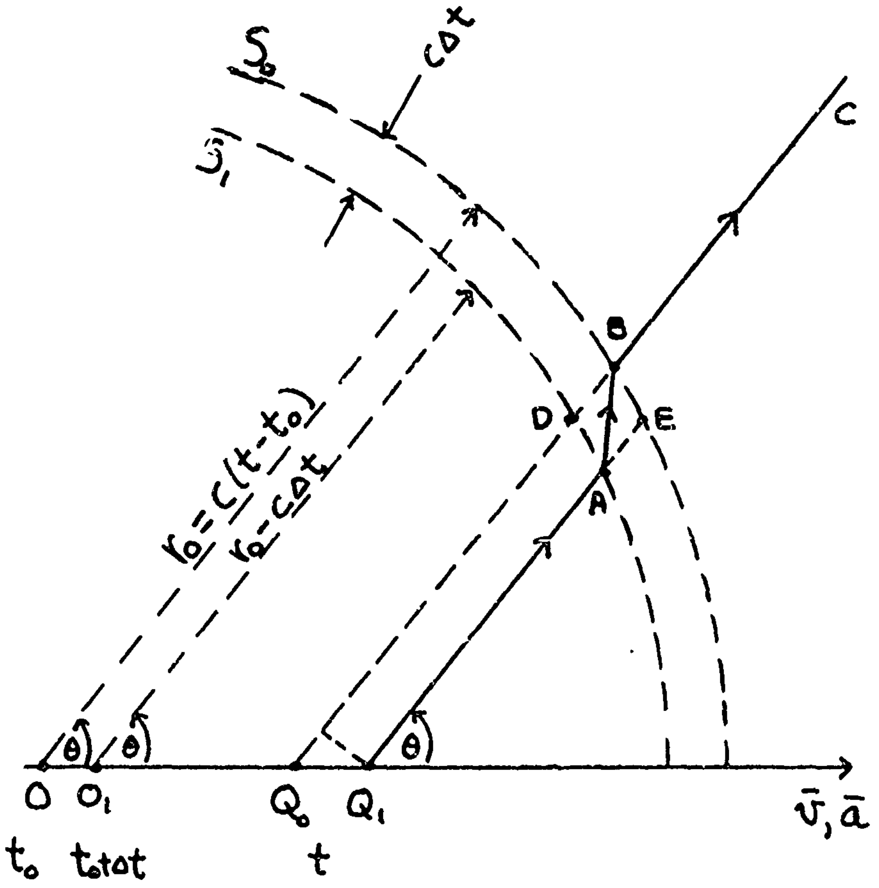

FIG. 6 Radiation due to an accelerated charge.

at the point Q_0, which is where the point where q would be at time t if it had not been accelerated. Hence the $\bar{E}$ line $\overline{BC}$ outside S_0 is shown diverging radially from Q_0.

Next draw a sphere S_1 centered at O_1 with radius $r_0 - c\Delta t$. Any signal traveling at velocity c reaching any point *inside* S_1 must have left q *after* it reached O_1 at time $t_0+\Delta t$, at which time it is moving with velocity $v+\Delta v$. Hence the field inside S_1 is the same as that of a charge moving at constant velocity $v+dv$, and therefore diverges as the line $\overline{Q_1 A}$ from Q_1, which point is actually reached by q at time t.

The thin shell of thickness $c\Delta t$ is the region where the acceleration effects must put a "kink" in the $\bar{E}$ line Q_1ABC as shown in Fig. 6. This kink travels along the $\bar{E}$ line at velocity c. Then,

$$a = \frac{\Delta v}{\Delta t} \tag{49}$$

$$\overline{OO_1} \approx v\Delta t \tag{50}$$

Since $v/c \ll 1$, then $\overline{OO_1} \ll c\Delta t$. Hence the shell is approximately due to two concentric spheres, with coincident centers at O. To an approximation which neglects terms of the order of (v/c) as well as (v^2/c^2), the situation is as shown in Fig. 6, with $\overline{Q_1 A} \approx r_0$ (Ref. 24, p. 340) in the limit of very small (v/c).

The $\bar{E}$ field segment $\overline{AB}$, which represents the acceleration effects, is resolved into two components:

$$\frac{E_\theta}{E_r} = \frac{\overline{AD}}{\overline{DB}} = \frac{\overrightarrow{Q_0Q_1}\sin\theta}{c\Delta t} \tag{51}$$

But

$$\overline{Q_0Q_1} = \overline{OQ_1} - \overline{OQ_0} \approx (t-t_0)(v+\Delta v) - (t-t_0)v$$

$$= (t-t_0)\Delta v$$

$$\therefore \overline{Q_0Q_1} \approx \frac{r_0\Delta v}{c} = \frac{r_0 a\Delta t}{c} \tag{52}$$

Hence

$$\frac{E_\theta}{E_r} = \frac{r_0 a\sin\theta}{c^2} \tag{53}$$

Continuity of the E_r component withthe usual radial field demands that

$$E_r = \frac{q}{4\pi\varepsilon_0 r^2} \tag{54}$$

Hence

$$E_\theta = \frac{q}{4\pi\varepsilon_0}\,\frac{n\theta}{c^2 r_0} \tag{55}$$

which agrees with Eq. (23) for the radiation field of an accelerating charge with velocity much less than c.

SECTION 3

RESPONSE OF A LINEAR WIRE ANTENNA TO PULSE EXCITATION AND RADIATION IN THE BROADSIDE DIRECTION

3.1 TRAVELING PULSE ON WIRE ANTENNA; THE SOURCE OF RADIATION

A current pulse traveling on a linear wire antenna is shown in Fig. 7. The current I(Z,t) satisfies a wave equation, assuming no attenuation for simplicity, given by (see Appendix III)

$$\frac{\partial^2 I}{\partial Z^2} - \frac{1}{c^2}\frac{\partial^2 I}{\partial t^2} = 0 \tag{56}$$

The solution to Eq. (56), for a wave traveling in the +Z direction is the well-known equation

$$I(t,Z) = I(t - Z/c) \tag{57}$$

For ordinary conductors, it may be assumed that the wave velocity is essentially the velocity of light c (see Appendix III). Skin effects will produce some round-off of sharp wave-fronts. In the central part of the pulse shown in Fig. 7, where the current is constant, no radiation is produced (a d.c. current does not radiate). This follows also from

$$\bar{I} = \bar{J}A = \rho\bar{v}\bar{A} = \text{constant} \equiv I_0 \tag{58}$$

Thus velocity $\bar{v}$ is constant, acceleration $\bar{a}$ is zero, and there is no radiation from that portion of the pulse where the current is constant.

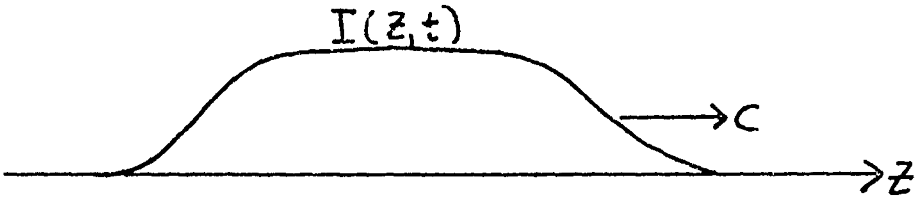

FIG. 7 Traveling current pulse on straight wire.

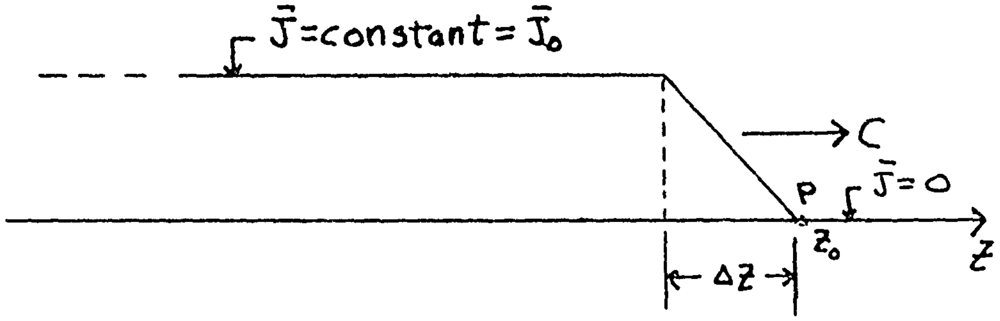

FIG. 8 Leading edge of traveling trapezoidal pulse shown at time t_o.

The radiation arises solely from the leading and trailing edges of the pulse, where the current (density) is changing with time, which results in acceleration of charges. To simplify the discussion of this phenomenon, consider an idealized trapezoidal pulse with a very short rise time = t_R seconds at its leading edge, as shown in Fig. 8. This figure shows the pulse at time t_0 (i.e., a "shapshot of J "frozen" at time t_0). In time

$$t_R = \Delta z / c \tag{59}$$

J at point O changes from zero to J_0 . Thus the partial derivative of J with respect to time is

$$\frac{\partial J}{\partial t} = \frac{J(t_0 + t_R, z_0) - J(t_0, z_0)}{t_R} = \frac{J_0 - 0}{t_R} = \frac{J_0}{t_R} \tag{60}$$

In Eq. (60), Z is fixed at its value Z_0 at point P. The partial derivative of J with respect to distance Z is

$$\frac{\partial J}{\partial z} = \frac{J(t_0, z_0) - J(t_0, z_0 - \Delta z)}{\Delta z} = \frac{0 - J_0}{\Delta z} = \frac{-J_0}{\Delta z} \tag{61}$$

From Eqs. (59,61),

$$\frac{\partial J}{\partial z} = -\frac{J_0}{c t_R} \tag{62}$$

Differentiating the equation $J=\rho v$ with respect to time results in

$$\frac{\partial J}{\partial t}=\rho\frac{\partial v}{\partial t}+v\,\frac{\partial \rho}{\partial t} \tag{63}$$

The continuity equation, for this one-dimensional case reduces to

$$-\frac{\partial \rho}{\partial t}=\nabla\cdot\bar{J}=\frac{\partial J}{\partial z} \tag{64}$$

Combining Eqs. (60-64 incl.), the result is

$$\frac{J_0}{t_R}=\rho\,\frac{\partial v}{\partial t}+\frac{v\,J_0}{c\,t_R} \tag{65}$$

Since v, the drift velocity of charges (electrons) in a conductor is many orders of magnitude less than c (see Appendix IV), Eq. (65) reduces to

$$\rho\,\frac{\partial v}{\partial t}=\frac{J_0}{t_R}\left(1-\frac{v}{c}\right)\approx\frac{J_0}{t_R} \tag{66}$$

Thus, although $\partial\rho/\partial t$ can approach large values for very small t_R, the term $v\,\partial\rho/\partial t$ turns out to be smaller than $\rho\,\partial v/\partial t$ by a factor equal to the ratio of the drift velocity to c, which is considered to be on the order of 10^{-8} or less (see Appendix IV).

The above results for the trapezoidal pulse are a special case of the more general result discussed in Appendix

III, which is

$$\rho\bar{a} = \rho\frac{\partial\bar{v}}{\partial t'} \approx \frac{\partial\bar{J}}{\partial t'} \qquad (67)$$

Hence, using Eq. (27), for charge q in length dZ,

$$\left[q\bar{a}\right]_{ret} = \frac{\partial}{\partial t}I(z, t-r/c)\,dz \qquad (68)$$

which is the same as Eq. (32). Thus the radiation arises from the time derivative of the current, i.e., from the edges of a flat-topped traveling pulse, as previously asserted. Insertion of Eq. (68) into Eqs. (23,24), and integration over the antenna length variable Z, taking into account the retardation factor, allows calculation of the radiation fields. Further discussion of this is given in Section 4 (e.g., see Eq. (74)).

3.2 RADIATION NORMAL TO A WIRE ANTENNA

To illustrate the use of some of the concepts concerning radiation which have been presented, they will be applied to a well-known paper concerning the calculated and experimental response of a thin cylindrical antenna to pulse excitation (Ref. 26). In Ref. 26 the radiated field of a monopole at $\theta = 90°$ is calculated by Fourier transform methods, and confirmed by measurements. The monopole, of height h over a conducting ground plane, is driven by a 50 ohm coaxial line, as shown in

Fig. 9. The antenna length-to-radius ratio (h/a) is given as 904. Several pulse lengths are used with space lengths $c\tau$ varying from 0.2 h/c to 2.0 h/c. The exact shapes of the pulses are specified in Ref. 26. In this report these shapes will be taken as almost rectangular, with short rise and decay times, which greatly simplifies the discussion. Further, it will be assumed that the input surge impedance of the monopole at its base is approximately 300 ohms. This produces a current reflection coefficient of 0.72 on a 50 ohm line, which, as shown below, gives good agreement with the published results.

The calculated radiated $\bar{E}$ field (Ref. 26, Fig. 4, top graph) for $\tau \simeq$ 0.2 h/c is sketched approximately in Fig. 10. The amplitudes have been normalized so that the first pulse has unity amplitude. The shape of this graph will now be explained.

As the leading edge of the pulse emerges from the coaxial line onto the monopole, there is a reflection back into the coaxial line, which is of no concern here, since that line is terminated in 50 ohms. As explained in Section 3.1, the leading edge of the pulse traveling on the monopole produces radiation due to accelerated electrons from the instant it emerges at local time $t' = 0$, which reaches $P(R, 90^\circ)$ at time $t = t' + R/c = R/c$. As the leading edge proceeds to a distance

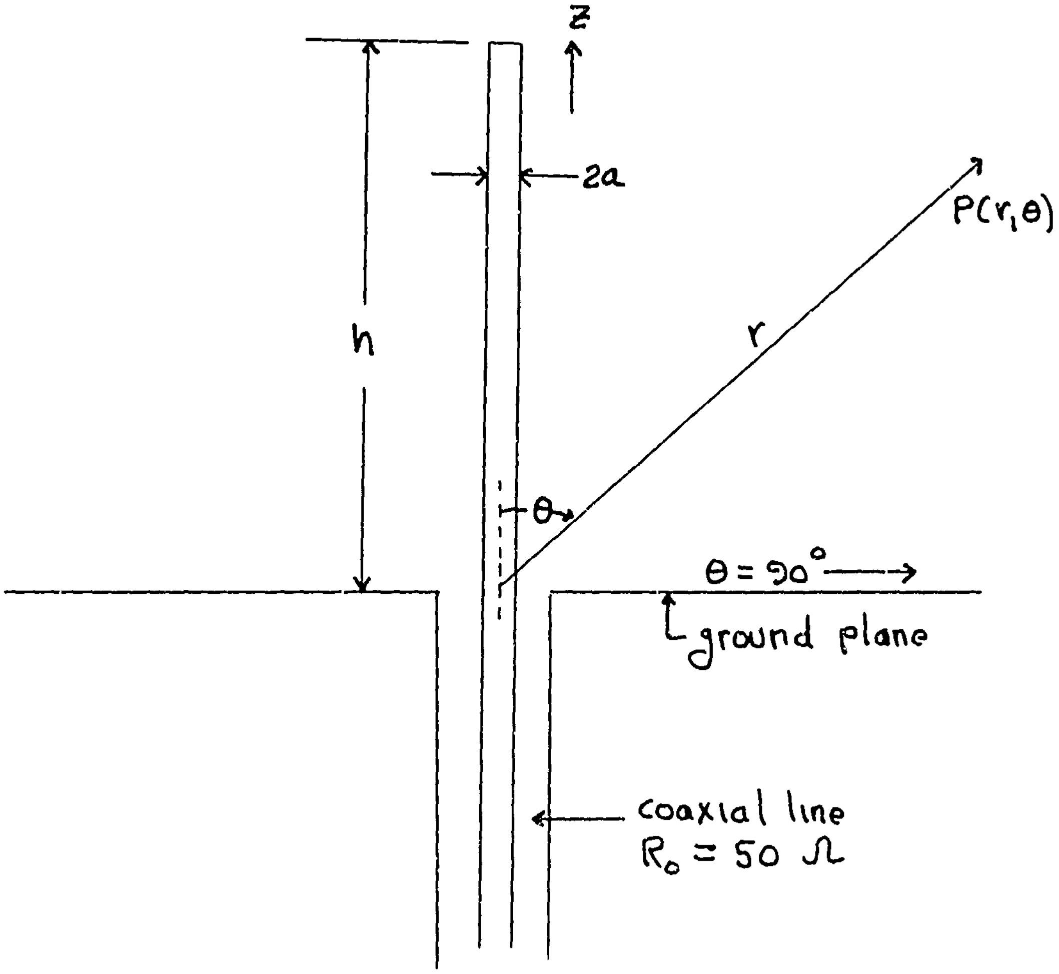

FIG. 9 Monopole over ground plane.

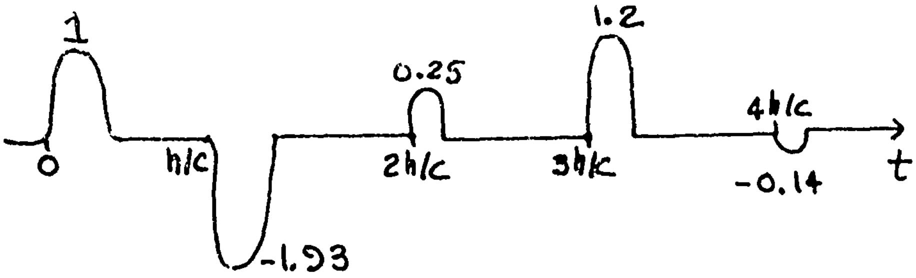

FIG. 10 Radiation field of monopole.

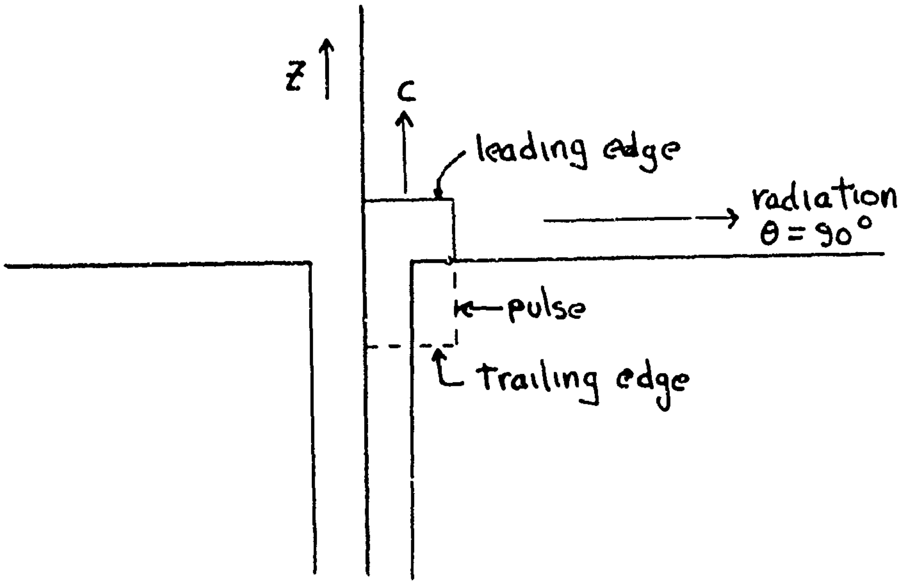

FIG. 11 Radiation from leading edge of pulse.

$z=ct'$, which is less than the space length of the pulse, radiation continues to be emitted from the leading edge, arriving at P at time $t = t'+R/c$. See Fig. 11. Hence the radiation emitted in a period of time t' is received over the same period of time at P. Neglecting line losses and the attenuation of the pulse due to radiation, this radiation continues to arrive at P from the leading edge, until the trailing edge of the pulse emerges at time $t'=\tau$ from the coaxial line. At this instant, radiation being emitted by deaccelerating electrons at the trailing edge, with radiation opposite to that of the leading edge, leaves to arrive at P at time $\tau+R/c$, where it cancels the radiation from the leading edge. Hence the radiation at P consists of a pulse of normalized amplitude equal to unity for a time interval equal to τ, and zero amplitude afterwards, during the time that the entire pulse is traveling up the monopole, and before the leading edge reaches the tip of the monopole. This state of affairs is illustrated in Fig. 12, where the common time delay of R/c has been dropped, and the traveling pulse has a normalized amplitude of $+1$. At the leading edge, charge is accelerated from zero velocity to unity (normalized) velocity, while at the trailing edge, charge is deaccelerated from unity to zero velocity. This is illustrated in Fig. 13, which shows

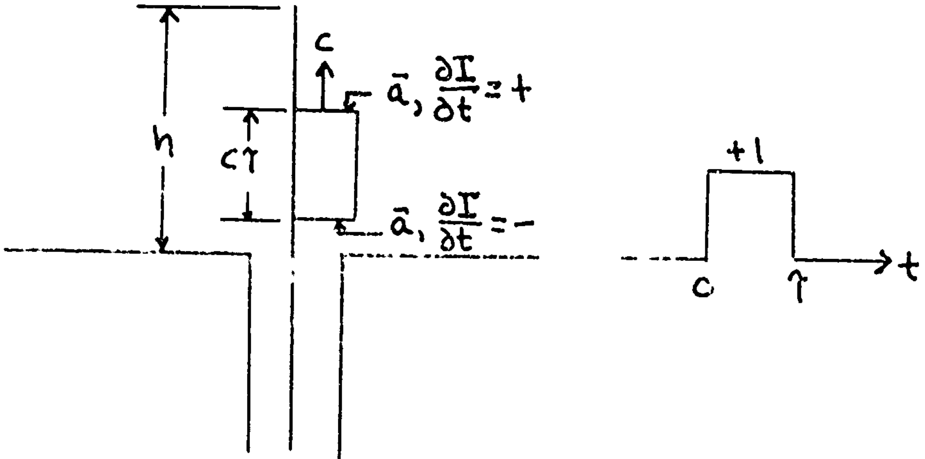
c
$\bar{a}, \frac{\partial I}{\partial t} = +$
h
$c\tau$
$\bar{a}, \frac{\partial I}{\partial t} = -$
+1
0
τ
t

(a) Pulse on monopole (b) Received waveform

FIG. 12 Initial radiated field when entire pulse is on monopole.

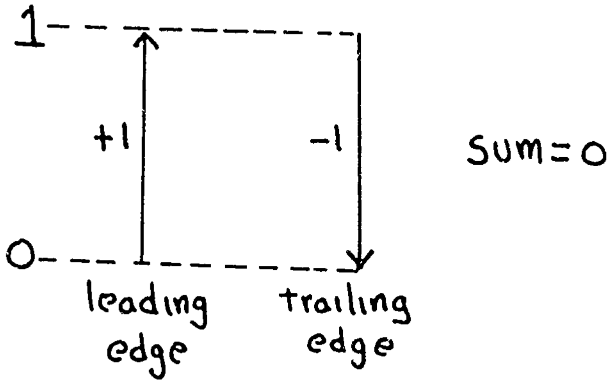

FIG. 13 Cancellation of radiation from leading and trailing edges.

the resultant cancellation between the two edges. Due to the ground plane, all of the above currents and charges have images. However, for $\theta = 90^\circ$, the images merely duplicate and double the radiation produced by the real monopole, so image effects need not be considered separately.

When the leading edge reaches the monopole tip at $z = h$, and time $t' = h/c$, the current goes to zero at the tip (approximately, since there can be current flow over the end cap, unless the end is sharpened to a needle-point (see Ref. 27)). Thus the pulse breaks up into an incident and a reflected pulse, which must appear as shown in Fig. 14 at some instant after the leading edge has reached the tip, but before the trailing edge has reached the tip. The combined space lengths of both pulses is $c\tau$. The radiation from the leading edge of the reflected pulse and the trailing edge of the incident pulse reinforce each other; hence the amplitude of the radiation field during the reflection period of duration τ is approximately -2 (normalized). That is, the field amplitude $\simeq -2$ in the time period $\frac{h}{c} < t \leq \frac{h}{c} + \tau$, omitting R/c. This reinforcement is illustrated in Fig. 15. The trailing edge of the incident pulse deaccelerates charge from unity to zero velocity, while the leading edge of the reflected pulse accelerates charge from zero to negative unity velocity. In fact,

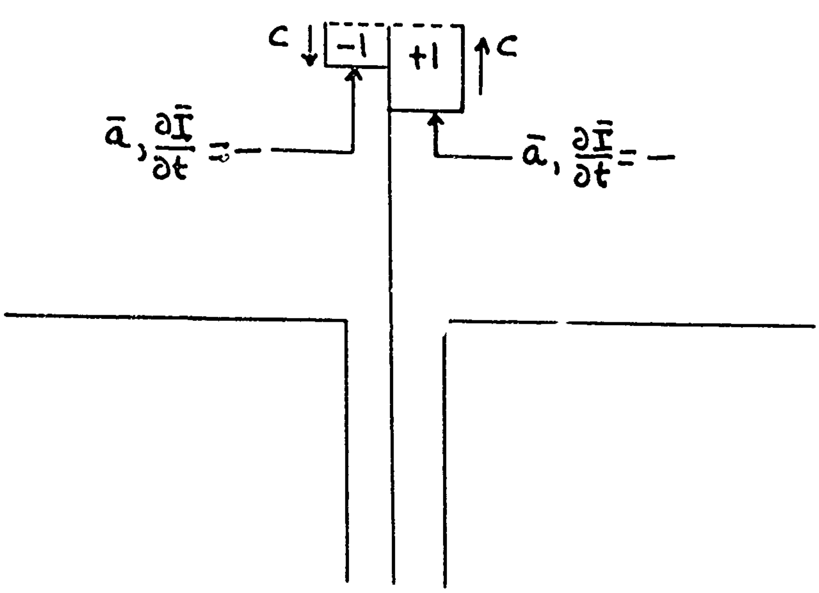
c
-1
+1
c
$\bar{a}, \frac{\partial \bar{I}}{\partial t} = -$
$\bar{a}, \frac{\partial \bar{I}}{\partial t} = -$

FIG. 14 Pulse after reflection at tip.

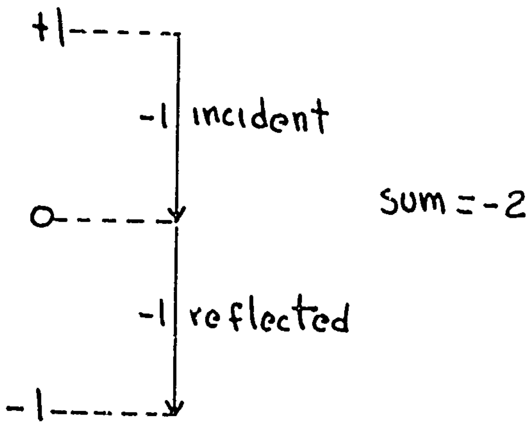

FIG. 15 Reinforcement of radiation from edges during reflection from tip.

the reflection from the end is probably not perfect, and a current reflection coefficient ≈ -0.5 leads to a field amplitude $\simeq -1.5$ which gives better agreement with the calculated field amplitude $\simeq -1.53$.

Summarizing the above, there is a burst of radiation as the pulse emerges from the coaxial line, which ceases and remains zero while the entire pulse length is traveling on the line. This is followed by another burst of radiation when the leading edge reaches the monopole tip, which ceases when the trailing edge completes its reflection from the tip. After the pulse has completed its first reflection from the tip, there results a negative current pulse of amplitude -0.5 traveling down the monopole, as shown in Fig. 16. Again, as previously described, the radiation from leading and trailing edges cancel, leading to zero radiation. Hence the radiated field appears as shown in Fig. 17.

When the reflected pulse shown in Fig. 16 reaches the base of the antenna, it is leaving a line with surge impedance of (approximately) 300 ohms and encountering a coaxial line of characteristic impedance $\simeq 50$ ohms. Assuming for simplicity that the surge impedance is largely resistive (there can be an appreciable reactive component; see Ref. (28), Figs. 5 and 6), the

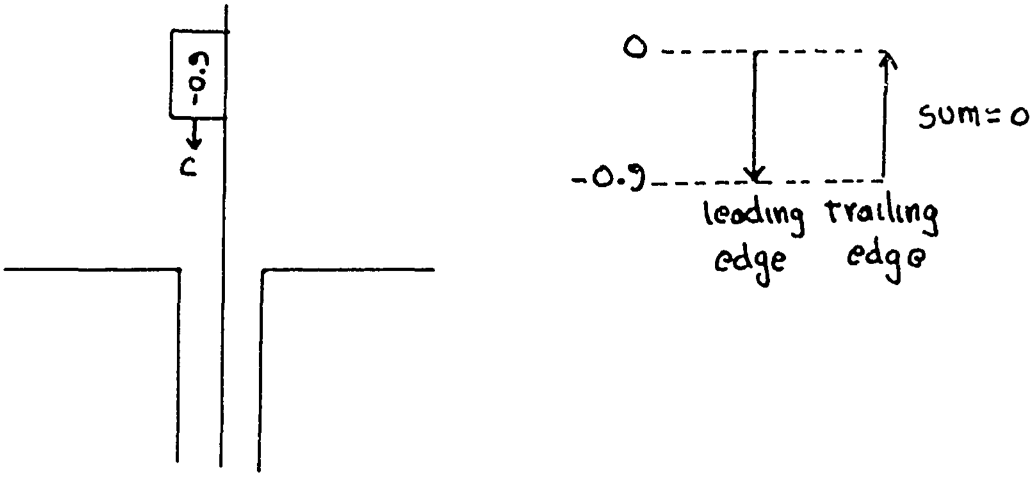

FIG. 16 Reflected pulse traveling back to base of monopole.

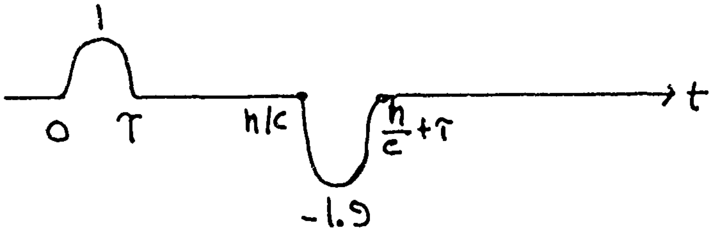

FIG. 17 Radiation field after first reflection.

current reflection coefficient is

$$\Gamma_c = \frac{R_o - R_L}{R_o + R_L} = \frac{300-50}{300+50} = 0.72 \qquad (69)$$

The situation during this base reflection period is shown in Fig. 18. The magnitude of the reflected current pulse is (-0.9) (0.72) = -0.65. The trailing edge of the incident pulse deaccelerates charge from -0.9 to zero amplitude, while the leading edge of the reflected pulse accelerates charge from zero to -0.65 amplitude. The radiation field subsequent to the reflection of the entire pulse from the base therefore appears as illustrated in Fig. 19.

The reflected pulse of amplitude -0.65 travels back up the antenna, and the previously described reflection phenomenon at the monopole tip reoccurs. Assume $\Gamma_c = -0.9$ at the tip; the reflected wave amplitude is 0.59, and the situation during this reflection is shown in Fig. 20. The lagging edge of the incident pulse deaccelerates charge from -0.65 to zero velocity, while the leading edge of the reflected pulse accelerates charge from zero to 0.59 velocity. The resultant radiation is then -(-0.65) + (0.59) = 1.24. The radiation waveform now appears as shown in Fig. 21.

Carrying the process through one more step, the reflected pulse of amplitude +0.59 returns to the base, where using

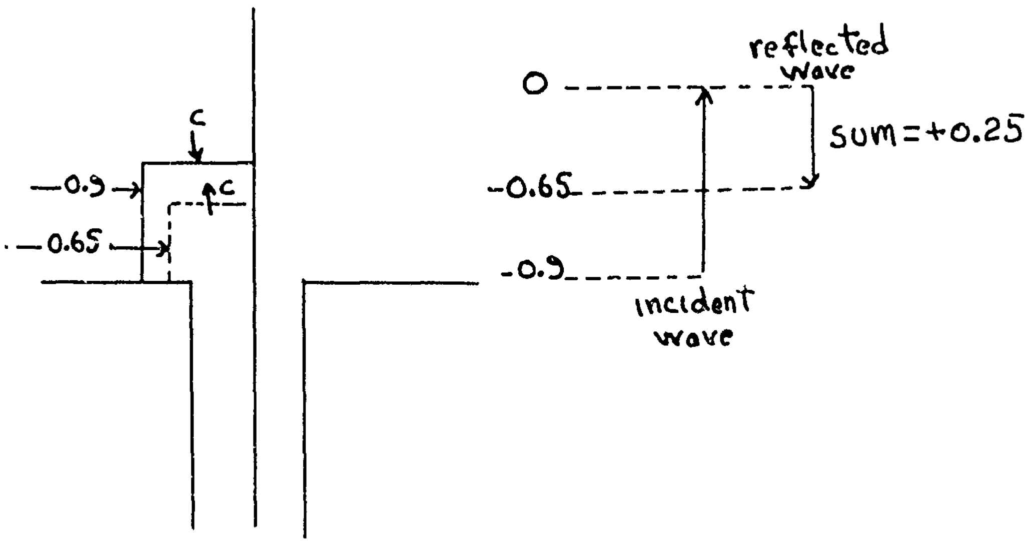

FIG. 18 Incident and reflected waves at base.

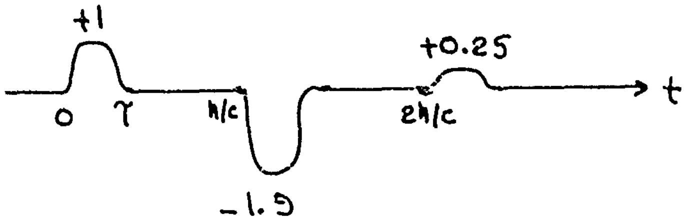

FIG. 19 Radiation field subsequent to reflection from base.

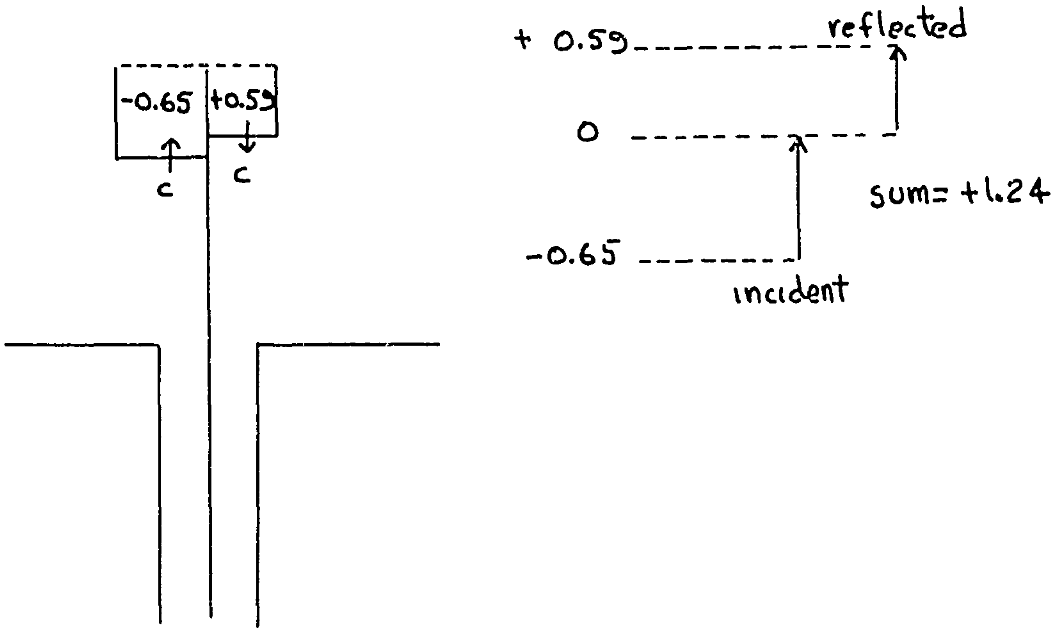

FIG. 20 Second reflection from tip.

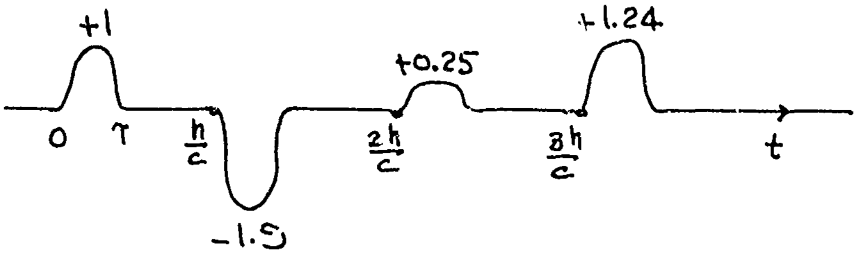

FIG. 21 Radiated waveform subsequent to second reflection from tip.

Γ_c = 0.72, another reflected wave of amplitude 0.43 starts back up the antenna. The situation during this second reflection at the base is shown in Fig. 22. The radiation waveform is shown in Fig. 23.

Comparison between the radiation waveforms of Fig. 23 and the calculated result (Ref. 26) shown in Fig. 10, shows a fairly good agreement. Of course, the surge impedance and reflection coefficients have been selected, using previously published data, so as to obtain good agreement. Nevertheless, it is evident that the principal radiation characteristics of the pulsed monopole antenna, at least for $\theta = 90^\circ$, can be explained with the aid of the radiation mechanisms described above and some simple transmission line calculations.

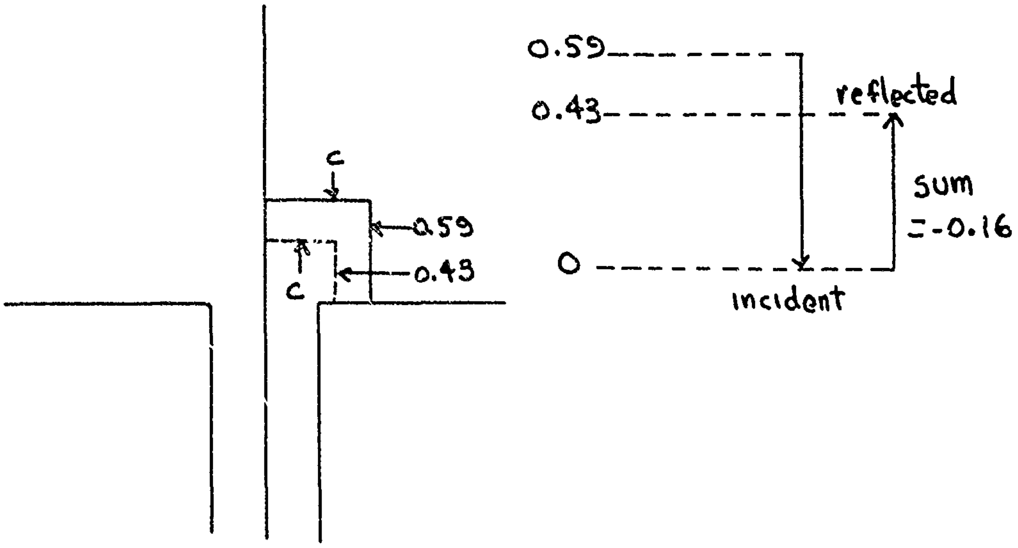

FIG. 22 Second reflection from base.

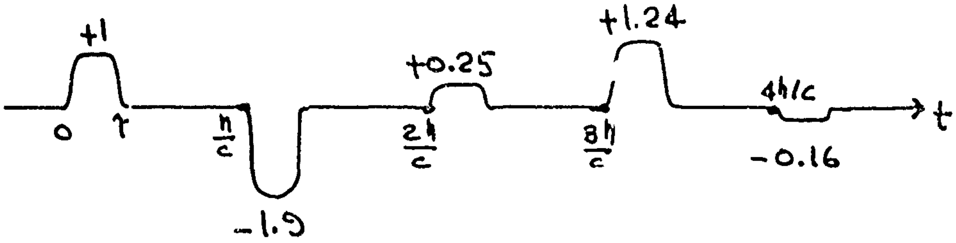

FIG. 23 Radiated waveform subsequent to second reflection from base.

SECTION 4

RADIATION OF A PULSE-EXCITED LINEAR WIRE ANTENNA IN ANY DIRECTION

4.1 DERIVATION OF EQUATIONS

In this section, the equations are derived for the radiation fields of a pulse-excited, linear, thin-wire antenna, in any general direction at angle θ with the antenna, using the accelerated charge concepts previously developed. See Fig. 24 which shows a standard center-fed linear antenna. However, the following discussion also pertains to any type of linear wire antenna, including a monopole over a ground plane. These equations agree with those given by Manneback (Ref. 29, Eq. 12), Schelkunoff (Ref. 30, pp. 102-109) and Ross et al (Refs. 31,32). For an infinitely thin wire antenna, Refs. 29-32 inclusive give the radiation field of a general current wave I (Z,t) traveling undispersed at light velocity c in the positive Z direction, originating at origin 0, as

$$H_\phi = \frac{I(t-r/c)}{4\pi r} \, \frac{1+\cos\theta}{\sin\theta} \tag{70}$$

$$E_\theta = \sqrt{\mu/\varepsilon} \; H_\phi \tag{71}$$

An alternative form of Eq. (70) also appears, using the trigonometric identity

$$\frac{1+\cos\theta}{\sin\theta} = \frac{\sin\theta}{1-\cos\theta} \tag{72}$$

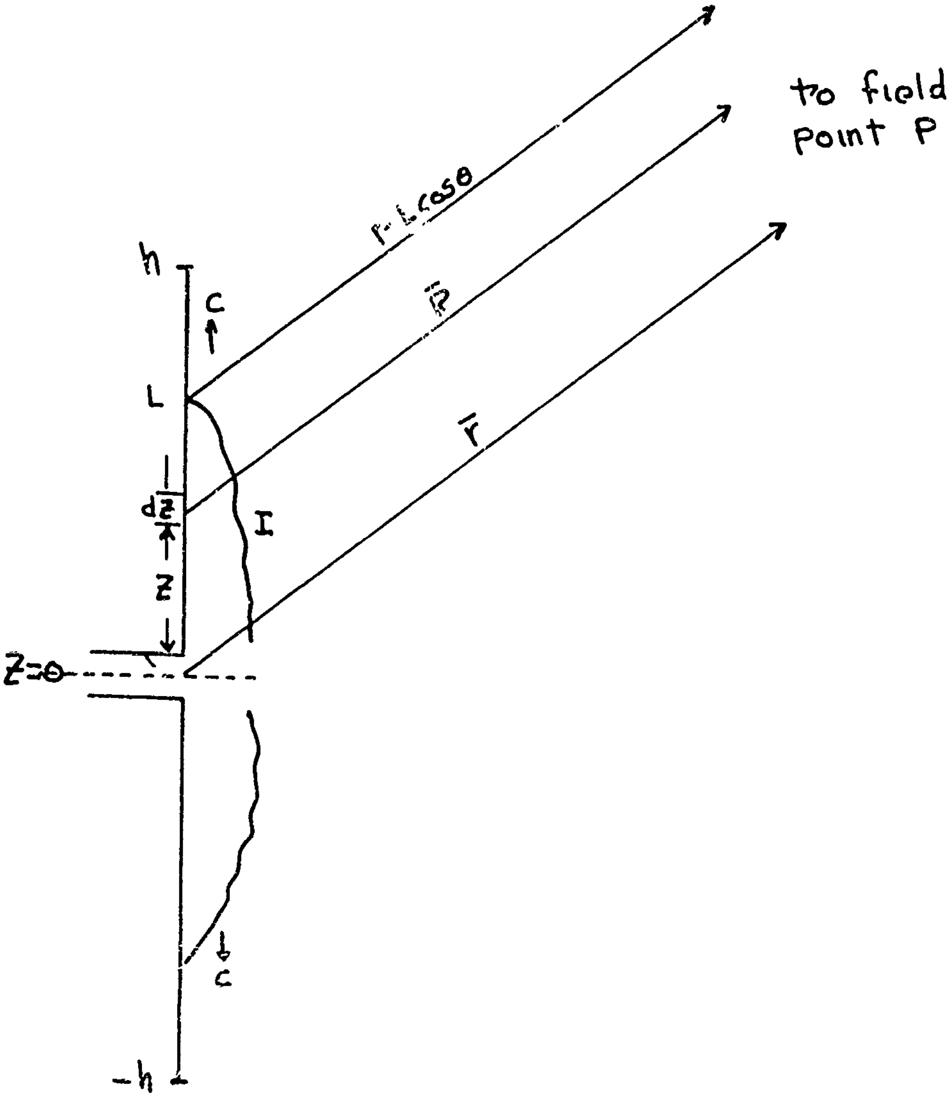

FIG. 24 Linear antenna geometry.

which is

$$H_\phi = \frac{I(t-r/c)}{4\pi r}\,\frac{\sin\theta}{1-\cos\theta} \tag{73}$$

From the accelerated charge viewpoint, the radiation field due to an accelerated differential charge q of length dZ is found by combining Eqs. (24) and (68) to give

$$dH_\phi = \frac{\sin\theta}{4\pi c R}\,\frac{\partial I(Z,t-R/c)}{\partial t}\,dZ \tag{74}$$

In Eq. (74), R appears in place of r as used in Eqs. (24) and (68). In Eqs. (24,68) the distance from radiating element dZ to field point P was designated as r, whereas in order to conform to Refs. 29-32 inclusive, r will be used to designate the radial distance from origin 0 to P, and R will designate the distance from dZ to P.

The radiation field given by Eq. (74) is also that of a Hertzian dipole, as given by Sommerfeld (Ref. 19), in the form shown as Eq. (V-2) in Appendix V, where the dipole length l = dZ, and

$$\ddot{p}(Z,t-R/c) = \frac{\partial^2}{\partial t^2}\left(q(Z,t-R/c)dZ\right) = \frac{\partial}{\partial t} I(Z,t-R/c)dZ \tag{75}$$

An equation equivalent to Eq. (74) also appears in Manneback (Ref. 29, Eq. (4)), where it is attributed to Hertz. In Appendix VII, it is demonstrated that the use of Eq. (74) for a number of standard antennas with a sinusoidally-time varying currents, such as a dipole and a traveling-wave antenna, leads to agreement with well-established results. In addition, in Appendix VII it is also shown that for arbitrary time variation, $d\overline{H}$ obtained from a vector potential $\overline{A}$ formulation is the same as given by Eq. (74).

Consider the field of a current wave traveling at velocity c in the positive Z direction on the upper half $0 \leq z \leq h$ of the antenna shown in Fig. 24. The field due to waves on the lower half $-h \leq z \leq 0$ of the antenna is calculated similarly as shown later. From Eq. (III-13), the traveling current wave is given by

$$I(z,t) = I(t - z/c) \tag{76}$$

In order to postpone, for the time being, inclusion of the effects of terminal conditions at the end of the antenna Z = h, (i.e., a reflected wave moving in the negative Z direction), let I at any particular time extend from Z = 0 to Z = L, where $L < h$, as shown in Fig. 24. The field at P is then found by integrating Eq (74) from Z = 0 to Z = L,

$$H_\phi = \frac{1}{4\pi c}\int_0^L \frac{\sin\theta}{R} \frac{\partial}{\partial t} I(z, t - R/c)\, dz \tag{77}$$

For point P sufficiently distant, the variable R in Eq. (77) may be replaced by the usual far-field approximation

$$R \approx r - z\cos\theta \tag{78}$$

Eq. (78) is based upon the assumption that at any time the largest spatial extent Z = L of the current on the antenna is small compared to R and r, and Eq. (77) is based upon the assumption that the current wave I has not yet reached the antenna end Z = h. Then, and only then, R may be replaced with negligible error by r in the denominator of the integrand in Eq. (77), and sin θ may be regarded as constant, since $\bar{R}$ and $\bar{r}$ approach parallelism when Eq. (78) holds true. Then Eq. (77) becomes

$$H_\phi = \frac{\sin\theta}{4\pi rc}\int_0^L \frac{\partial}{\partial t} I(Z, t-R/c)\, dZ \tag{79}$$

The function I (Z,t-R/c) in Eq. (79), can be rewritten, using Eqs. (76,78), as

$$I(Z, t-R/c) = I\left(t - \frac{Z}{c} - \frac{R}{c}\right) = I\left(t - \frac{r}{c} - \frac{Z}{c}(1-\cos\theta)\right) \tag{80}$$

Thus Eq. (79) becomes

$$H_\phi = \frac{\sin\theta}{4\pi rc}\int_0^L \frac{\partial}{\partial t} I\left(t - \frac{r}{c} - \frac{Z}{c}(1-\cos\theta)\right) dZ \tag{81}$$

Now

$$\frac{\partial}{\partial t} I\left(t - \frac{r}{c} - \frac{Z}{c}(1-\cos\theta)\right) = I' \frac{\partial}{\partial t}\left(t - \frac{r}{c} - \frac{Z}{c}(1-\cos\theta)\right) = I' \tag{82}$$

where I' denotes the derivative of $I\left(t-\frac{r}{c}-\frac{z}{c}(1-\cos\theta)\right)$ with respect to the argument $\left(t-\frac{r}{c}-\frac{z}{c}(1-\cos\theta)\right)$.

Similarly

$$\frac{\partial}{\partial z} I\left(t-\frac{r}{c}-\frac{z}{c}(1-\cos\theta)\right)=-\frac{1-\cos\theta}{c} I' \tag{83}$$

From Eqs. (82,83),

$$\frac{\partial I\left(t-\frac{r}{c}-\frac{z}{c}(1-\cos\theta)\right)}{\partial t}=\frac{-c}{1-\cos\theta}\frac{\partial}{\partial z} I\left(t-\frac{r}{c}-\frac{z}{c}(1-\cos\theta)\right) \tag{84}$$

Eq. (84) is typical of the relationship between the t and Z partial derivatives for traveling waves. Substitution of Eq. (84) into Eq. (81) gives

$$H_\phi=-\frac{\sin\theta}{1-\cos\theta}\frac{1}{4\pi r}\int_0^L \frac{\partial}{\partial z} I\left(t-\frac{r}{c}-\frac{z}{c}(1-\cos\theta)\right) dz \tag{85}$$

The partial derivatives of I with respect to either Z or t cannot have infinite values, in the actual case. The slopes of any real wave I traveling on a wire may be very large, but must be finite, even for a hypothetical square pulse applied to the input terminals. This is discussed in more detail in Appendix III, subsection 3, entitled "Wave Travel of Step Functions and Pulses on Lossy Lines." However, the employment of step and delta waveforms in concept, or as models of actual waveforms is so useful and important that their radiation properties must be analyzed. This is done in Section 4.2. At this point, assuming that I has no infinite slopes, the integral in Eq. (85) reduces simply to

$$H_{\phi}(t,r) = \frac{f(\theta)}{4\pi r}\left[I(t - r/c) - I(t - r/c - L(1-\cos\theta)/c\right] \tag{86a}$$

$$f(\theta) \equiv \frac{\sin\theta}{1-\cos\theta} = \frac{1+\cos\theta}{\sin\theta} \tag{86b}$$

The retardation time r/c identifies the first term in the brackets of Eq. (86) as the current that was at the origin 0 at time r/c ago. The retardation time

$$\frac{r}{c} + \frac{L}{c}(1-\cos\theta) = \frac{L}{c} + \frac{r-L\cos\theta}{c} \tag{87}$$

of the second term is the sum of the time L/c for the leading edge of the current wave I to travel along the antenna from the origin to Z = L, plus the time $(r-L\cos\theta)/c$ for propagation of the field from Z = L to point P. This identifies the second term as the current that was at the origin 0 at time $\left(\frac{r+L(1-\cos\theta)}{c}\right)$ ago, which is the current at the leading edge of I. But for the use of non-infinite derivatives of I, the leading-edge current must be zero, as illustrated in F 25. Hence Eq. (86)

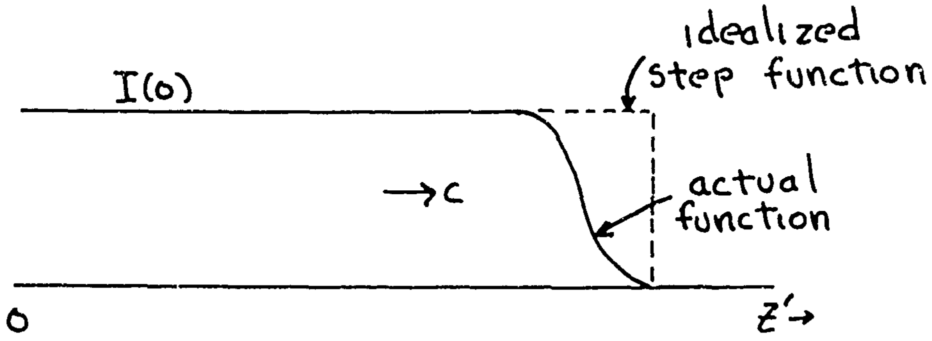

FIG. 25 Leading edge detail.

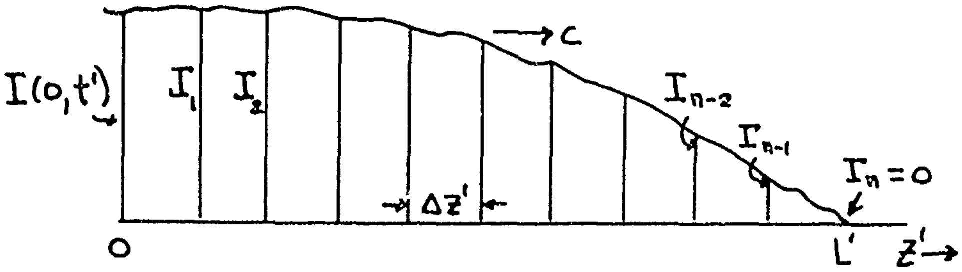

FIG. 26 Finite-slope function $I(z', t')$ at fixed time t'.

reduces to

$$H_\phi(t,r) = \frac{I(t-r/c)}{4\pi r} \quad \frac{1+\cos\theta}{\sin\theta} \tag{88}$$

Eq. (88) is the same as Eq. (70) or Eq. (73). The field appears to be radiated in spherical waves from the origin. Thus, although the radiation emanates from all parts of the traveling wave where there is acceleration of charge (i.e., a non-zero time derivative of current), the integration of this derivative along the wave produces the interesting result that the far-field radiation acts as if it emanated only from the point of initial excitation, the origin. Similar results, but for differing reasons appear in Refs. (29-32 inclusive).

Eq. (88) can be derived in an alternative manner, which is shorter and instructive. In Eq. (85) make the following substitutions:

$$t' \equiv t - r/c \tag{89a}$$

$$z' \equiv z(1-\cos\theta) \tag{89b}$$

$$L' \equiv L(1-\cos\theta) \tag{89c}$$

Then

$$H_\phi\left(t'+\frac{r}{c}, r\right) = \frac{-\sin\theta}{1-\cos\theta} \, \frac{1}{4\pi r} \int_0^{L'} \frac{\partial}{\partial z'} I\left(t' - \frac{z'}{c}\right) dz' \tag{90}$$

Let $I(t', Z')$ be a finite-slope function, as shown in Fig. 26. Replace the integral in Eq. (90), using equi-valued intervals

$\Delta z'$ given by

$$\Delta z' = L'/m \tag{91}$$

by summation shown below:

$$\int_0^{L'} \frac{\partial}{\partial z'} I(t' - z'/c)\, dz' = \sum_m \frac{\partial}{\partial z'} I(t' - z'/c) \Delta z'$$

$$\approx \left[\frac{I_1 - I(0)}{\Delta z'} + \frac{I_2 - I_1}{\Delta z'} + \cdots + \frac{0 - I_{n-1}}{\Delta z'} \right] \Delta z'$$

Hence

$$\int_0^{L'} \frac{\partial}{\partial z'} I(t' - z'/c)\, dz' \approx -I(0, t') \tag{92}$$

Since I (0,t') is the current at the origin, i.e.,

$$I(z'=0, t') = I(t - r/c) \tag{93}$$

then Eq. (90) reduces to Eq. (88), i.e.,

$$H_\phi(t, r) = \frac{I(t - r/c)}{4\pi r} \cdot \frac{1 + \cos\theta}{\sin\theta} \tag{94}$$

4.2 RADIATION DUE TO STEP-FUNCTION EXCITATION

The above method, based upon Eq. (90), also allows a simple derivation of the radiation field due to current waves with infinite derivatives, such as step-functions, rectangular pulses, or impulses. The transformation from the time derivative of Eq. (81) to the space derivative of Eq. (85) continues to hold, even for these cases, as can be shown by a limiting process going from non-finite slopes to infinite slopes. Thus Eq. (90), based upon Eq. (85), continues to hold.

Consider the traveling-wave step function

$$I(z,t) = I_0\, U(t - z/c) \qquad (95)$$

where U(x) is the standard step function given by U=1 for $x > 0$ and U=0 for $x < 0$. Then Eq. (90) yields

$$H_\phi = \frac{-\sin\theta}{1-\cos\theta}\,\frac{1}{4\pi r}\int_0^{L'} \frac{\partial}{\partial z'}\left(I(0)\,U(t' - z'/c)\right) dz' \qquad (96)$$

The derivative of the step function inside the integral in Eq. (96) yields a delta function, which can be integrated. However, the integral can be evaluated alternatively by first allowing the traveling-wave to have a steep, but finite slope at its leading edge, performing the integration, and passing to the limit of an infinite slope. See Fig. 27. This mathematical process, has real physical significance, since it shows how a hypothetical step function can be approximated as closely as desired by an increasingly steep but finite-slope wavefront. Hence

$$\int_0^{L'} \frac{\partial}{\partial z'}\left(I(0)\,U(t' - z'/c)\right) dz' = \lim_{\Delta z' \to 0} \int_0^{L'} \frac{\partial}{\partial z'} I(z',t')\, dz' \qquad (97)$$

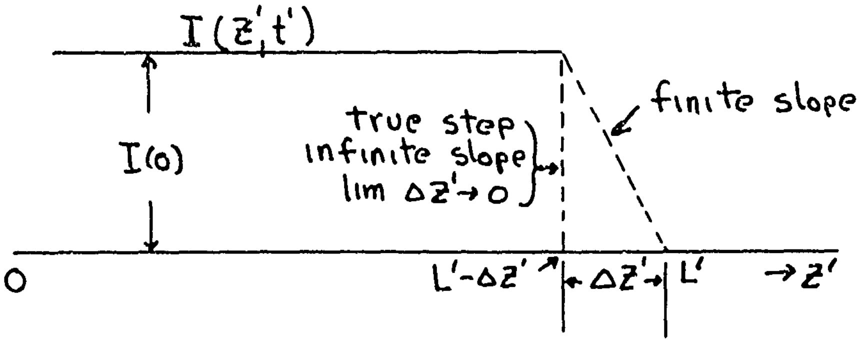

FIG. 27 Step function as a limiting process.

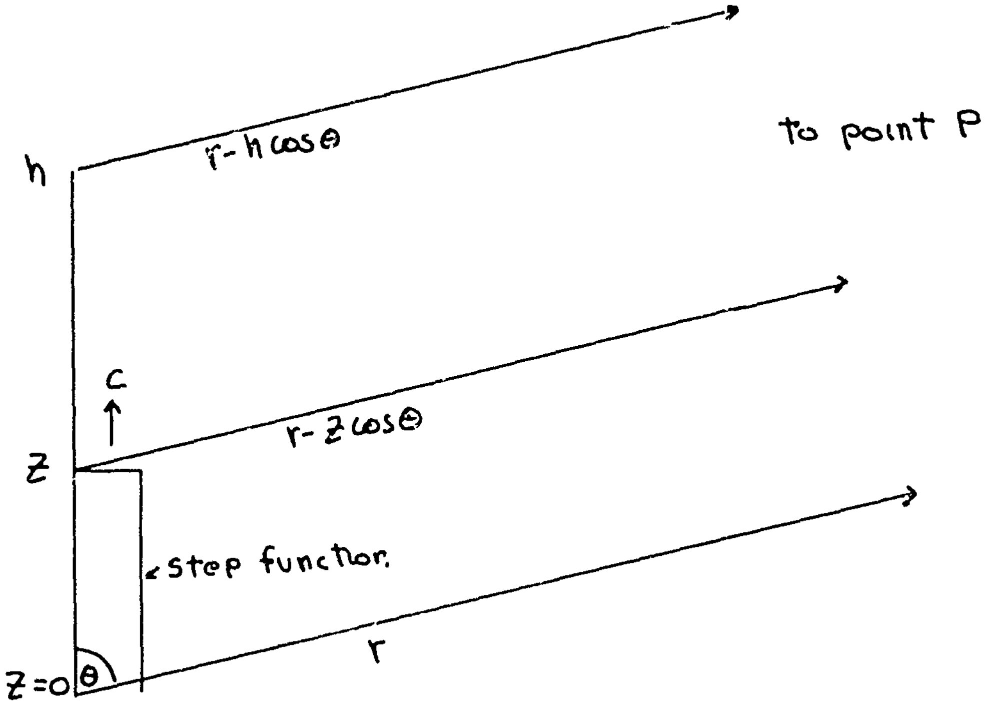

FIG. 28 Geometry for traveling step function.

where $I(Z',t')$ is the finite-slope function shown in Fig. 27. Since

$$\frac{\partial}{\partial z'} I(z',t') = -\frac{I(0)}{\Delta z'} \qquad (L'-\Delta z' \le z' \le L') \tag{98a}$$

$$= 0 \qquad (0 \le z' \le L'-\Delta z') \tag{98b}$$

then

$$\int_0^{L'} \frac{\partial}{\partial z'}\left(I(0)\, U\left(t'-\frac{z'}{c}\right)\right) dz' = \int_{L'-\Delta z'}^{L'} -\frac{I(0)}{\Delta z'}\, dz' = -I(0) \tag{99}$$

Since for a step function I(0) is also the current at the origin 0, then as before, $I(0) = I(Z'=0,t') = I(t-r/c$, and Eqs. 96, 99) yield again Eq. (94).

An alternative derivation of Eq. (94), using the formal mathematical properties of step and delta functions, proceeds directly from Eq. (81). A traveling step function, using Eq. (95), becomes

$$I(z, t-R/c) = I_o U\left(t - \frac{r}{c} - \frac{z}{c}(1-\cos\theta)\right) \tag{100}$$

The derivative in Eq. (81) is

$$\frac{\partial}{\partial t}\, I_o U\left(t-\frac{r}{c}-\frac{z}{c}(1-\cos\theta)\right) = I_o\, \delta\left(t-\frac{r}{c}-\frac{z}{c}(1-\cos\theta)\right) \tag{101}$$

where δ is the standard delta function. Eq. (81) becomes

$$H_\phi = I_o \frac{\sin\theta}{4\pi r c} \int_0^L \delta\left(t-\frac{r}{c}-\frac{z}{c}(1-\cos\theta)\right) dz \tag{102}$$

Substitute*

$$\chi = -\frac{z(1-\cos\theta)}{c} \tag{103}$$

$$dz = -\frac{c}{1-\cos\theta}\,d\chi \tag{104}$$

Eq. (102) becomes

$$H_\phi = \frac{1+\cos\theta}{\sin\theta}\,\frac{I_0}{4\pi r}\int_{-\frac{L}{c}(1-\cos\theta)}^{0}\delta\left(\chi-\left(\frac{r}{c}-t\right)\right)d\chi \tag{105}$$

$$\therefore\ H_\phi = \frac{1+\cos\theta}{\sin\theta}\,\frac{I_0}{4\pi r} \qquad -\frac{L}{c}(1-\cos\theta) \le \frac{r}{c}-t \le 0 \tag{106a}$$

$$= 0 \qquad \text{otherwise} \tag{106b}$$

The interval $-\frac{L}{c}(1-\cos\theta) \le \frac{r}{c}-t \le 0$ can be rewritten as $\frac{r}{c} \le t \le \frac{r}{c}+\frac{L}{c}(1-\cos\theta)$. Using h for L, Eq. (106) becomes

$$H_\phi(r,t) = \frac{1+\cos\theta}{\sin\theta}\,\frac{I_0 U(t-r/c)}{4\pi r} \tag{107}$$

$$\frac{r}{c} \le t \le \frac{r}{c}+\frac{h}{c}(1-\cos\theta) \tag{107b}$$

Thus the initial pulse of the radiation waveform [illegible] step function excitation has the amplitude given by Eq. (106a) and lasts over a duration time interval of $\frac{h}{c}(1-\cos\theta)$ seconds, not $\frac{h}{c}$ seconds. This is discussed further below.

---

*An alternative evaluation of the integral in Eq. (102) is given in Appendix VI.

Since any function can be represented as a sum (superposition) of step functions, and Eq. (107) is the response of the antenna to a step function input, then by the linear superposition theorem (Ref. (33), p. 113), the antenna response to a general current function input I, will be

$$H_\phi(r,t) = \frac{I(t-r/c)}{4\pi r}\;\frac{1+\cos\theta}{\sin\theta} \tag{108a}$$

$$\frac{r}{c} \le t \le \frac{r}{c} + \frac{h}{c}(1-\cos\theta) \tag{108b}$$

Eq. (108) is the same as Eq. (94).

The radiated waveform for an input step function is thus given by Eq. (107). Actually, according to the accelerated-charge radiation concepts, the source of the radiation is in the moving leading edge (step) of this waveform. The distance R between this moving step and P varies, but for P sufficiently far away, R may be replaced in the denominator by r in Eq. (77), which is why r appears in the denominator of Eq. (107).

The radiated field as observed at P commences at time r/c after the instant the step function enters the antenna at the origin 0, and remains constant at the value given by Eq. (107) until the traveling current step wavefront reaches the antenna end Z = h, where a reflected wave is initiated. The field at P remains constant at the value given by Eq. (107) until the radiation from the reflected wave reaches P. Therefore the duration of this initial constant field at P is $\frac{h}{c}(1-\cos\theta)$ and not h/c. This can be seen by examination of the following table and Fig. 28

Event	Location of step wavefront	Local time at antenna	Observed time of arrival of radiation at P
1	entry at origin	0	r/c
2	Z	Z/c	$r/c + Z(1-\cos\theta)/c$
3	reflection at h	h/c	$r/c + h(1-\cos\theta)/c$
4	return to origin	2h/c	$r/c + 2h/c$

In the local time frame at the antenna the timespan between events 3 and 1 is h/c, but to the observer at P, this time span is h/c $(1-\cos\theta)$, as measured by his observations of the received field. This is illustrated by the upper waveform in Fig. 29.

The fact that the radiation-producing step is traveling towards the observer produces the observed time compression factor of $(1-\cos\theta)$. Similarly, the time span between events 4 and 3 is again h/c in the local antenna time, but is h/c $(1+\cos\theta)$ as measured by the observer at P. This is because the radiating wavefront is now traveling away from the observer, resulting in a time expansion factor of $(1+\cos\theta)$. The time span between events 4 and 1 is 2h/c to both an observer at the antenna and at P, as it should be, since both events occur at a fixed point, the origin.

The reflection of an incident current wave I at the open end Z = h is equivalent to starting two waves from that end, each -I(t-h/c). One continues in the +Z direction (supposed to be extended) along with the incident wave, thus canceling the incident wave for all $Z > h$, and the other propagates back in the -Z direction (Ref. 29, p. 298), also (Ref. 30, p. 105). The fields due to these two new waves are as follows (Ref. 30, pp. 104, 105 and Ref. 31, p. 144)

$$+Z \text{ wave: } H_\phi = \frac{-I(t-h/c-r'/c)}{4\pi r'} \frac{1+\cos\theta'}{\sin\theta'} \tag{109}$$

$$-Z \text{ wave: } H_\phi = \frac{-I(t-h/c-r'/c)}{4\pi r'} \frac{1-\cos\theta'}{\sin\theta'} \tag{110}$$

In Eqs. (109,110), r' is the magnitude of the vector $\bar{r}'$ drawn from the end Z = h to P, and θ' is the angle between the +Z axis and $\bar{r}'$. For P sufficiently far, r' may be replaced by r in the denominators, and θ' by θ. The radiation from these two waves thus appears to emanate from the end Z = h.

To calculate the H_ϕ field for step-function excitation of a center-fed dipole, or a monopole over a ground plane, it is necessary to take into account the radiation from both arms of the dipole, or the image in a ground plane. The table below gives the observed magnitudes and time durations of the received radiation pulses due to both up and down-going current waves on each arm, over one time cycle of wave travel, starting with the step at the origin, followed by travel along the antenna, then perfect reflection at the ends Z = $\pm$ h, and return to the origin where perfect absorption (no reflection) is assumed for simplicity. Fig. 29(a) shows the radiation wave-forms for H_ϕ . multiplied by the common factor $(4\pi r/I_0)$. The $\pm$ Z symbols in Fig. 29(a) show the directions of travel of the step on the antenna.

Arm	Number in Fig. 29	Direction of wave travel	$H_\phi\left(\frac{4\pi r}{I_0}\right)$	Duration of radiation pulse
Upper	1	+Z (initial wave)	$\frac{1+\cos\theta}{\sin\theta}$	$0 < t < \frac{h}{c}(1-\cos\theta)$
Upper	2	-Z (reflected wave)	$-\frac{1-\cos\theta}{\sin\theta}$	$\frac{h}{c}(1-\cos\theta) < t < \frac{2h}{c}$
Lower	3	-Z (initial wave)	$\frac{1-\cos\theta}{\sin\theta}$	$0 < t < \frac{h}{c}(1+\cos\theta)$
Lower	4	+Z (reflected wave)	$-\frac{1+\cos\theta}{\sin\theta}$	$\frac{h}{c}(1+\cos\theta) < t < \frac{2h}{c}$

The radiation response due to an impulsive excitation may be found by taking the time derivative of the response due to a step excitation. Thus the radiation due to an impulse, as shown in Fig. 29(b), is obtained by time differentiation of the radiation wave-form shown in Fig. 29(a) due to a step. For $\theta = 90^\circ$ the two inner impulses in Fig. 29(b) merge at h/c to form a negative impulse with amplitude twice that of the two outer positive impulses, as shown in Fig. 30(b). This impulsive response at $\theta = 90^\circ$, as well as for other values of θ, can also be obtained from the response to a rectangular pulse of width τ, by letting τ approach zero. It should be kept in mind that these results assume no reflection at the origin. The case when there is reflection at the origin is considered below.

For $\theta = 90^\circ$, the radiation waveforms of Fig. 29 reduce to those shown in Fig. 30.

If the feeder transmission line impedance is not matched to the surge impedance of the antenna, then the step wavefronts are reflected on return to the origin Z = 0. Let the current reflection coefficient at the origin be κ_o (= 0.72 in Section 3). Further, for the sake of completeness, assume nonperfect reflection at the ends $Z = \pm h$, and let the reflection coefficients there be κ_e (= -0.9 in Section 3). Then the radiation waveforms shown in Fig. 29 must be modified in amplitude and extended in time as shown in Fig. 31. For the sake of definiteness, $\theta = 45^\circ$, $\kappa_o = 0.72$, and $\kappa_e = -0.9$ in Fig. 31.

4.3 RADIATION DUE TO PULSE EXCITATION; COMPARISON WITH A FREQUENCY-DOMAIN ANALYSIS

In this subsection, the radiation due to a rectangular pulse will be calculated using the time domain techniques

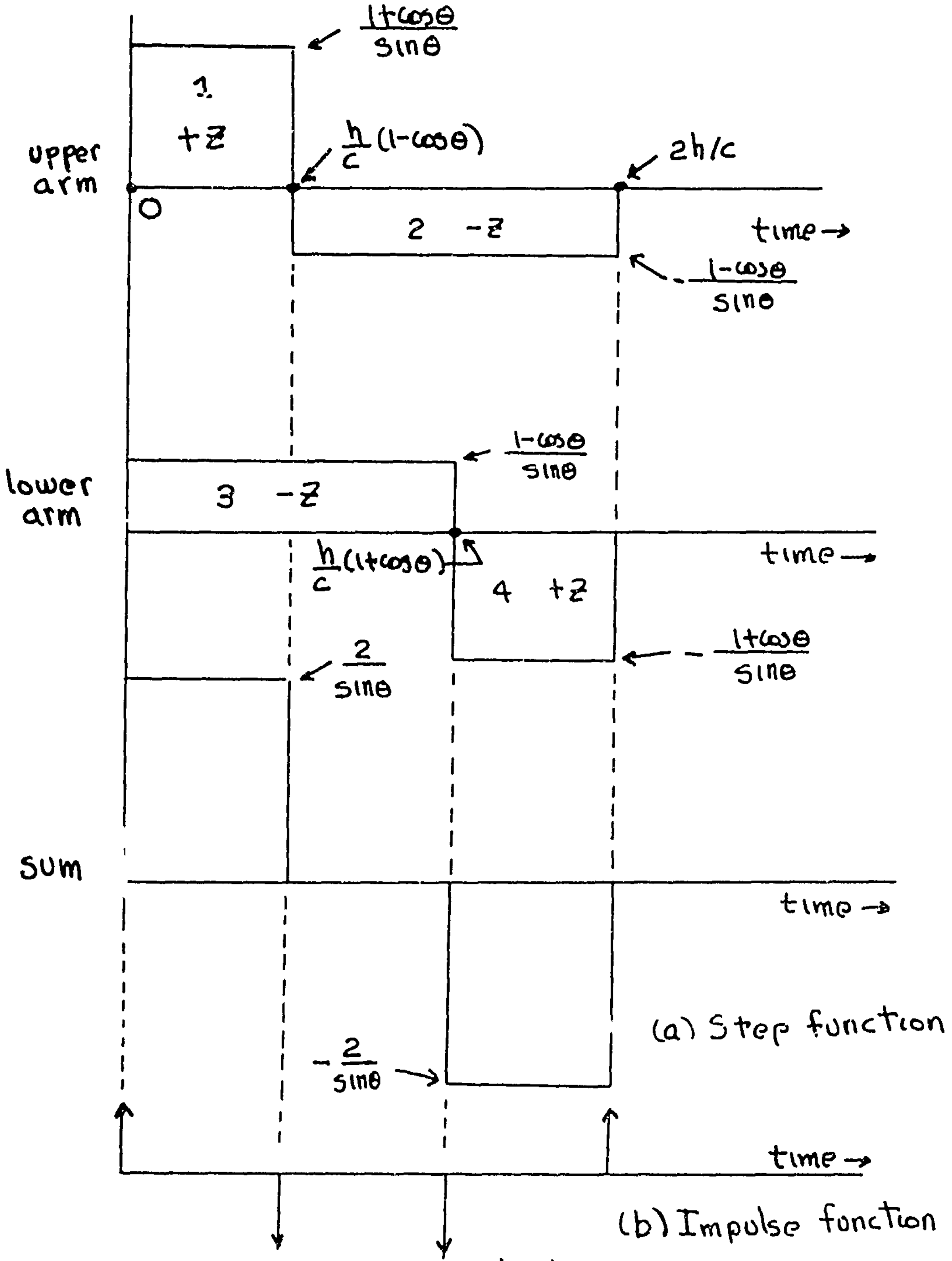

$\frac{1+\cos\theta}{\sin\theta}$
1
+z
upper arm
0
$\frac{h}{c}(1-\cos\theta)$
2h/c
2 -z
time →
$\frac{1-\cos\theta}{\sin\theta}$
lower arm
$\frac{1-\cos\theta}{\sin\theta}$
3 -z
$\frac{h}{c}(1+\cos\theta)$
time →
4 +z
$\frac{1+\cos\theta}{\sin\theta}$
$\frac{2}{\sin\theta}$
sum
time →
$-\frac{2}{\sin\theta}$
(a) Step function
time →
(b) Impulse function

FIG. 29 Radiation $H_\phi(4\pi r/I_o)$ due to step and impulse functions on a dipole, no reflection at input.

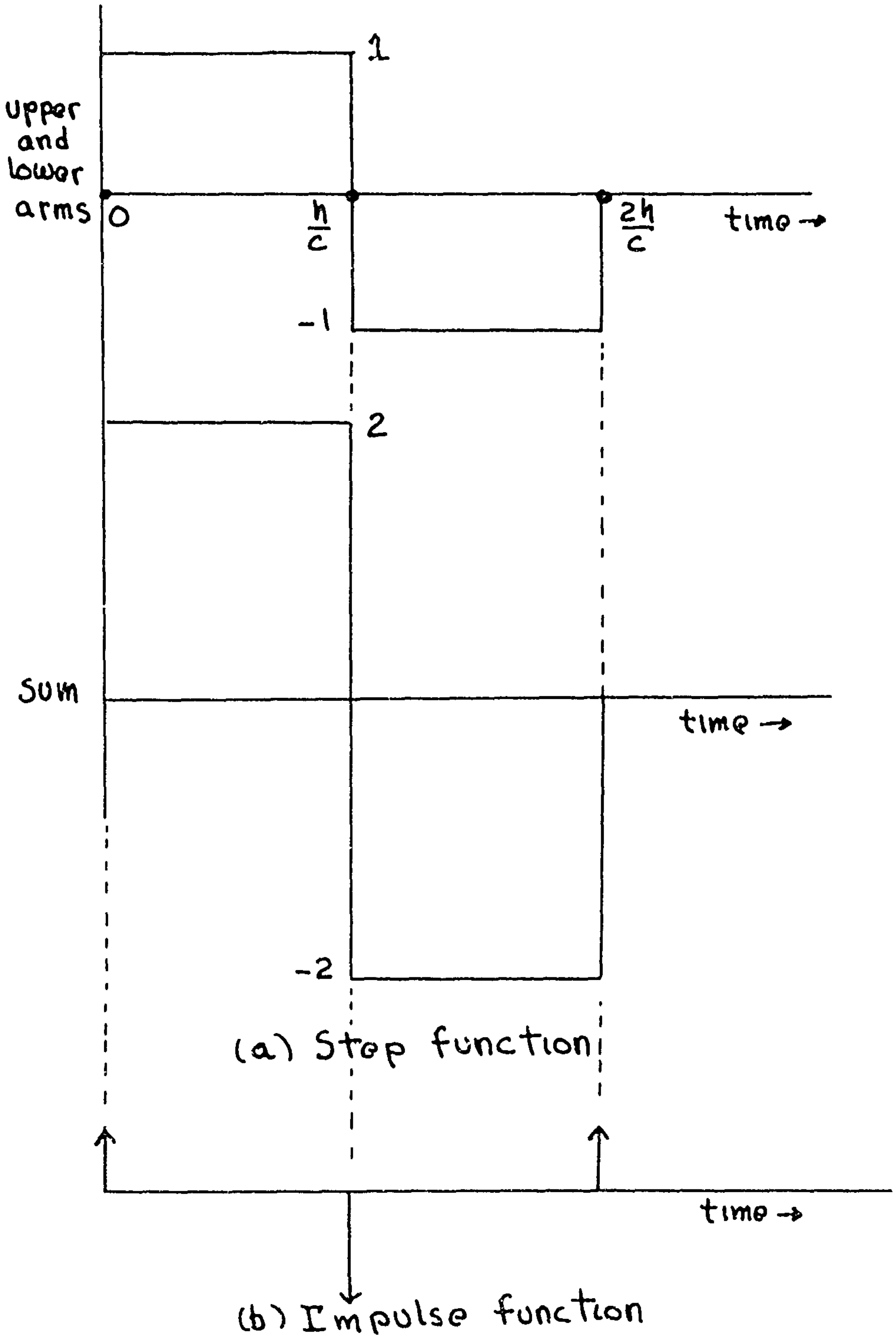

FIG. 30 Radiation $H_\phi(4\pi r/I_0)$ at $\theta = 90°$ due to step and impulse functions on a dipole, no reflection at input.

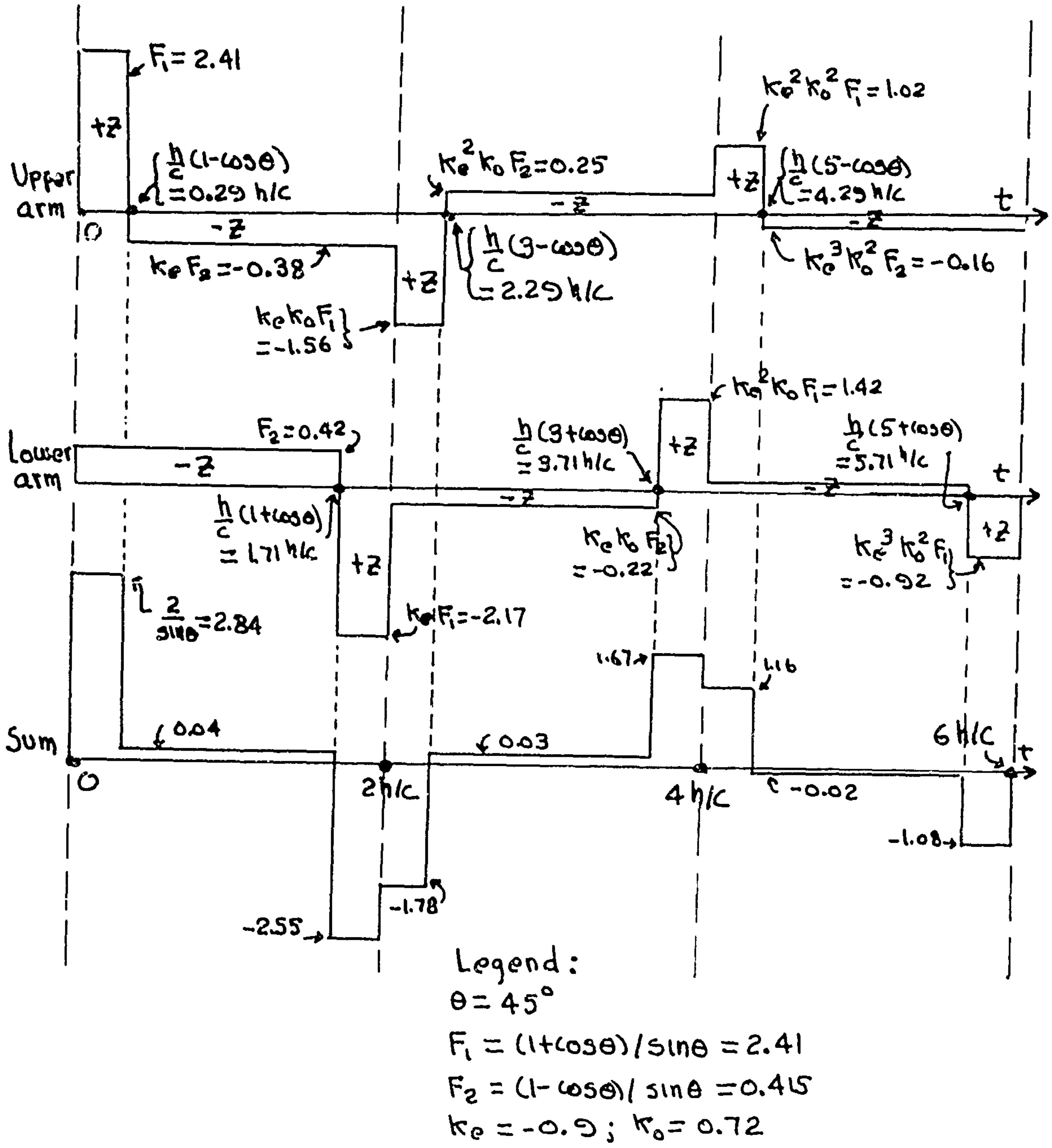

FIG. 31 Radiation $H_\phi(4\pi r/I_o)$ due to step function on a dipole.

discussed in the previous subsections. Let the pulse duration be τ seconds, where τ is less than the travel time h/c on either arm of length h of a center-fed dipole as shown in Fig. 24, or on the length h of a monopole over a ground plane. Such a pulse traveling on each arm of the antenna may be represented before reflection at the ends as the sum of two traveling step functions as follows:

upper arm: $U(t - z/c) - U(t - \tau - z/c)$ (111a)

lower arm: $U(t + z/c) - U(t - \tau + z/c)$ (111b)

The time history of the radiation waveforms due to the first terms (leading edge of the pulse) in Eqs. (111a,111b), including reflections at the ends $Z = \pm h$ and at the origin $Z = 0$ has been illustrated in Fig. 31. The radiation waveform due to the second term (trailing edge of the pulse) has a similar shape, except that the sign is revised due to multiplication by -1, and the waveform is shifted to the right along the time axis by τ, due to the time delay of τ seconds between leading and trailing edges. Addition of the two sets of waveforms thus gives the radiation waveforms for rectangular pulse excitation of a center-fed dipole, with a current reflection coefficient k_σ at the dipole ends, and k_0 at the input ($Z = 0$), for a pulse width less than the antenna travel time h/c.

The details of this time-domain calculation have been carried out, but are not repeated here, to permit comparison with an example given in Ref. (34). In Ref. (34), the center-driven cylindrical antenna has a length to radius ratio $\frac{h}{a} = 904$, with a source excitation pulse of trapezoidal shape with a base width of about 0.55 h/c, a flat top width of about 0.26 h/c, and a width of about 0.38 h/c at the 50 percent peak amplitude point. The transmission line has a 50 ohm impedance. To definitize the comparison, the following numerical values were assumed:

$$\begin{aligned} \tau &= 0.4\, h/c \\ k_e &= -0.9 \\ k_o &= \frac{300-50}{300+50} = 0.12 \end{aligned} \tag{112}$$

The patterns in Ref. (34) are calculated for the far-zone field using an inverse Fourier transform of the response to sinusoidal excitation $e^{j\omega t}$. A comparison between these patterns as given in Ref. (34), and those calculated as explained above, assuming a rectangular pulse of width τ = 0.4 h/c are presented in Fig. 32, for different values of polar angle θ. The patterns of Ref. (34), as shown in Fig. 32 have been simplified in that small amplitude oscillations have been omitted, however the indicated amplitudes, widths and times of the principal pulses follow the values given in Ref. (34) as closely as can be read from the curves presented therein. The time-domain results have been normalized so that the first pulse for $\theta = 90^\circ$ (broadside) has the same amplitude (=1.55) as the corresponding pulse in Ref. (34), thereby affording ready comparison.

Inspection of the two sets of curves in Fig. 32 shows a fairly reasonable agreement, considering the relatively approximate nature of the time-domain calculations, except as θ approaches small angles. For $\theta = 90^\circ$, 70°, 60°, and 45°, the agreement is fairly good as measured by the number of pulses, their amplitudes, widths, and positions. For example, as θ decreases, the amplitude of the first pulse increases approximately as predicted by the $(1+\cos\theta)/\sin\theta$ factor of Eq. (107a), until $\theta = 20^\circ$. Further, using time-domain analysis, it is simple to show that as θ decreases from 90 , the received pulse width remains constant at τ until the angle θ is reached at which the quantity $(1-\cos\theta)h/c$ becomes less than τ. For θ less than this angle, the pulse width, for an ideal rectangular pulse, becomes $(1-\cos\theta)h/c$. For $\tau = 0.4\ h/c$, this angle is 53°. Inspection of the curves given in Ref. (34) shows that the received pulse width begins to decrease for θ around 55°, in agreement with the time-domain prediction, and continues to decrease as θ decreases, again in agreement with the time-domain analysis.

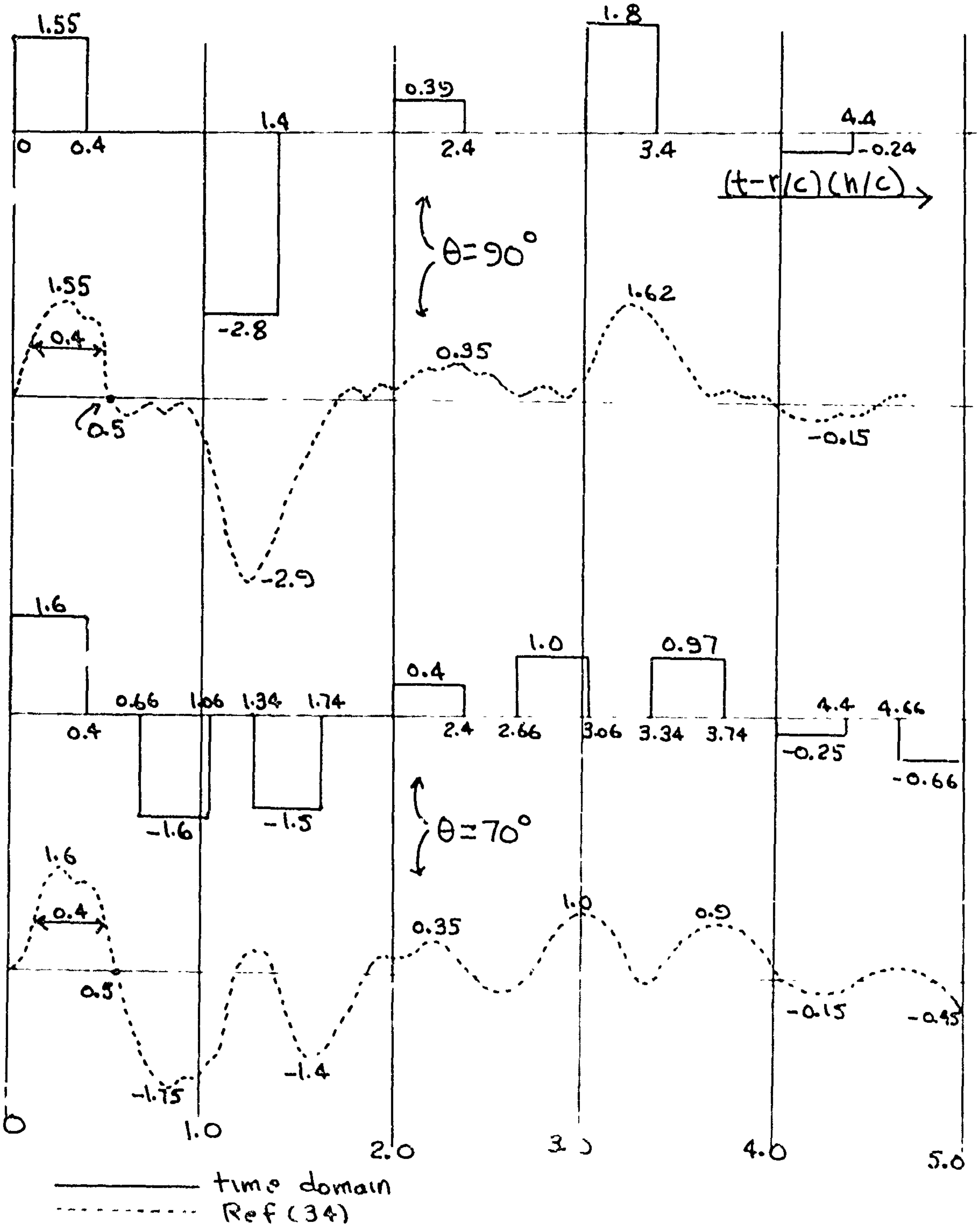

FIG. [illegible] [illegible] [illegible] $\theta = 90^\circ, 70^\circ$.

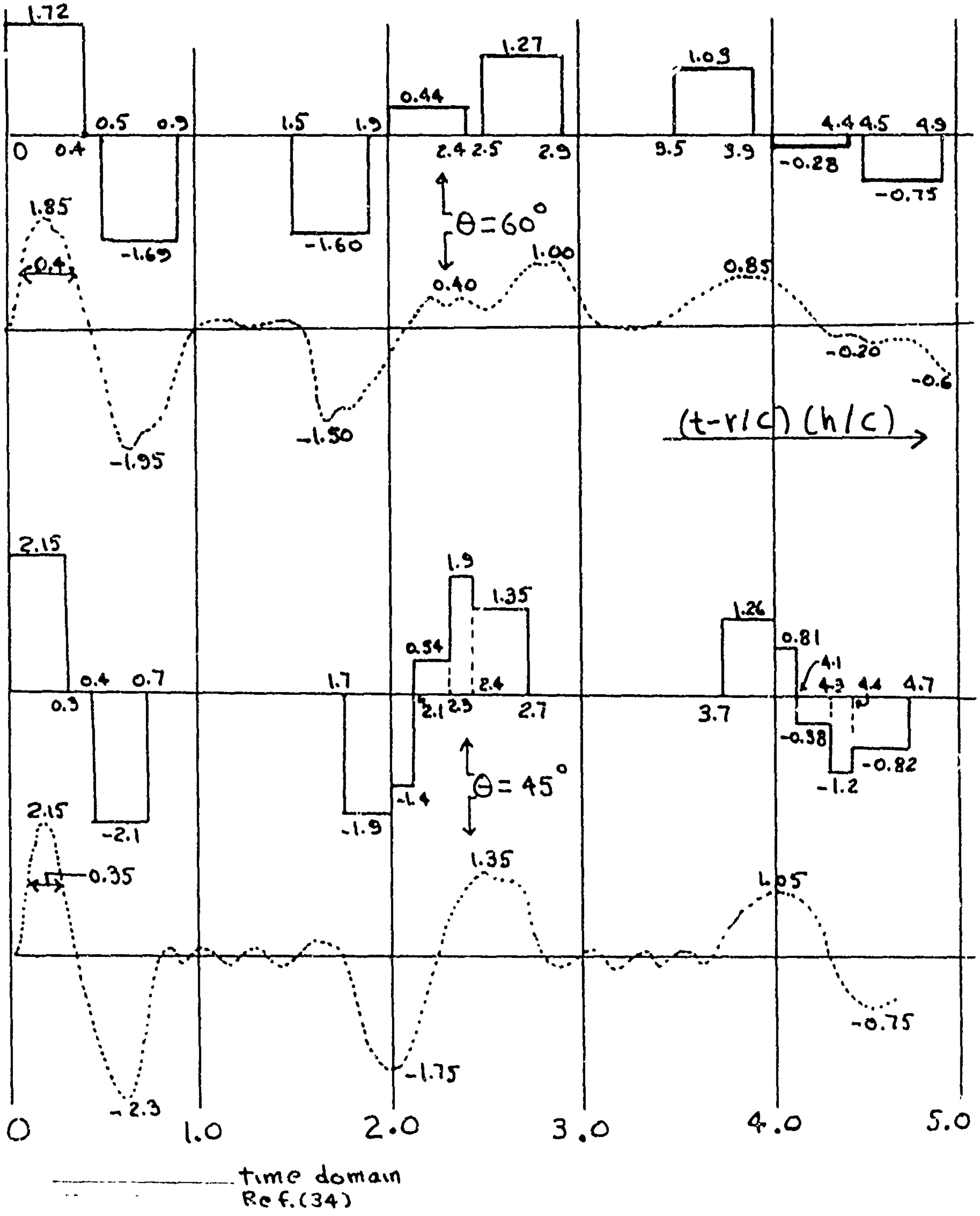

FIG. 32(1) Radiation waveforms for θ= 60°, 45° .

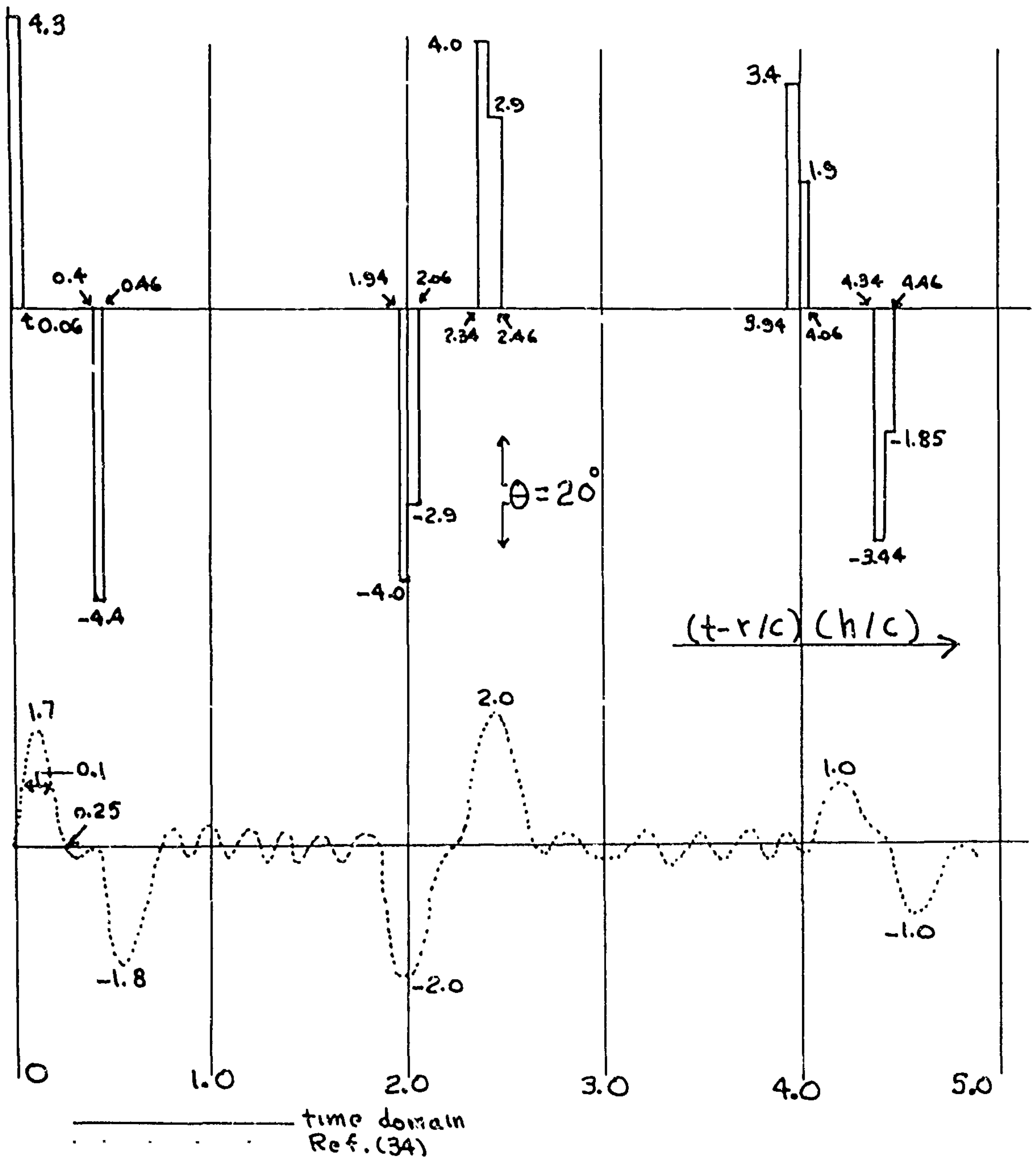

FIG. 32(c) Radiation waveforms for θ = 20°.

However, it is clear that there is serious disagreement between the two sets of results for $\theta \leq 20^\circ$. The time-domain analysis as presented in this report, which leads to equations such as Eqs. (70) and (107), which agree with previously published work (Refs. 29-32 incl.), predicts a field which continues to increase with decreasing θ as

$$\lim_{\theta \to \text{small}} \frac{1+\cos\theta}{\sin\theta} = \frac{2}{\theta} \tag{113}$$

On the other hand, while the frequency-domain analysis of Ref. (34), presents curves which show a field which does increase approximately as $(1+\cos\theta)/\sin\theta$, from 90° to 40°, the $\theta = 20^\circ$ curve distinctly shows a field which has begun to decrease again. The disagreement arises in the singular behaviour predicted by Eqs. (70,107,113) for the field which increases without limit as θ approaches zero. This behaviour is discussed in more detail in subsection 4.4 below.

However, it is stated in advance that while this discussion shows that the total radiated energy of the pulsed dipole antenna remains finite, and that the fields do not go to infinity as $\theta \to 0$ for an infinite-length antenna, nevertheless the disagreement noted above for small values of θ remains unresolved. Experimental investigation of the fields of a pulsed dipole for θ = small might help to resolve this point.

4.4 DISCUSSION OF PULSED WIRE-ANTENNA RADIATION, ESPECIALLY AT SMALL VALUES OF θ

Eqs. (70,71) have been derived in this report for a current wave traveling in the +Z direction on a finite-length linear antenna, such as a dipole, the effect of the ends not being included. The same equations are derived using the retarded vector potential $\bar{A}$ for a finite-length antenna by Ross et al (Ref. 31, pp. 17, 117) and also for an infinite-length antenna using a Green's function by Ross et al (Ref. 31, p. 142). The effect of the ends is accounted for by a reflected current wave by Ross et al (Ref. 32, p. 115). The same equations were presented without derivation by Manneback (Ref. 29, p. 294) for an infinite-length wire; he showed that these expressions satisfy Maxwell's equations, neglecting $1/r^2$ terms compared to $1/r$ terms, and that for θ small, Eqs. (70,71) reduce to the expected fields E_θ, H_ϕ of a plane electromagnetic wave traveling at velocity c along a wire. Manneback also took into account end effects by partial or total reflection at the ends; see Eqs. (109,110). Schelkunoff (Ref. 30) shows that Eqs. (70,71) are really exact, including $1/r^2$ terms, for an infinite-length wire; he also accounts for end effects by equations such as Eqs. (109,110).

The purpose of the above discussion is to show that the radiation equations for finite-length antennas are the same as for the infinite-length antennas, except that provision must be made for end effects. For infinite-length antennas there are no end discontinuities; the fields in the direction of the antenna (small θ) travel with the current wave along the antenna at velocity c. For the finite-length case, the ends represent a discontinuity, such as partial or total reflection, or absorption. The radiation from the finite-length antenna is thus calculated using the same equations as for the infinite-length case, modified by appropriate reflection coefficients for terminal conditions, with due regard to the direction of current wave travel and time delays (e.g., Eqs. (109,110)).

For an infinite-length antenna, Eqs. (70,71) present no special problems as $\theta \to 0$. Ross et al (Ref. 31, p. 137) show that Ampere's law in the form

$$\oint \bar{H} \cdot d\bar{l} = I \tag{114}$$

is satisfied by Eq. (70) for $\theta \to 0$. See Fig. 33. Thus

$$l = r \sin\theta$$

$$\oint \bar{H}(\bar{r},t) \cdot d\bar{l} = H_\phi(r,t) 2\pi l = H_\phi(r,t) 2\pi r \sin\theta$$

$$= \frac{I(t-r/c)}{4\pi r} \cdot \frac{1+\cos\theta}{\sin\theta} \cdot 2\pi r \sin\theta$$

Using $1+\cos\theta \rightarrow 2$ and $r \rightarrow z$ as $\theta \rightarrow 0$,

$$\oint \bar{H}(\bar{r}_1 t) \cdot d\bar{l} = I(t - z/c) \tag{115}$$

Thus the line integral of $\bar{H}$ near the wire at distance Z from the origin, at time t, is the current that was at the origin at time Z/c ago. Since the current is assumed to travel undispersed along the wire at velocity c, this is exactly the current that is now (at time t) at Z, and has reached the loop area. It is pointed out that Eq. (114) is not the complete form of Ampere's law, which is, for stationary boundaries,

$$\oint \bar{H} \cdot d\bar{l} = \int_S \bar{J} \cdot d\bar{S} + \varepsilon \frac{\partial}{\partial t} \int_S \bar{E} \cdot d\bar{S} \tag{116}$$

The first term in the RHS of Eq. (116) is the conduction current, and the second term is the displacement current. However, as $\theta \rightarrow 0$, and the surface of the wire is approached, $d\bar{S} \rightarrow dS\,\hat{a}_z$, the radial component (Z-component) of $\bar{E} \rightarrow 0$, and therefore $\bar{E} \cdot d\bar{S} \rightarrow 0$. Thus Eqs. (114,115) hold as $\theta \rightarrow 0$. Schelkunoff (Ref 30, p. 109) arrives at the same results using a conductor which is a semi-infinite cone of half-angle ψ . As $\theta \rightarrow \psi$ (surface of the cone), Ampere's law in the form of Eq (114) is invoked, the radial component of $\bar{E}$ being zero at the surface. See Fig. 34.

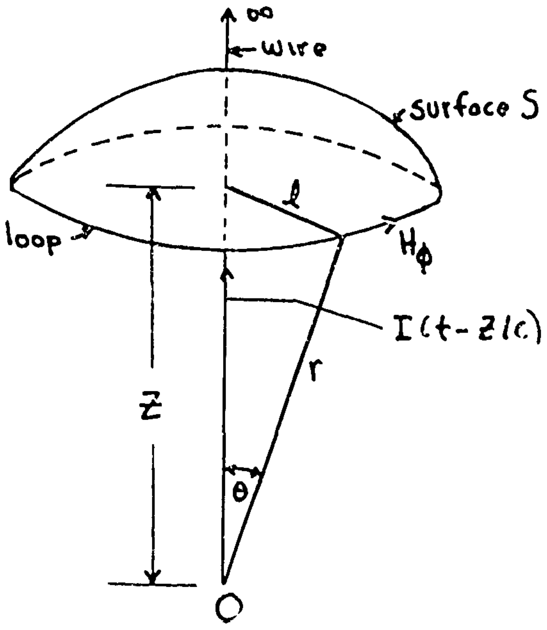

FIG. 33 Line integral of H for semi-infinite wire.

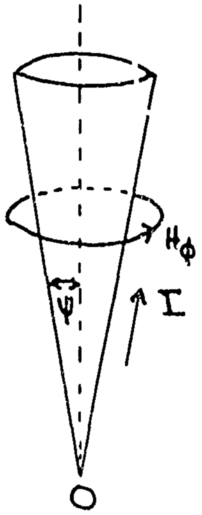

FIG. 34 Line integral of H for semi-infinite cone.

The foregoing discussion indicates that as far as calculation of the fields due to traveling waves on infinite wires is concerned, including the case of $\theta \to 0$, there is agreement among the various writers cited. Fig. 35 illustrates how the fields wavefront travels with the current wave along the antenna at velocity c. Two wavefronts are shown at time t. The leading wavefront is due to a current element $I_1 dz$ now at $z = r_1$, and formerly at the origin at time $t - r_1/c$, the second wavefront is due to a current element $I_2 dz$ now at $z = r_2$, and formerly at the origin at time $t - r_2/c$.

For a finite-length antenna, Fig. 36 illustrates how the radiation field at a far-field point P varies in time. Assume a step-function excitation. The initial radiation to reach P is due to the current wave traveling in the +Z direction. At time $h(1-\cos\theta)/c$ later, the radiation from the reflected current wave arrives at P. At exactly $\theta = 0$, the two wavefronts are just tangent. Calculation of the resultant field at $\theta = 0$ is beset with a number of difficulties such as the boundary conditions at the end $Z = h$, the effects of a finite wire diameter, the discontinuity experienced by the traveling field wavefront as it moves off the end of the wire into space, and the zero duration of this field. However, at non-zero values of θ, it is clear that the radiation that arrives first at P is due only

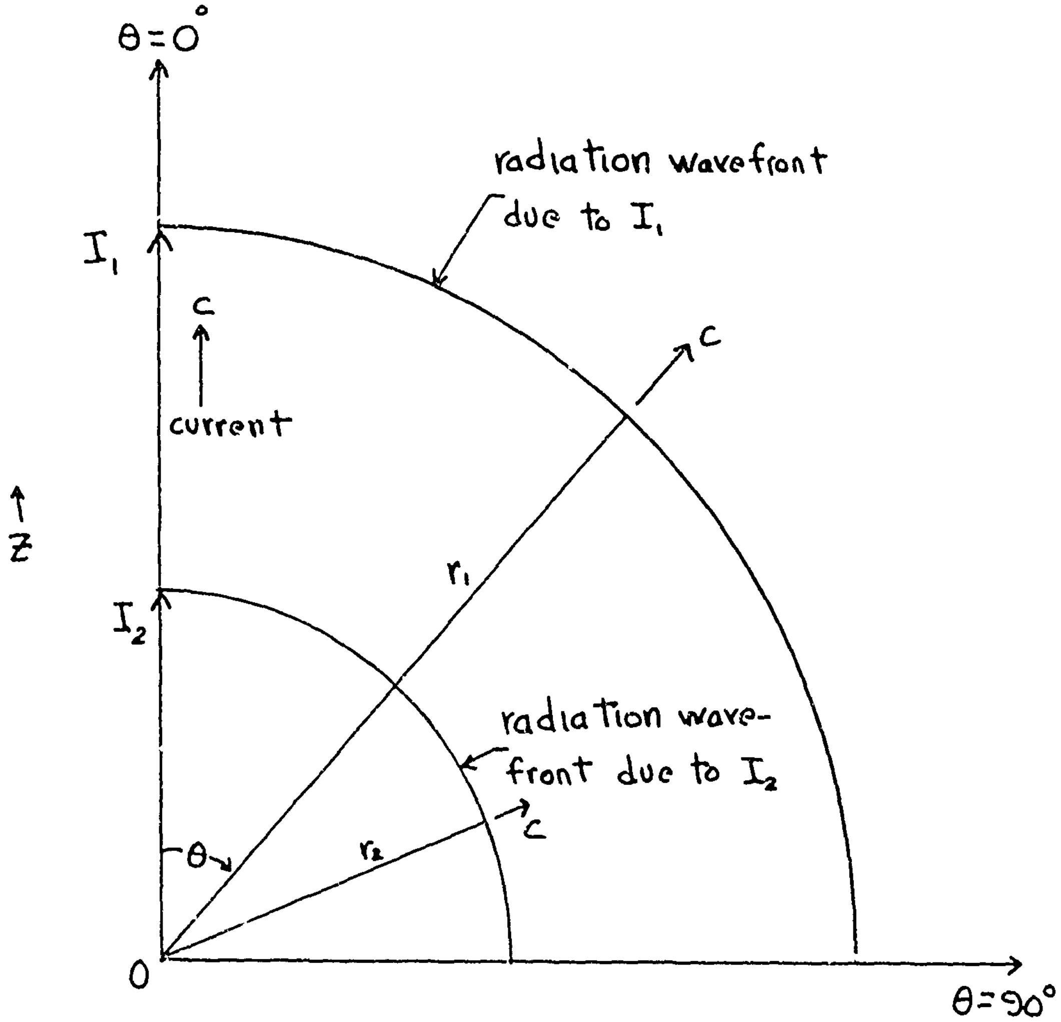

FIG. 35 Currents and wavefronts for current wave on semi-infinite wire.

to the initial current wave traveling in the +Z direction; the radiation change due to arrival of the current wave at the end h reaches P at time $h(1-\cos\theta)/c$ later. Hence during the time interval $0 \le t \le h(1-\cos\theta)/c$, the current step has not yet reached the antenna end, and the radiation at P must be independent of what occurs at Z = h. Therefore, during this non-zero time interval, unaffected as yet by end conditions, the field is given by Eq. (107a) for a step waveform, and by Eq. (108a) for a general current waveform. All the cited references (Ref. 29-32 incl.) agree on this form of the radiation equation. Hence the bothersome question remains as to the behaviour of this field for small θ as $2/\sin\theta$, which disagrees with the calculations of Ref. (34).

In terms of field amplitude or power per unit area, the linear pulsed antenna appears to act as an end-fire antenna. Ordinary (sinusoidal time variation) traveling wave linear antennas also act to tilt the radiation pattern in the forward direction, the tilt increasing with the ratio of antenna length to wavelength. However, such antennas are terminated at the ends so as to eliminate standing waves, i.e., an absorption termination instead of an open end. Hence any comparison with ordinary traveling wave antennas must be treated with caution.

In terms of radiated energy, some interesting conclusions are easily arrived at for the pulsed dipole antenna. Assume step excitation, for simplicity, and perfect end reflection. For one cycle of current travel on the antenna $0 \le t \le 2h/c$, Fig. 29(a) shows the radiated field, for $\theta \le \pi/2$. For $\frac{\pi}{2} \le \theta \le \pi$, it is simple to show that the total radiation waveform remains unchanged in form, consisting of two pulses as shown of the same amplitude and time duration as for $\theta \le \pi/2$. Hence the radiated energy per unit area (two pulses) at any angle θ is

$$\mathcal{E}(\theta) = \int_0^{2h/c} \sqrt{\mu/\varepsilon}\, H^2 dt = 2\sqrt{\frac{\mu}{\varepsilon}}\, \frac{4 I_0^2}{(4\pi r)^2 \sin^2\theta}\, \frac{h}{c}(1-|\cos\theta|)$$

$$\therefore\ \mathcal{E}(\theta) = \sqrt{\frac{\mu}{\varepsilon}}\ \frac{I_0^2}{2\pi^2 r^2}\ \frac{h}{c}\ \frac{1}{1+|\cos\theta|} \qquad (117)$$

$$\frac{\mathcal{E}(0)}{\mathcal{E}(\pi/2)} = \frac{1}{2} \qquad (118)$$

Thus the energy per unit area is finite at all angles. Also the broadside $(\theta = 90^\circ)$ energy per unit area is twice that in the endfire directions $(\theta = 0^\circ, 180^\circ)$, decreasing smoothly from the broadside maximum. The singular behaviour in radiated amplitude and power as $\theta \to 0^\circ, 180^\circ$ is not manifested in the energy. In terms of radiated energy, the antenna does not act as an end-fire type.

The total energy $\mathcal{E}_t$ radiated in one cycle $0 \le t \le 2h/c$ by a step excitation on a dipole antenna is found by integrating Eq. (117) over the surface of a sphere. This leads to

$$\mathcal{E}_t = \sqrt{\frac{\mu}{\varepsilon}}\,\frac{I_0^2}{2\pi^2}\,\frac{h}{c}\,2\int_0^{2\pi}\!\!\int_0^{\pi/2} \frac{r^2 \sin\theta\, d\theta\, d\phi}{r^2(1+\cos\theta)}$$

Using

$$\int_0^{\pi/2} \frac{\sin\theta\, d\theta}{1+\cos\theta} = \ln 2$$

$$\mathcal{E}_t = I_0^2 \sqrt{\frac{\mu}{\varepsilon}}\,\frac{h}{c}\,\frac{2}{\pi}\ln 2 \qquad (119)$$

Hence the total radiated energy is finite.

Before leaving the subject of the singular behaviour of the field amplitudes as $\theta \to 0$, it is pertinent to note what happens if the velocity of propagation v_p of the traveling current wave along the antenna is very slightly less than c. Then the factor of $(1+\cos\theta)/\sin\theta = \sin\theta/(1-\cos\theta)$ in Eq. (107a) is replaced by $\beta\sin\theta/(1-\beta\cos\theta)$, where $\beta \equiv v_p/c < 1$ (Ref. 32, p. 123).

The significance of this is that the "infinity catastrophe" at $\theta=0$ disappears. The field now goes to zero at $\theta=0$, and has a maximum at $\theta_m=\cos^{-1}\beta$ given by $\beta/\sin\theta_m$. For example, for $\beta=0.98$, $\theta_m=11.5^\circ$. It is only a conjecture if some effects of this nature are indeed taking place on bare wire antennas. The discussion of propagation of sharp wavefronts on lossy lines in Appendix III indicates that the definition of an effective velocity of propagation depends upon the details of build-up of the wavefront at a point along the antenna.

SECTION 5

RADIATION FROM LOOP ANTENNAS

5.1 INTRODUCTION

In this section, the radiation of a circular loop antenna is examined. Two examples are given. The first is a loop driven with sinusoidal time-varying excitation, for which the solution is well-known. The radiation field is derived from the accelerated charge Eqs. (V-7,32), which for a linear element dZ lead to Eq. (74). This example illustrates that these equations produce correct results for known cases. The second example is a loop driven by pulsed excitation, for which a solution has recently been made available using both frequency and time-domain analysis (Ref. 35). The time-domain analysis is examined to verify that its formulation in the time domain agrees with that developed in this report.

5.2 SINUSOIDAL TIME-VARYING EXCITATION

The loop is taken in the XY-plane, with radius b sufficiently small compared to wavelength so that the current can be assumed to be constant around the loop, to a good approximation (Ref. 22, p. 56). In Appendix V it is shown that Eq (V-7), for the radiation field of an accelerated charge moving at low relativistic velocities, becomes Eq. (V-32). For a loop, differential length dZ is replaced by the differential circumferential length

$$d\bar{L} = dL\,\hat{a}_{\phi}' = b\,d\phi'\,\hat{a}_{\phi}' \tag{120}$$

See Fig. 37. The coordinates of the current source element $\overline{dL}$ are ($b, \pi/2, \phi'$), and those of the field point P are (r, θ, ϕ). Eq. (V-32) becomes

$$d\bar{H} = \frac{1}{4\pi c}\left[\frac{\dot{I}\,d\bar{L}\times\hat{n}}{R}\right]_{ret} \tag{121}$$

For point P in the far field, R may be replaced by r in the denominator of Eq. (121). Using

$$\left[\dot{I}\right]_{ret} = \frac{\partial}{\partial t} I(t-R/c) \tag{122}$$

$$I = I_0 e^{j\omega t} \tag{123}$$

it follows that

$$\frac{\partial}{\partial t} I(t-R/c) = j\omega I_0 e^{-jkR} e^{j\omega t} \tag{124}$$

Hence

$$d\bar{H} = \frac{j\omega I_0 e^{-jkR}}{4\pi c r}\, d\bar{L}\times\hat{n}\, e^{j\omega t} \tag{125}$$

For P in the far field, $\bar{R}$ is essentially parallel to $\bar{r}$, so unit vector $\hat{n}$ may be replaced by unit vector $\hat{a}_r$, and

$$R \approx r - b\cos\psi \tag{126}$$

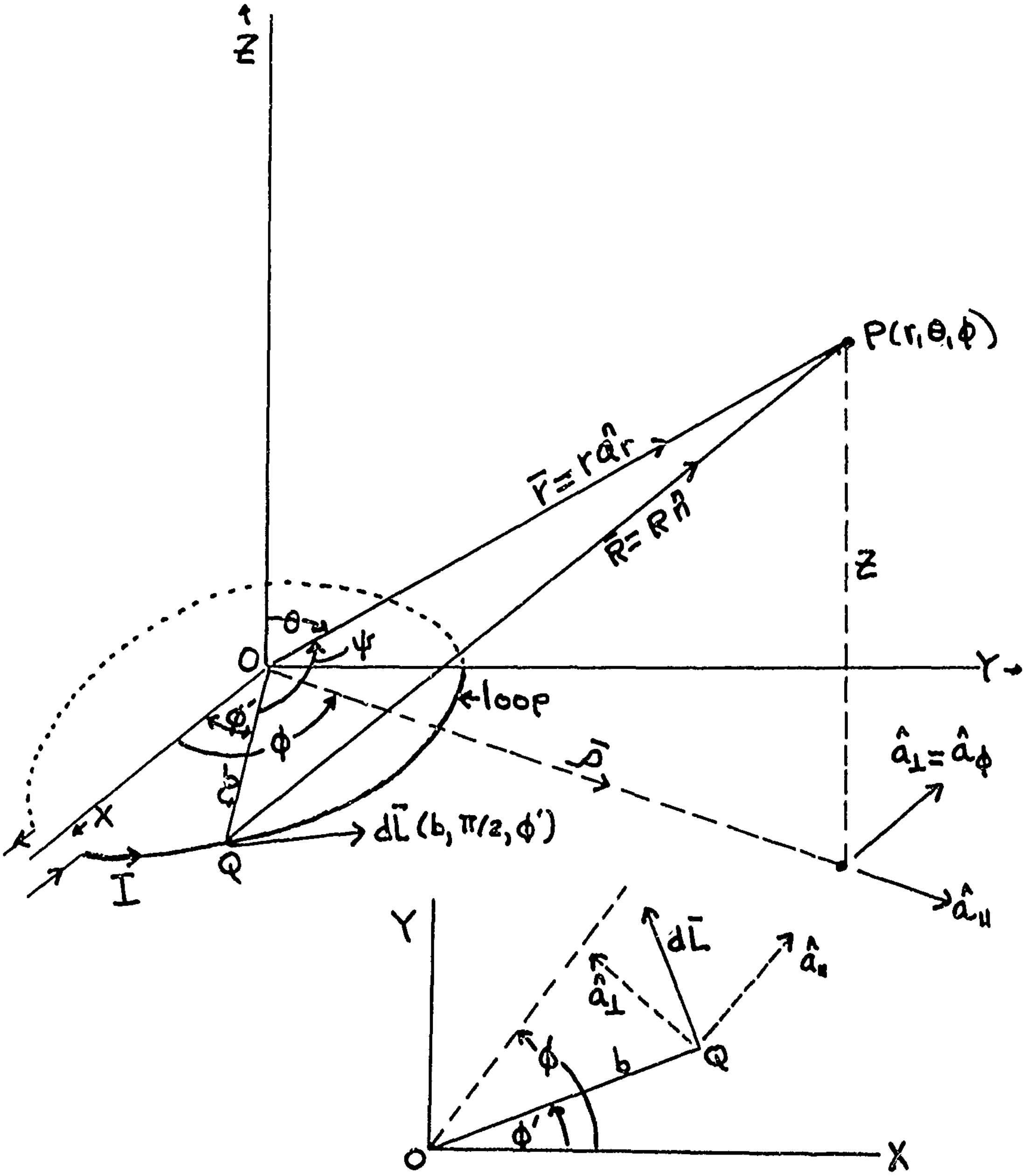

FIG. 37 Loop geometry.

where, from spherical trigonometry

$$\cos\psi = \cos(\phi-\phi')\sin\theta \tag{127}$$

Hence

$$e^{-jkR} = e^{-jkr} e^{jkb\cos\psi} = e^{-jkr} e^{jkb\cos(\phi-\phi')\sin\theta} \tag{128}$$

By hypothesis, $kb = 2\pi b/\lambda \ll 1$, hence

$$e^{-jkR} \approx e^{-jkr}(1+jkb\cos(\phi-\phi')\sin\theta) \tag{129}$$

Resolving $d\bar{L}$ along the directions $\hat{a}_{\parallel}$ parallel to $\bar{\rho}$, the projection of $\bar{r}$ on the XY-plane, and $\hat{a}_{\perp}$ $(=\hat{a}_{\phi})$ perpendicular to $\bar{\rho}$,

$$d\bar{L} = dL\left[\cos(\phi-\phi')\,\hat{a}_{\perp} + \sin(\phi-\phi')\,\hat{a}_{\parallel}\right] \tag{130}$$

Substituting Eqs. (120,129,130) into Eq. (125) and integrating over the variable ϕ',

$$\bar{H} = \frac{j\omega I_o}{4\pi c r} e^{-jkr} e^{j\omega t}\, b \int_0^{2\pi} \left[1+jkb\sin\theta\cos(\phi-\phi')\right] \cdot \left[\cos(\phi-\phi')\,\hat{a}_{\perp} + \sin(\phi-\phi')\,\hat{a}_{\parallel}\right] d\phi' \times \hat{a}_r$$

$$\bar{H} = \frac{j\omega I_o b}{4\pi c r} e^{-jkr} e^{j\omega t} (jkb\pi\sin\theta)(\hat{a}_{\perp} \times \hat{a}_r)$$

Using loop area $A = \pi b^2$, $k = \omega/c$, magnetic moment $M_o \equiv I_o A$, and $\hat{a}_\perp = \hat{a}_\phi$,

$$\bar{H} = \frac{-M_0 k^2}{4\pi r} \sin\theta \, e^{j(\omega t - kr)} \hat{a}_\theta \tag{131}$$

which is a well-known result (Ref. 21, p. 95).

5.3 PULSE EXCITATION

In Ref. (35) the loop is as shown in Fig. 37. The $\bar{E}$ field is calculated in (Ref. 35) using the radiation field of an infinitesimal dipole given by Sommerfeld. Using the equations developed in this report, $\bar{E}$ is given by Eqs. (II-34, V-37) as

$$\bar{E} = \sqrt{\mu/\epsilon}\,(\bar{H} \times \hat{n}) \tag{132}$$

Hence Eq. (121) can be used, to yield

$$d\bar{E} = \frac{1}{4\pi\epsilon c^2}\left[\frac{(\dot{\bar{I}}\, d\bar{L} \times \hat{n})}{R} \times \hat{n}\right]_{ret} \tag{133}$$

From Eq. (V-22) for the differential current element $\bar{h} = d\bar{L}$,

$$\frac{\partial^2}{\partial t^2} \bar{P}(t - R/c) = \dot{\bar{I}}(t - R/c)\, d\bar{L} \tag{134}$$

In the far field R is replaced by r (except in the arguments of $\bar{P}$ or $\bar{I}$), and since $\bar{R}$ and $\bar{r}$ are parallel, then $\hat{n} = \bar{r}/r = \hat{a}_r$. Hence Eq. (133) can be written as

$$d\bar{E} = \frac{1}{4\pi\epsilon c^2 r^3}\left\{\frac{\partial^2}{\partial t^2} \bar{P}(t - R/c) \times \bar{r}\right\} \times \bar{r} \tag{135}$$

Eq. (135) is identical to the equation for $d\bar{E}$ developed in (Ref. 35, p. 28).

In Ref. (35) the source and field point coordinates are $(b, \frac{\pi}{2}, \phi_L)$ and (R_0, θ_0, ϕ_0) respectively, whereas here they are $(b, \frac{\pi}{2}, \phi')$ and (r, θ, ϕ). The distance between source and field points is r in Ref. (35), whereas here it is R. Taking this into account, Eq. (135) is the same as that used in Ref. (35) (p. 28, Eq. (4)).

Returning to Eq. (133), using Eq. (130), $\hat{a}_\perp = \hat{a}_\phi$, $\hat{n} = \hat{a}_r$, there is obtained

$$(d\bar{L} \times \hat{n}) \times \hat{n} = -dL\left[\cos(\phi-\phi')\hat{a}_\phi + \sin(\phi-\phi')\cos\theta \, \hat{a}_\theta\right] \tag{136}$$

From Eq. (133), $d\bar{E}$ has two components

$$dE_\theta = -\frac{1}{4\pi\varepsilon c^2 r} \frac{\partial}{\partial t} I(t-R/c) \, dL \sin(\phi-\phi')\cos\theta \tag{137a}$$

$$dE_\phi = -\frac{1}{4\pi\varepsilon c^2 r} \frac{\partial}{\partial t} I(t-R/c) \, dL \cos(\phi-\phi') \tag{137b}$$

In Ref. (35), the excitation is a pulse applied to the input terminals shown in Fig. 37. Similar to the case of the linear dipole discussed in subsection 4.3, this produces a current pulse traveling circumferentially on each arm of the loop, in opposite ϕ' directions. Each pulse is represented, as in subsection 4.3, as the sum of two separated step functions, resulting in four step functions in all. It will suffice, for the purposes of this report, to investigate the radiation due to one step function; the detailed results of the superposition of the four step functions is given in Ref. 35.

A step function of current traveling at linear velocity c on a loop is given by an equation similar to Eq. (95), with Z replaced by circumferential length $L = b\phi'$. Thus

$$I = I_0 \, U\left(t - \frac{b\phi'}{c}\right) \tag{138}$$

Using Eqs. (126,127,138)

$$R = r - b\cos(\phi-\phi')\sin\theta \tag{139}$$

$$I(t-R/c) = I_0 \, U\left(t - \frac{r}{c} - \frac{b}{c}\left[\phi' - \cos(\phi-\phi')\sin\theta\right]\right) \tag{140}$$

$$\therefore \frac{\partial I(t-R/c)}{\partial t} = I_0 \, \delta\left(t - \frac{r}{c} - \frac{b}{c}\left[\phi' - \cos(\phi-\phi')\sin\theta\right]\right) \tag{141}$$

Substituting Eq. (141) into Eq. (137), using $dL = b\,d\phi'$, and integrating over the variable ϕ' gives

$$E_\theta = -\frac{b\cos\theta \, I_0}{4\pi\varepsilon c^2 r}\int_0^{2\pi} \sin(\phi-\phi')\,\delta\left(t - \frac{r}{c} + f(\phi')\right) d\phi' \tag{142a}$$

$$E_\phi = -\frac{b\, I_0}{4\pi\varepsilon c^2 r}\int_0^{2\pi} \cos(\phi-\phi')\,\delta\left(t - \frac{r}{c} + f(\phi')\right) d\phi' \tag{142b}$$

$$f(\phi') \equiv -\frac{b}{c}\left[\phi' - \cos(\phi-\phi')\sin\theta\right] \tag{143}$$

The integrals in Eq. (142) are of the type discussed in Appendix VI,

$$\int g(\phi')\delta\left[f(\phi')-\lambda\right]d\phi'' = \frac{g(\phi'_i)}{\left|\frac{df(\phi')}{d\phi'}\right|_{\phi'=\phi''_i}} \tag{144}$$

Here ϕ'_i is a zero of the argument of the delta function, i.e., $f(\phi'_i)=\lambda$. From Eq. (143),

$$\left|\frac{df(\phi')}{d\phi'}\right|_{\phi'_i} = \frac{b}{c}\left|1-\sin(\phi-\phi'_i)\sin\theta\right| \tag{145}$$

Hence Eqs. (142) become

$$E_\theta = -\frac{I_0\cos\theta}{4\pi\varepsilon c r}\,\frac{\sin(\phi-\phi'_i)}{\left|1-\sin(\phi-\phi'_i)\sin\theta\right|} \tag{146a}$$

$$E_\phi = -\frac{I_0\cos(\phi-\phi'_i)}{4\pi\varepsilon c r}\,\frac{1}{\left|1-\sin(\phi-\phi'_i)\sin\theta\right|} \tag{146b}$$

Eqs. (146) are the same as those in Ref. (35) (p. 31,32, Eqs. (12,13)), using v_i (traveling-wave velocity) = c, except that there is a + sign in front of the $\sin(\phi-\phi'_i)\sin\theta$ term. This may be traced back to what appears to be a typographical or a sign error in Ref. (35). If one substitutes the equation

$$r = R_0 - b\cos(\phi_0 - \phi_L)\sin\theta_0$$ (Ref. 35, p. 30)

into the argument of the delta function

$$\delta\left(t - T_i - \frac{b\phi_L}{v_i} - \frac{r}{c}\right)$$ (Ref. 35, p. 30,31 Eqs. (10,11))

one obtains the argument

$$t - T_i - \frac{b\phi_L}{v_i} - \frac{R_0}{c} + \frac{b}{c}\cos(\phi_0 - \phi_L)\sin\theta_0$$

whereas a $-$ sign appears in front of the $\cos(\phi_0 - \phi_L)\sin\theta_0$ term in Ref. 35 (p. 31).

It is concluded that the time-domain analysis of the pulsed loop problem in Ref. (35) and the analysis developed in this report are very similar to each other in basic formulation.

SECTION 6

TRANSIENT RADIATION FROM APERTURE ANTENNAS

1. INTRODUCTION

The radiation from aperture antennas such as horns and paraboloids is calculated in many analyses from diffraction of the aperture fields $\bar{E}_s$, $\bar{H}_s$. For reflector types the reflector-surface fields or currents can also be used (Ref. 21, p. 144). For wire antennas the preceding sections have shown that the use of accelerated-charge radiation leads to a time-domain formulation in terms of the time-derivative of the currents on the antennas. A similar analysis for reflector-aperture antennas, using the accelerated charges on the actual conducting surfaces to calculate the transient radiation has not been attempted as yet. Instead, in this report, a general time-domain method of calculating the transient radiation from aperture antennas developed by Chernousov (Ref. 37) is reviewed, and some important results are noted. This method uses the antenna surface or the aperture fields and the Huygens-Kirchhoff principle to calculate the radiated fields. It is shown in this report that the radiation from the equivalent current sheets which replace the aperture fields in Chernousov's analysis, may also be obtained from equivalent accelerating charge sheets over the aperture. It is also shown that Chernousov's results for the radiation of a planar in-phase aperture in principal planes reduce to the results for a one-dimensional antenna given by Cheng and Tseng (Ref. 38). Some recent work by Maddox (Ref. 3) is also described.

2. REVIEW OF CHERNOUSOV PAPER (REF. 37)

Consider the antenna aperture fields $\bar{E}(\bar{r}_s,t), \bar{H}(\bar{r}_s,t)$, which must be known, and their equivalent currents, which are arbitrary functions of time,

$$\bar{K}_E(\bar{r}_s,t) = \hat{n} \times \bar{H}(\bar{r}_s,t) \tag{147a}$$

$$\bar{K}_H(\bar{r}_s,t) = -\hat{n} \times \bar{E}(\bar{r}_s,t) \tag{147b}$$

where $\bar{K}_E, \bar{K}_H$ are the usual equivalent ficticious electric-and magnetic-current sheet densities over aperture S (Ref. 6, p. 486). The retarded potentials are (Ref. 6, Chap. 13)

$$\bar{A}_E(\bar{r},t) = \frac{\mu}{4\pi}\int_S \frac{\bar{K}_E(\bar{r}_s,t-R/v)}{R}\,dS \tag{148a}$$

$$\bar{A}_H(\bar{r},t) = \frac{\varepsilon}{4\pi}\int_S \frac{\bar{K}_H(\bar{r}_s,t-R/v)}{R}\,dS \tag{148b}$$

See Fig. 38. $\bar{r}_s$ is the vector from origin 0 to aperture area element dS, and v is the propagation velocity in the medium.

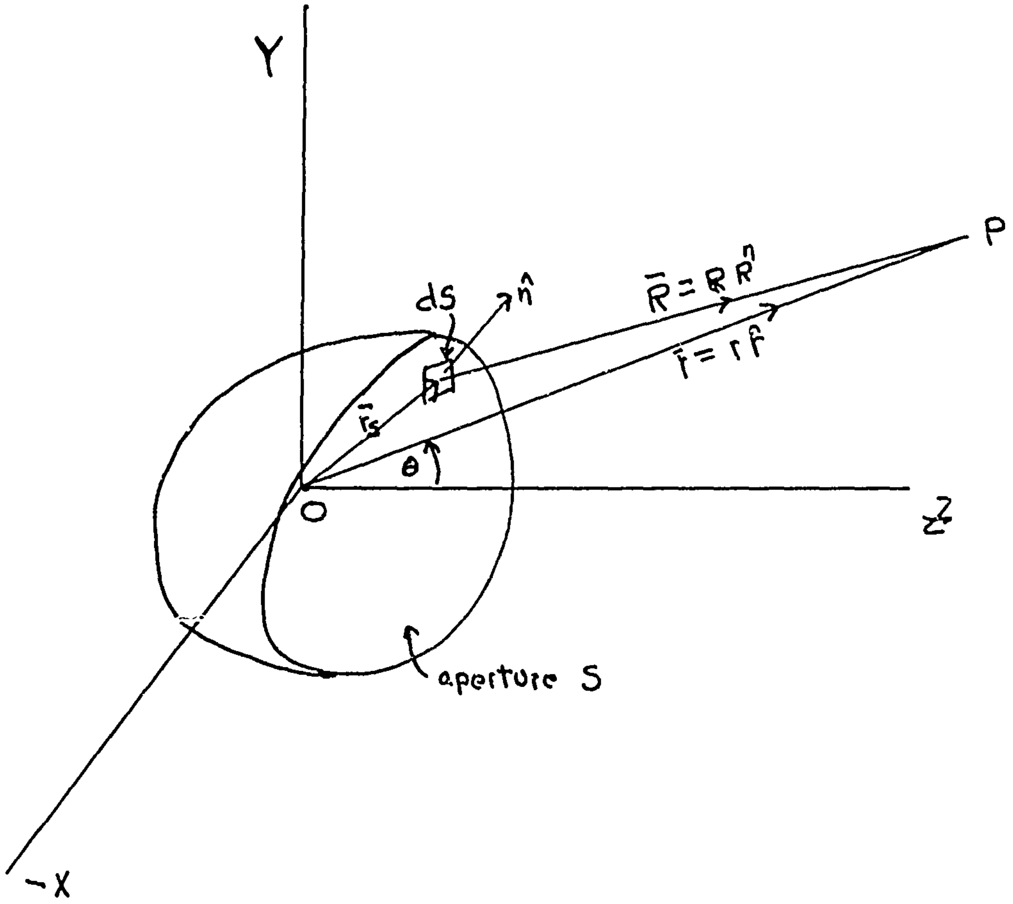

FIG. 38 Aperture antenna.

Then, following well-known methods, the fields $\bar{E}(\bar{r},t)$, $\bar{H}(\bar{r},t)$ at P are expressed in terms of vector operations on $\bar{A}_E$ and $\bar{A}_H$. The results, which are not repeated here, are given in Ref. (37), and hold for near-as well as far-fields.

Chernousov defines the far field by the following equations,

$$\frac{1}{v}\left|\frac{\partial \bar{F}(\bar{r}_s,t)}{\partial t}\right| \gg \frac{1}{R}\left|\bar{F}(\bar{r}_s,t)\right| \tag{149a}$$

$$\frac{1}{v}\left|\bar{F}(\bar{r}_s,t)\right| \gg \frac{1}{R}\left|\int_0^t \bar{F}(\bar{r}_s,t)\,dt\right| \tag{149b}$$

plus the requirement that $R \gg$ linear dimensions of the antenna, where $\bar{F}$ denotes $\bar{E}$ or $\bar{H}$. To illustrate these equations, for conventional sinusoidal time-varying excitation, let $\bar{F} = \bar{f}(\bar{r}_s)e^{j\omega t}$. Using $v = c$, Eq. (149) reduces to $R \gg \lambda/2\pi$, which is a well-known criterion for the far field for $e^{j\omega t}$ excitation. For arbitrary time variation, using Chernousov's results (Ref. 37, Eq. (8)) and Eq. (147), the radiation field can be shown to be

$$\bar{H}(\bar{r},t) = -\frac{\hat{r}}{4\pi c r}\times\int_S\left\{\frac{\partial}{\partial t}\bar{K}_E\left(\bar{r}_s, t'+\frac{\bar{r}_s\cdot\hat{r}}{v}\right) + \frac{\hat{r}}{\sqrt{\mu/\epsilon}}\times\frac{\partial}{\partial t}\bar{K}_H\left(\bar{r}_s, t'+\frac{\bar{r}_s\cdot\hat{r}}{v}\right)\right\}ds \tag{150}$$

where $t' = t - r/v$, and $\hat{r}$ is a unit vector along $\bar{r}$.

3. ACCELERATED-CHARGE VIEWPOINT

It will now be shown that Eq. (150) is consistent with the accelerated-charge radiation results developed in Eqs. (68, 74, V-7). For a one-dimensional current flow along the Z-axis, these equations show that

$$d\bar{H}(\bar{r},t) = \frac{1}{4\pi c R}\,\frac{\partial \bar{I}}{\partial t}(z, t - \frac{R}{c})\,dz \times \hat{R} \qquad (151)$$

where $\hat{R}$ is a unit vector along $\bar{R}$, the vector from dZ to field point P. In a similar fashion to Eq. (68), which replaces the charge-acceleration product by a product of the time derivative of the current and dz, for a surface sheet current flow $\bar{K}_E$ amps/meter, the charge-acceleration product would be replaced by the following product:

$$[qa]_{ret} = \frac{\partial}{\partial t}\bar{K}_E(\bar{r}_s, t - \frac{R}{c})\,dS \qquad (152)$$

Then the radiation due to the equivalent (ficticious) electric current sheet $\bar{K}_E$ which replaces the true aperture field $\bar{H}(\bar{r}_s,t)$ can equally well be considered as arising from the radiation of equivalent (ficticious) accelerated charges as given by Eq. (152), leading to the following two-dimensional generalization of Eq. (151):

$$d\bar{H}(\bar{r},t) = \frac{1}{4\pi c R}\,\frac{\partial \bar{K}_E(\bar{r}_s, t-R/c)}{\partial t}\,dS \times \hat{R} \qquad (153)$$

For the far field, $R \approx r - \bar{r}_s \cdot \hat{r}$, $\bar{R}$ is parallel to $\bar{r}$, and Eq. (153) becomes

$$d\bar{H}(\bar{r},t) = -\frac{\hat{r}}{4\pi c r} \times \frac{\partial}{\partial t}\bar{K}_E\left(\bar{r}_s, t - \frac{r}{c} + \frac{\bar{r}_s\cdot\hat{r}}{c}\right) \qquad (154)$$

Eq. (154) is identical to the $\bar{K}_E$ term in Eq. (150) from Chernousov's paper. A corresponding term arises from the $\bar{K}_H$ current; this is the $\bar{K}_H$ term in Eq. (150). Thus the Chernousov results for aperture fields can be interpreted in terms of equivalent accelerating charges.

In the case of linear antennas, the charge-acceleration product was formulated in terms of the time derivative of the actual current. For an aperture antenna, the above shows that a similar correspondence obtains between the time derivatives of the equivalent (ficticious) aperture currents and fictiaperture charge acceleration products. A transient radiation analysis in terms of the actual reflector currents has not been attempted, but presumably would produce a similar correspondence between these current time-derivatives and the actual surface charge-acceleration products.

4. PLANAR IN-PHASE APERTURE

Chernousov examines transient radiation from a planar, rectangular aperture excited in-phase such that the aperture field at any time has the same value at all points in the aperture. Thus the aperture excitation may be written as

$$\bar{E}_s(\bar{r}_s, t) = E_s(t)\,\bar{E}_s(\bar{r}_s) \tag{155}$$

where $\bar{E}_s(\bar{r}_s)$ may be equated to unity over the aperture. The aperture is taken in the XY-plane, radiating in the Z-direction, of dimensions $-a/2 \leq x \leq a/2$, $-b/2 \leq y \leq b/2$. The aperture field $\bar{E}_s$ is polarized in the Y direction, and $\bar{H}_s$ is in the -X direction. For the case where $\bar{E}_s$, $\bar{H}_s$ form the front of a free-space TEM wave, Chernousov shows that the radiation pattern in a principal plane such as XZ is of the form

$$E(\bar{r}, t) = \frac{ab\,(1+\cos\theta)}{4\pi c r}\,\frac{1}{2\tau_a}\left\{E_s(t'+\tau_a) - E_s(t'-\tau_a)\right\} \tag{156}$$

where θ is the usual polar angle with respect to the Z-axis, $t' = t - r/c$, and $\tau_a = a\sin\theta/(2c)$. Since τ_a is the time difference between radiation from the aperture edges and the origin, it is seen that the radiation is the sum of two waves, which appear to originate at the aperture ends, and have the same time form as the excitation field.

Cheng & Tseng (Ref. 38) consider a one-dimensional antenna with current excitation $i(x, t)$. When this function is separable then $i(x,t) = A(x)\, f(t)$. For a comparable example with the above Chernousov case, select the example in Ref. (38) where $A(x) = 1$ for $-a/2 \leq x \leq a/2$. For $\cos\theta \approx 1$ (Ref. 38, footnote 3) so that $(1+\cos\theta) \approx 2$, the radiated field is (Ref. 38, Eq. (13))

$$E(\theta,t) = \frac{\mu_0 a}{8\pi r u}\left\{f([t]+u) - f([t]-u)\right\} \tag{157}$$

where $u = a\sin\theta/(2c) = \tau_a$, and $[t] = t - r/c = t'$. Hence apart from differing amplitude factors, which is expected since one analysis is based on aperture fields and the other on currents, the two patterns of Eqs. (156,157) are identical.

5. SOME ADDITIONAL RESULTS

Using Chernousov's formulation, Maddox (Ref. 3) has investigated the scattered far-field due to a conducting disk whose surface is perpendicular to an incident pulse-type plane wave. In the broadside direction $(\theta = 0)$, the time waveform of this field is shown to be the negative time-derivative of the incident waveform. Thus the response to an impulse illumination is an inverted doublet. This has been verified experimentally (Ref. 39). Maddox (Ref. 3) has also derived the equations for the radiation $\overline{E}$ field on the axis of a paraboloid antenna illuminated by a pulse-type sperical wave whose origin is at the focus, again using the Chernousov formulation. Calculations and interpretation of the results are not yet complete; however it appears, depending upon the geometry of the problem, that it is not always true that the radiated field is the negative time derivative of the incident excitation.

A limited amount of experimentation has been done, using available equipment. The transmitter is a Spencer-Kennedy Laboratory pulse generator (mercury switch), with a one nanosecond pulse width (one foot resolution) and a rise time of about 350 picoseconds. This excites a long vertical monopole from a coaxial line. For a receiving antenna a linear string of five carbon resistors has been used (Ref. 26). The display oscilloscope is a H. P. 185B with a 187B preamplifier. With this equipment in a non-anechoic room, measurements have been made of the returns from a parabola (3 ft. diameter, 9 in. focal length) and two disks (1, 2 ft. diameter). Qualitative agreement has been obtained with published results (Ref. 40). More refined experiments on aperture and wire antennas would require test equipment with considerably higher resolution.

SECTION 7

CONCLUSIONS AND RECOMMENDATIONS

Based upon the results presented in this final report, the problem of radiation from antennas excited by impulsive signals can be approached in the time domain from the viewpoint of radiation from accelerated charges. The transition to antennas is accomplished through derivation of a radiation equation which expresses the accelerated-charge radiation in terms of the time-derivative of the antenna currents, either real or equivalent. Applied to pulse-excited dipoles, linear antennas and aperture antennas, this radiation equation produces a result derived previously by retarded potential and other methods. For a pulse-excited loop, the result is the same as that obtained by another investigator using the Sommerfeld radiation equation for an infinitesimal dipole. For sinusoidal time excitation, the above radiation equation reproduces well-known results for standard antennas such as small dipoles and loops, a half-wave length dipole, and a linear traveling-wave antenna.

It has been shown that the radiation characteristics of antennas may be expressed in the time domain in a number of equivalent ways, involving the integration of either the retarded potentials, or the Sommerfeld dipole radiation formula, or the radiation from accelerated charges over the differential elements of the antenna. If one accepts the premise, as preferred by this writer, that the basic physical radiation mechanism is the presence of accelerated charges, then the other methods may be interpreted as alternative mathematical formulations.

In this report, the radiation fields due to accelerating charges in all cases have been expressed in terms of the time-derivative of the actual or equivalent currents on the antenna, which are assumed to be known. Then the method of retarded potentials, for example, could also be used, without any reference to accelerating charges. Thus, based upon the work completed thus far, it is concluded that while the accelerated charge radiation approach provides, in the time domain, a direct physical explanation of and an analytic basis for impulsive antenna radiation, it has not been demonstrated that it has significant advantages compared to other methods which also use known or assumed antenna currents in their formulation. It is probable that this conclusion will be altered by the results of further work on transient antennas with new configurations, where the currents or aperture fields are unknown and must be solved for (i.e., time-domain boundary value problems), or must be controlled by new and novel techniques.

In the report, the radiation from a pulse-excited dipole is examined at various angles, using a time-domain equation which has also been derived by others. Comparison with a published frequency-domain analysis shows reasonably good agreement at all angles except for angles close to the end-fire direction. Further work on this point is recommended. Experimental data on the radiation from a pulsed dipole (or monopole) at all angles is also recommended.

The receiving characteristics of antennas in incident transient fields have not been investigated in this report. It is noted that the receiving response of a monopole over a ground plane, matched at the base, to an incident impulsive plane wavefront, as given by Ross (Ref. 27) has a waveform identical to that for the transmitted radiation of a step function given in Fig. 29(a) (Ross's θ is the complement of the θ used in this report). Investigation of receiving characteristics and reciprocity relationships with transmitting characteristics is an obvious recommendation.

A promising method due to Chernousov for analysis of the performance of transient high-gain aperture-type antennas has been identified and described. This is a gener oach, based upon replacement of known or assumed apertu by equivalent surface current sheets. It is shown in this report that the Chernousov results can be recast alternatively in terms of equivalent surface accelerating charge sheets. For a one-dimensional case, it is shown that the Chernousov formulation reduces to results derived previously by Cheng and Tseng. It is recommended that the analysis of impulsive high-gain aperture-type antennas be extended both in scope and in detail, including primary feed antennas, to further the state-of-the-art of this important class of antennas.

SECTION 8

REFERENCES

1. Jackson, J. D., Classical Electrodynamics, John Wiley, N. Y. (1962).

2. Panofsky, W. K. H., and Phillips, M., Classical Electricity and Magnetism, Addison-Wesley, Reading, Mass., 2nd Ed. (1962).

3. Maddocks, H. C., dissertation research, Elec. Engr. Dept., Univ. of Vermont, Burlington, Vt. (1971).

4. Sherwin, C. W., Basic Concepts of Physics, Holt, Rinehart and Winston, N. Y. (1961).

5. Magnusson, P. C., Transmission Lines and Wave Propagation, Allyn and Bacon, Boston, 2nd Ed. (1970).

6. Jordan, E. C., and Balmain, K. G., Electromagnetic Waves and Radiating Systems, Prentice-Hall, Englewood Cliffs, N. J., 2nd Ed. (1968).

7. Jones, D. S., The Theory of Electromagnetism, MacMillan, N. Y. (1964).

8. Pocklington, H. C., Proc. Camb. Phil. Soc., 9,324 (1897).

9. Torre, E. D., and Longo, C. V., The Electromagnetic Field, Allyn and Bacon, Boston (1969).

10. Stratton, J. H., Electromagnetic Theory, McGraw-Hill, N. Y. (1941).

11. Paris, D. T., and Hurd, K. F., Basic Electromagnetic Theory, McGraw-Hill, N. Y. (1969).

12. Garbuny, M., Optical Physics, Academic Press, N. Y. (1965).

13. Elliot, R. S., Electromagnetics, McGraw-Hill, N. Y. (1966).

14. Becker, R., Electromagnetic Fields and Interactions, Blaisdell, N. Y., Vol. I (1964).

15. Silvester, P., Modern Electromagnetic Fields, Prentice-Hall, Englewood Cliffs, N. J. (1968).

16. Sherwin, C. W., loc. cit.

17. Ruehli, E. A., "An Integral Equation Equivalent Circuit Solution to a Large Class of Interconnection Systems," Ph.D. dissertation, Dept. of Elec. Engr., Univ. of Vermont, Burlington, Vt. (1972).

18. Moore, R. K., Traveling-Wave Engineering, McGraw-Hill, N. Y. (1960).

19. Sommerfeld, A., Electrodynamics, Academic Press, N. Y. (1964).

20. Ramo, S., and Whinnery, J. R., Fields and Waves in Modern Radio, John Wiley, N. Y., 2nd Ed. (1953).

21. Silvers S., Microwave Antenna Theory and Design, McGraw-Hill, N. Y. (1949).

22. Weeks, W. L., Antenna Engineering, McGraw-Hill Book Co., N. Y. (1968).

23. French, A. P., Principles of Modern Physics, John Wiley, N. Y. (1958).

24. Rossi, B., Optics, Addison-Wesley, Reading, Mass. (1957).

25. Lorrain, P. and Corson, D. R., Electromagnetic Fields and Waves, Freeman and Co., San Francisco, Cal., 2nd Ed. (1970).

26. Schmitt, H. J., Harrison, C. W., Jr., and Williams, C. S., Jr., "Calculated and Experimental Response of Thin Cylindrical Antennas to Pulse Excitation," IEEE Trans. on Ant. and Prop., Vol. AP-14, No. 2, 120-127 (March, 1966).

27. Ross, G. F., "A New Wideband Antenna Receiving Element," NEREM, pp. 78-79, Nov. (1967).

28. King, R. W. P., and Schmitt, H. J., "The Transient Response of Linear Antennas and Loops," IEEE Trans. on Ant. and Prop., Vol. AP-10, pp. 222-228, May (1962).

29. Manneback, C., "Radiation from Transmission Lines," Trans. A.I.E.E., Vol. 42, pp. 289-301, Feb. (1923).

30. Schelkunoff, S. A., Advanced Antenna Theory, John Wiley and Sons, N. Y. (1952).

31. Ross, G., Bates, R. H. T., Hanley, G., Susman, L. and Robbins, K., Transient Behavior of Radiating Elements, Rome Air Development Center Interim Report RADC-TR-66-441, Sept. (1966).

32. Ross, G. F., Bates, R. H. T., Susman, L., Hanley, G., Smith, R., and Robbins, K., Transient Behavior of Radiating Elements, Rome Air Development Center Final Technical Report, RADC-TDR-66-790, Nov. (1966).

33. Goldman, S., Transformation Calculus and Electrical Transients, Prentice-Hall, N. Y. (1949).

34. Palciauskas, J. R. and Beam, R. E., "Transient Fields of Thin Cylindrical Antennas," IEEE Trans. on Ant. and Prop., Vol. AP-18, pp. 276-278, March (1970).

35. Abo-Zena, A. M., "Transient Electromagnetic Fields of Pulsed-Excited Wire and Aperture Antennas," pp. 1-43 "The Circular Loop," Ph.D. dissertation, Dept. of Elec. Engr., Northwestern Univ., Evanston, Ill. (June, 1972).

36. Bracewell, R., The Fourier Transform and Its Applications, McGraw-Hill, N. Y. (1965).

37. Chernousov, V. S., "Nonstationary Radiation of Antenna Systems," Radio Engineering and Electronic Systems (Russian, English translation), Vol. 10, No. 8, pp. 1246-1252 (1965).

38. Cheng, D. K. and Tseng, F. I., "Transient and Steady-State Antenna Pattern Characteristics for Arbitrary Time Signals," IEEE Trans. on Ant. and Prop., Vol. AP-12, No. 4, pp. 492-493 (1964).

39. DeLorenzo, J. D., "Video Time-Domain Scattering Range," Northeast Electronics Research and Engineering Meeting, IEEE NEREM record, pp. 80-81 (Nov. 1967).

40. Cronson, H. M. and Proud, J. M., Jr., "Time-Domain Ray Analysis," Proc. IEEE, Vol. 58, No. 9, pp. 1383-1384 (Sept., 1970).

APPENDIX I

LIENARD-WIECHERT POTENTIALS

1. SCALAR AND VECTOR POTENTIALS

The Lienard-Wiechert potentials are the potentials resulting from charges with arbitrary spatial and temporal distributions. From these potentials the E and H fields due to accelerating charges may be found. For the sake of completeness a derivation of those potentials is included in this Appendix.

Maxwell's equations in Gaussian units (Ref. 1) are

$$\nabla \times \bar{H} = \frac{4\pi}{c}\bar{J} + \frac{1}{c}\frac{\partial \bar{D}}{\partial t} \qquad \text{(I-1)}$$

$$\nabla \times \bar{E} = -\frac{1}{c}\frac{\partial \bar{B}}{\partial t} \qquad \text{(I-2)}$$

$$\nabla \cdot \bar{D} = 4\pi\rho \qquad \text{(I-3)}$$

$$\nabla \cdot \bar{B} = 0 \qquad \text{(I-4)}$$

The constitutive equations are

$$\bar{D} = \varepsilon\bar{E}\,; \quad \bar{B} = \mu\bar{H}\,; \quad \bar{J} = \sigma\bar{E} \qquad \text{(I-5)}$$

Because of Eq. (1-4) and the vector identity div curl = 0, $\bar{B}$ can be derived from the curl of a vector potential $\bar{A}$:

$$\bar{B} = \nabla \times \bar{A} \qquad \text{(I-6a)}$$

Similarly, because curl grad = 0, $\bar{E}$ may be derived from a scalar potential Φ and $\bar{A}$ by

$$\bar{E} = -\nabla\Phi - \frac{1}{c}\frac{\partial \bar{A}}{\partial t} \qquad \text{(I-6b)}$$

Thus the curl of Eq. (I-6b) recovers Eq. (I-2). The Lorentz condition (Ref. 1, p. 180) defines div $\bar{A}$ by

$$\nabla \cdot \bar{A} = -\frac{1}{c}\frac{\partial \Phi}{\partial t} \tag{I-7}$$

Vector manipulation of the above equations leads to the standard wave equations

$$\nabla^2 \Phi - \frac{1}{c^2}\frac{\partial^2 \Phi}{\partial t^2} = -4\pi\rho \tag{I-8}$$

$$\nabla^2 \bar{A} - \frac{1}{c^2}\frac{\partial^2 \bar{A}}{\partial t^2} = -\frac{4\pi}{c}\bar{J} \tag{I-9}$$

where $\bar{J}$ is the impressed current density due to external sources.

For static fields Eqs. (I-8,9) reduce to the Poisson equations

$$\nabla^2 \Phi = -4\pi\rho \tag{I-10}$$

$$\nabla^2 \bar{A} = -\frac{4\pi}{c}\bar{J} \tag{I-11}$$

The solutions of the static Eqs. (I-10,11) are the particular integrals

$$\Phi(\bar{x}) = \int \frac{\rho(\bar{x}')}{R} d^3x' \tag{I-12}$$

$$\bar{A}(\bar{x}) = \int \frac{\bar{J}(\bar{x}')}{R} d^3x' \tag{I-13}$$

Here $\bar{x}$ is the position vector of the field point $P(x_1, x_2, x_3)$, $\bar{x}'$ is the position vector of the source volume $d^3x' = dx_1' dx_2' dx_3'$

at point $P'(x_1', x_2', x_3')$, and R is the magnitude of the vector $\bar{R} = \bar{x} - \bar{x}'$ from P' to P. See Fig. 39.

For dynamic fields, the time-dependent Eqs. (I-8,9) are of the form

$$\nabla^2\psi - \frac{1}{c^2}\frac{\partial^2\psi}{\partial t^2} = -4\pi f(\bar{x},t) \qquad \text{(I-14)}$$

The time-retarded solution of Eq. (I-14) is (Ref. 1, p. 186)

$$\psi(\bar{x},t) = \int \frac{\delta(t'-t+R/c)}{R} f(\bar{x}',t')d^3x'dt' \qquad \text{(I-15)}$$

where δ is the Dirac delta function. The integration over t', using the properties of the delta function

$$\delta(t'-t+R/c) = 0 \qquad \text{(I-16)}$$

except at

$$t' = t - R/c \qquad \text{(I-17)}$$

yields

$$\psi(\bar{x},t) = \int \frac{[f(\bar{x}',t']_{ret}}{R} d^3x' \qquad \text{(I-18)}$$

where $[\;\;]_{ret}$ means that t' is the "retarded time" given by Eq. (I-17). The time-varying solution Eq. (I-18) of the dynamic Eq. (I-14) is a generalization of the static solution Eq. (I-12) of the static Eq. (I-10), incorporating time retardation.

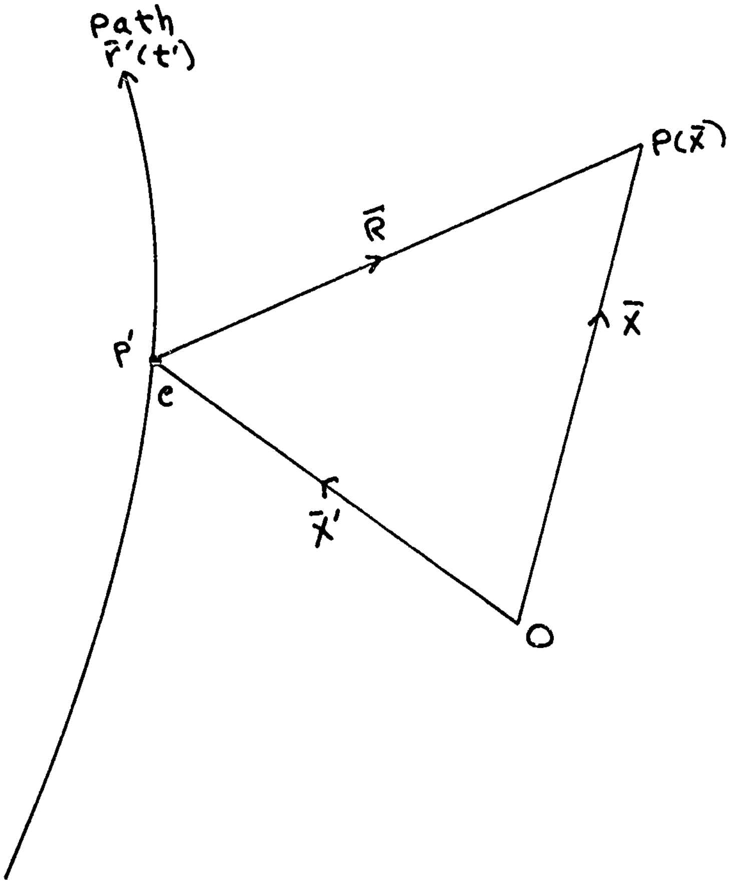

FIG. 39 Charge e moving on path $\bar{r}'(t')$.

From Eqs. (I-8,9,14, and 18), the integrals for ϕ and $\bar{A}$ are

$$\Phi(\bar{x},t)=\iint \frac{\rho(\bar{x}',t')}{R}\,\delta(t'-t+R/c)\,d^3x'\,dt' \qquad \text{(I-19)}$$

$$\bar{A}(\bar{x},t)=\iint \frac{\bar{J}(\bar{x}',t')}{R}\,\delta(t'-t+R/c)\,d^3x'\,dt' \qquad \text{(I-20)}$$

2. LIENARD-WIECHERT POTENTIALS

The Lienard-Wiechert potentials are given in the literature for moving point charges of fixed magnitude. These potentials can be extended to the case of a fixed-position charge of time-varying magnitude, as shown in this appendix.

Consider first a fixed-magnitude charge e moving on a prescribed path $\bar{r}'(t')$ with prescribed velocity (see Fig.39)

$$\bar{v}(t')\equiv c\,\bar{\beta}(t') \qquad \text{(I-21)}$$

The current density at a point $\bar{r}'$ due to e is (Ref. 1, p. 465)

$$\bar{J}(\bar{x}',t')=\rho\bar{v}=ec\,\bar{\beta}(t')\,\delta\left[\bar{x}'-\bar{r}'(t')\right] \qquad \text{(I-22)}$$

The vector delta function in Eq. (I-22) is defined such that

$$\int_V f(\bar{x}')\,\delta(\bar{x}'-\bar{r}')\,d^3x'=f(\bar{r}') \qquad \text{(I-23)}$$

if volume V contains point $\bar{r}'$, otherwise the integral is zero. Substitution of Eq. (I-22) into (I-20) gives

$$\bar{A}(\bar{x},t)=e\iint\frac{\bar{\beta}(t')}{R}\,\delta(\bar{x}'-\bar{r}')\,\delta(t'-t+R/c)\,d^3x'\,dt' \qquad \text{(I-24)}$$

Integration of Eq. (I-24) over x_i' gives

$$\bar{A}(\bar{x},t) = e\int \frac{\bar{\beta}(t')}{R(t')}\,\delta(t'-t+R(t')/c)\,dt' \tag{I-25}$$

where

$$\bar{R}(t') = \left[\bar{x}-\bar{x}'(t')\right]_{\bar{x}'(t')=\bar{r}'(t')} = \bar{x}-\bar{r}'(t') \tag{I-26}$$

Similarly, write for the charge density at $\bar{r}'(t')$

$$\rho(\bar{x}',t') = e\delta\left[\bar{x}'-\bar{r}'(t')\right] \tag{I-27}$$

which, when substituted into Eq. (A-19), and integrated over x_i' yields

$$\Phi(\bar{x},t) = e\int \frac{1}{R(t')}\,\delta(t'-t+R(t')/c)\,dt' \tag{I-28}$$

Consider now a charge in fixed position at $\bar{r}'$, but with time-varying amplitude $q(t')$. Such a charge must, of course, be supplied by a current, to satisfy the continuity equation $\nabla\cdot\bar{J} = -\partial\rho/\partial t$. Then the charge density at $\bar{r}'(t')$ can be written as

$$\rho(\bar{x}',t') = q(t')\,\delta\left[\bar{x}'-\bar{r}'(t')\right] \tag{I-29}$$

Substitution of Eq. (I-29) into Eq. (I-19) gives

$$\Phi(\bar{x},t) = \iint \frac{q(t')}{R}\,\delta(t'-t+R/c)\,\delta(\bar{x}'-\bar{r}'(t'))\,d^3x'\,dt' \tag{I-30}$$

The vector potential $\bar{A}$ for $q(t')$ is zero, since $q(t')$ has zero velocity.

Returning to fixed-magnitude moving charges, Eqs. (I-25,28) are now reduced to the standard Lienard-Wiechert forms (Ref. 1, p. 465). Write Eq. (I-25) in more convenient notation as

$$\bar{A} = e\int \frac{\bar{\beta}(t')}{R(t')}\,\delta\left(f(t')-t\right)dt' \qquad \text{(I-31)}$$

where

$$f(t') \equiv t' + R(t')/c \qquad \text{(I-32)}$$

The integral in Eq. (I-31) is evaluated using the following property of the delta function (Ref. 1, p. 465):*

$$\int g(x)\,\delta\left(f(x)-a\right)dx = \left.\frac{g(x)}{\left|\frac{df}{dx}\right|}\right|_{f(x)=a} \qquad \text{(I-33)}$$

Hence

$$\bar{A} = \frac{e\bar{\beta}(t')}{R(t')} \Big/ \frac{d}{dt'}\left(t'+R(t')/c\right) \qquad \text{(I-34)}$$

where Eq. (I-34) must be evaluated at

$$t'+R(t')/c = t$$

i.e., at the retarded time

$$t' = t - R(t')/c \qquad \text{(I-35)}$$

---

*See Appendix VI.

Now

$$\frac{df(t')}{dt'} = \frac{d}{dt'}\left(t' + R(t')/c\right) = 1 + \frac{1}{c}\frac{dR(t')}{dt'} \qquad \text{(I-36)}$$

The derivative $dR(t')/dt'$ is found from

$$R(t') = \left[\sum_{i=1}^{3}\left(x_i - x_i'(t')\right)^2\right]^{1/2} \qquad \text{(I-37)}$$

which shows $R(t')$ as an explicit function of x_i' . Hence

$$\frac{dR(t')}{dt'} = \sum_i \frac{\partial R(t')}{\partial x_i'}\frac{dx_i'}{dt'}$$

$$= -\frac{1}{R(t')}\sum_i (x_i - x_i')\frac{dx_i'}{dt'}$$

$$= -\frac{\bar{R}(t')}{R(t')}\cdot\bar{v}(t')$$

Define the unit vector $\hat{n}$ from source charge at $\bar{x}'$ to field point at $\bar{x}$. Then

$$\hat{n} = \bar{R}(t')/R(t) \qquad \text{(I-38)}$$

Hence

$$\frac{dR(t')}{dt'} = -\hat{n}(t')\cdot\bar{v}(t') \qquad \text{(I-39)}$$

From Eqs. (A-21, A-36), it follows that

$$L(t') \equiv \frac{df(t')}{dt'} = 1 - \hat{n}(t')\cdot\bar{\beta}(t') \geq 0 \qquad \text{(I-40)}$$

Hence Eq. (I-34) becomes

$$\bar{A}(\bar{x},t) = e\left[\frac{\bar{\beta}(t')}{R(t')L(t')}\right]_{ret} \qquad \text{(I-41)}$$

Comparing Eqs. (I-24) and (I-28), the solution Eq. (I-41) to Eq. (I-24) implies that the solution to Eq. (I-28) is

$$\Phi(\bar{x},t) = e\left[\frac{1}{R(t')L(t')}\right]_{ret} \qquad \text{(I-42)}$$

Equations (I-41,42) are the standard Lienard-Wiechert potentials which apply to a point charge of fixed magnitude e , moving at prescribed velocity $\bar{v}(t')$ on prescribed path $\bar{r}'(t')$.

Consider now a point charge $q(t')$, fixed in position, but varying in magnitude with time. Integrating Eq. (I-30) first in x' gives

$$\Phi(\bar{x},t) = \int \frac{q(t')}{R(t')}\,\delta(f(t')-t)\,dt' \qquad \text{(I-43)}$$

Using Eqs. (I-33, I-40), and the fact that for this case $\bar{\beta}(t') = \bar{v}(t')/c = 0$, so $L(t') = 1$, Eq. (I-43) yields

$$\Phi(\bar{x},t) = \left[\frac{q(t')}{R(t')}\right]_{ret} \qquad \text{(I-44)}$$

Equations (I-41, I-42, I-44) can be combined to give the following generalized forms of the Lienard-Wiechert potentials:

$$\bar{A}(\bar{x},t) = \left[\frac{q(t')\,\bar{\beta}(t')}{R(t')\,L(t')} \right]_{ret} \qquad \text{(I-45)}$$

$$\Phi(\bar{x},t) = \left[\frac{q(t')}{R(t')\,L(t')} \right]_{ret} \qquad \text{(I-46)}$$

For a fixed-magnitude charge $q(t') = e$, while for a stationary charge $L(t') = 1$, so that Eqs. (I-45, I-46) reduce in each of these cases to Eqs. (I-41, I-42) and Eq. (I-44) respectively. Equations (I-45, I-46) were derived by Maddocks (Ref. 3).

In MKS units, and using the notation of Ref. 2, Eqs. (41, 42) become

$$\bar{A}(\bar{x},t) = \frac{\mu_0 e}{4\pi} \left[\frac{\bar{v}}{s} \right]_{ret} \qquad \text{(I-47)}$$

$$\Phi(\bar{x},t) = \frac{e}{4\pi\varepsilon_0} \left[\frac{1}{s} \right]_{ret} \qquad \text{(I-48)}$$

where

$$s \equiv r - \bar{r}\cdot\frac{\bar{v}}{c} = r - \bar{r}\cdot\bar{\beta} \qquad \text{(I-49)}$$

and $\bar{r}$ is used in place of $\bar{R} = \bar{x} - \bar{x}'$.

APPENDIX II

THE FIELDS OF MOVING CHARGES

1. EQUATIONS FOR THE FIELDS

The fields of moving charges may be derived from the Lienard-Wiechert potentials Eqs. (I-41,42) and the differential operations of Eqs. (I-5,6) (Ref. 1, p. 466 in CGS units; Ref. 2, p. 345 in MKS units). The derivation below follows Ref. 1 closely, and is included here only for the sake of completeness.

From Eqs. (I-5,25)

$$\bar{B}(\bar{X},t)=e\int \nabla_{X_i}\times\left[\bar{\beta}(t')\delta(t'-t+R/c)/R\right]dt' \qquad \text{(II-1)}$$

The ∇_{X_i} operator is in X_i coordinates and operates only on the R inside the integral. Using

$$\nabla_{X_i}\times\left[h(X_i)\bar{F}(X_i)\right]=\nabla_{X_i}h(X_i)\times\bar{F}(X_i) \qquad \text{(II-2)}$$

Eq. (II-1) becomes

$$\bar{B}(\ldots,t)=e\int \nabla_{X_i}\left[\delta(t'-t+R/c)/R\right]\times\bar{\beta}(t')dt' \qquad \text{(II-3)}$$

Define

$$g(R)\equiv\delta(t'-t+R/c)/R \qquad \text{(II-4)}$$

Using Eqs. (I-37,38)

$$\frac{\partial g(R)}{\partial x_i} = \frac{\partial g(R)}{\partial R}\cdot\frac{\partial R}{\partial x_i} = \frac{\partial g(R)}{\partial R}\cdot\frac{x_i - x_i'}{R}$$

$$\nabla g(R) = \sum_{i=1}^{3} \frac{\partial g(R)}{\partial x_i}\,\hat{a}_{x_i} = \frac{\partial g}{\partial R}\,\hat{m} \qquad \text{(II-5)}$$

Thus the ∇_{x_i} operation is equivalent to

$$\nabla_{x_i} = \hat{m}\,\frac{\partial}{\partial R} \qquad \text{(II-6)}$$

where $\hat{m}$ is the unit vector along $\bar{R}$. Hence

$$\nabla_{x_i}\left[\delta(t'-t+R/c)/R\right] = -\hat{n}\,\delta(t'-t+R/c)/R^2 + \frac{\hat{m}}{Rc}\,\delta'(t'-t+R/c) \qquad \text{(II-7)}$$

where $(\ )'$ denotes differentiation with respect to the argument of $(\ )$. Eq. (II-3) becomes

$$\bar{B} = e\int\left[\frac{\delta(t'-t+R/c)}{R^2} - \frac{1}{cR}\,\delta'(t'-t+R/c)\right](\bar{\beta}\times\hat{m})\,dt' \qquad \text{(II-8)}$$

Similarly, from Eqs. (I-6,25,28,32, II-7)

$$\bar{E} = -\nabla\Phi - \frac{1}{c}\frac{\partial\bar{A}}{\partial t}$$

$$\nabla\Phi = e\int \nabla\left[\delta(t'-t+R/c)/R\right] dt'$$

$$-\nabla\Phi = e\int\left[\frac{\delta(t'-t+R/c)}{R^2}\,\hat{m} - \frac{\delta'(t'-t+R/c)}{cR}\,\hat{m}\right]dt' \qquad \text{(II-9)}$$

$$-\frac{1}{c}\,\frac{\partial\bar{A}}{\partial t} = -\frac{e}{c}\int \frac{\bar{\beta}(t')}{R}\,\frac{\partial}{\partial t}\,\delta(t'-t+R/c)\,dt' \qquad \text{(II-10)}$$

Using

$$\frac{\partial}{\partial t}\,\delta(t'-t+R/c) = -\delta'(t'-t+R/c)$$

Eq. (II-10) becomes

$$-\frac{1}{c}\,\frac{\partial\bar{A}}{\partial t} = e\int \frac{\bar{\beta}(t')}{cR}\,\delta'(t'-t+R/c)\,dt' \qquad \text{(II-11)}$$

Hence

$$\bar{E} = e\int\left[\frac{\hat{m}}{R^2}\,\delta(t'-t+R/c) + \frac{1}{cR}(\bar{\beta}-\hat{m})\,\delta'(t'-t+R/c)\right]dt' \qquad \text{(II-12)}$$

The integrals in Eqs. (II-8,12) are evaluated using the properties of the δ -function given by Eq. (I-33) and by Eq. (II-13) below (Ref. 1, p. 4).

$$\int h(x)\delta'(x-a)\,dx = -h'(a) \tag{II-13}$$

The first integral in Eq. (I-8) is reduced as follows:

$$f \equiv t' + R(t')/c \tag{II-14}$$

$$\frac{df}{dt'} = 1 + \frac{1}{c}\frac{dR}{dt'} \equiv L(t') \tag{II-15}$$

$$\therefore\ dt' = df/L(t') \tag{II-16}$$

Then

$$e\int \frac{(\bar{\beta}\times\hat{n})}{R^2}\delta(t'-t+R/c)\,dt' = e\int\frac{(\bar{\beta}\times\hat{n})}{R^2L}\delta(f-t)\,df$$

$$= \left.\frac{e(\bar{\beta}\times\hat{n})}{R^2L}\right|_{f=t}$$

$$= e\left[\frac{\bar{\beta}\times\hat{n}}{R^2L}\right]_{ret}$$

Using

$$\delta'(t'-t+R/c)\,dt'=\delta'(f-t)\,df/L$$

the second integral in Eq. (B-8) becomes

$$-\frac{e}{c}\int\frac{(\bar{\beta}\times\hat{n})}{RL}\delta'(f-t)\,df=\frac{e}{c}\frac{d}{df}\left(\frac{\bar{\beta}}{R}\frac{1}{L}\right)\Big|_{f=}$$

$$=\frac{e}{cL}\frac{d}{dt'}\left(\frac{\bar{\beta}\times\hat{n}}{RL}\right)\Big|_{f=t}$$

$$=\frac{e}{cL}\left[\frac{d}{dt'}\,\frac{\bar{\beta}\times\hat{n}}{RL}\right]_{ret}$$

The equation $f=t$ means that $f=t'+\frac{R}{c}=t$, or that the retarded time $t'=t-R/c$. Eq. (II-8) becomes

$$\bar{B}(\bar{x},t)=e\left[\frac{\bar{\beta}\times\hat{n}}{R^2L}+\frac{1}{cL}\frac{d}{dt'}\left(\frac{\bar{\beta}\times\hat{n}}{RL}\right)\right]_{ret} \qquad \text{(II-17)}$$

In similar fashion the integrals in Eq. (II-12) can be reduced by comparison with the integrals in Eq. (II-8) reduced to the forms appearing in Eq. (II-17). It is seen that

$$\bar{E}(\bar{x},t)=e\left[\frac{\hat{n}}{R^2L}+\frac{1}{cL}\frac{d}{dt'}\left(\frac{\hat{n}-\bar{\beta}}{RL}\right)\right]_{ret} \qquad \text{(II-18)}$$

Henceforth, the $[\;]_{\mathrm{ret}}$ symbol will be omitted; it being understood that the R.H.S. of equations for $\bar{B}$ and $\bar{E}$ are evaluated at retarded time t'.

To decompose the fields given by Eqs. (II-17,18) into "static," "velocity," and "acceleration" components, the differential operations in these equations must be evaluated.

$$\frac{1}{c}\frac{d\hat{n}}{dt'} = \frac{1}{c}\frac{d}{dt'}(\bar{R}/R) = -\frac{\bar{R}}{cR^2}\frac{dR}{dt'} + \frac{1}{cR}\frac{d\bar{R}}{dt'}$$

$$= \frac{1}{cR}\left(-\hat{n}\frac{dR}{dt'} + \frac{d\bar{R}}{dt'}\right)$$

Now

$$\frac{d\bar{R}}{dt'} = \frac{d}{dt'}\sum_{i=1}^{3}(x - x_i')\hat{a}_{x_i} = \sum_{i} -\frac{dx_i'}{dt'}\hat{a}_{x_i} = -\bar{v}(t') \qquad \text{(II-19)}$$

Using Eqs. (I-39, II-18),

$$\frac{1}{c}\frac{d\hat{n}}{dt'} = \frac{1}{cR}\left[\hat{n}(\hat{n}\cdot\bar{v}) - \bar{v}\right] = \frac{\hat{n}\times(\hat{n}\times\bar{\beta})}{R} \qquad \text{(II-20)}$$

The derivative in Eq. (II-17) is

$$\frac{d}{dt'}\left(\frac{\bar{\beta}\times\hat{n}}{RL}\right) = \frac{d}{dt'}\left(\frac{\bar{\beta}}{RL}\right)\times\hat{n} + \frac{\bar{\beta}}{RL}\times\frac{d\hat{n}}{dt'}$$

$$= \frac{d}{dt'}\left(\frac{\bar{\beta}}{RL}\right)\times\hat{n} + \frac{\bar{\beta}}{RL}\times\frac{c}{R}\left[(\hat{n}\cdot\bar{\beta})\hat{n} - \bar{\beta}\right] \qquad \text{(II-21)}$$

Equation (II-17) becomes

$$\bar{B} = e\left[\frac{\bar{\beta}\times\hat{n}}{R^2L} + \frac{1}{cL}\frac{d}{dt'}\left(\frac{\bar{\beta}}{RL}\right)\times\hat{n} + \frac{\bar{\beta}}{R^2L^2}\times\left\{(\hat{n}\cdot\bar{\beta})\hat{n} - \bar{\beta}\right\}\right]$$

which, after some recombination, reduces to

$$\bar{B} = e\left[\frac{\bar{\beta}}{R^2L^2} + \frac{1}{cL}\frac{d}{dt'}\left(\frac{\bar{\beta}}{RL}\right)\right]\times\hat{n} \qquad \text{(II-22)}$$

Equation (II-18) becomes

$$\bar{E} = e\left[\frac{\hat{n}}{R^2L} + \frac{1}{cL}\frac{d}{dt'}\left(\frac{\hat{n}}{RL}\right) - \frac{1}{cL}\frac{d}{dt'}\left(\frac{\bar{\beta}}{RL}\right)\right]$$

which, after considerable recombination, reduces to

$$\bar{E} = e\left[\frac{\hat{n}}{R^2L^2} - \frac{\bar{\beta}}{R^2L^2} + \frac{\hat{n}}{cL}\frac{d}{dt'}\left(\frac{1}{RL}\right) - \frac{1}{cL}\frac{d}{dt'}\left(\frac{\bar{\beta}}{RL}\right)\right] \qquad \text{(II-23)}$$

From Eq. (II-23) it is seen that

$$\hat{n}\times\bar{E} = e\left[\frac{\bar{\beta}}{R^2L^2} + \frac{1}{cL}\frac{d}{dt'}\left(\frac{\bar{\beta}}{RL}\right)\right]\times\hat{n}$$

Hence

$$\bar{B}\Big|_{tot} = \hat{n}\times\bar{E}\Big|_{tot} \qquad \text{(II-24)}$$

Thus, $\bar{E}$, $\bar{B}$, and $\hat{n}$ form a mutually orthogonal set of vectors.

The derivatives in Eqs. (II-22,23) are now evaluated. Denoting differentiation on t' by a dot,

$$\frac{d}{dt'}\left(\frac{\bar{\beta}}{RL}\right) = \frac{\dot{\bar{\beta}}}{RL} - \frac{\bar{\beta}}{R^2L^2}\left(R\dot{L} + L\dot{R}\right) \qquad \text{(II-25)}$$

From Eq. (I-40)

$$\dot{L} = -\hat{n}\cdot\dot{\bar{\beta}} - \dot{\hat{n}}\cdot\bar{\beta} \qquad \text{(II-26)}$$

Using Eq. (I-39)

$$\frac{d}{dt'}(RL) = R\dot{L} + L\dot{R} = R(-\hat{n}\cdot\dot{\bar{\beta}} - \dot{\hat{n}}\cdot\bar{\beta}) + L(-\hat{n}\cdot c\bar{\beta})$$

which, after some recombinations, becomes

$$\frac{d}{dt'}(RL) = R\hat{n}\cdot\dot{\bar{\beta}} + c\beta^2 - c\bar{\beta}\cdot\hat{n} \tag{II-27}$$

Equation (I-25 then reduces to

$$\frac{d}{dt'}\left(\frac{\bar{\beta}}{RL}\right) = \frac{\dot{\bar{\beta}}}{RL} + \frac{(\hat{n}\cdot\dot{\bar{\beta}})\bar{\beta}}{RL^2} - \frac{c\beta^2\bar{\beta}}{R^2L^2} + \frac{c(\bar{\beta}\cdot\hat{n})\bar{\beta}}{R^2L^2} \tag{II-28}$$

Similarly, Eq (I-23) becomes

$$\bar{E} = e\left[\hat{n}\left\{\frac{1}{R^2L^2} - \frac{\beta^2}{R^2L^3} + \frac{\hat{n}\cdot\bar{\beta}}{R^2L^3}\right\} - \bar{\beta}\left\{\frac{1}{R^2L^2} - \frac{\beta^2}{R^2L^3} + \frac{\hat{n}\cdot\bar{\beta}}{R^2L^3}\right\} + \frac{\hat{n}(\hat{n}\cdot\dot{\bar{\beta}})}{cRL^3} - \frac{\dot{\bar{\beta}}}{cRL^2} - \frac{\bar{\beta}(\hat{n}\cdot\dot{\bar{\beta}})}{cRL^3}\right] \tag{II-29}$$

Now

$$\frac{1}{R^2L^2} - \frac{\beta^2}{R^2L^3} + \frac{\bar{\beta}\cdot\hat{n}}{R^2L^3} = \frac{1}{R^2L^3}\left(L + \bar{\beta}\cdot\hat{n} - \beta^2\right) = \frac{1-\beta^2}{R^2L^3} \tag{II-30}$$

Also

$$\frac{\hat{n}(\hat{n}\cdot\dot{\bar{\beta}})}{cRL^3} - \frac{\dot{\bar{\beta}}}{cRL^2} - \frac{\bar{\beta}(\hat{n}\cdot\dot{\bar{\beta}})}{cRL^3}$$

$$= \frac{1}{cRL^3}\left[(\hat{n}\cdot\dot{\bar{\beta}})\hat{n} - L\dot{\bar{\beta}} - (\hat{n}\cdot\dot{\bar{\beta}})\bar{\beta}\right]$$

$$= \frac{1}{cRL^3}\,\hat{n}\times\left[(\hat{n}-\bar{\beta})\times\dot{\bar{\beta}}\right] \tag{II-31}$$

Substituting Eqs. (II-30,31) into Eq. (II-29), there is obtained (Ref. 1, p. 467)

$$\bar{E} = e\left[\frac{1}{R^2L^3}(\hat{n}-\bar{\beta})(1-\beta^2) + \frac{1}{cRL^3}\hat{n}\times\left\{(\hat{n}-\bar{\beta})\times\dot{\bar{\beta}}\right\}\right] \tag{II-32}$$

From Eq. (II-24),

$$\bar{B} = e\left[\frac{1}{R^2L^3}(1-\beta^2)(\bar{\beta}\times\hat{n}) + \frac{1}{cRL^3}\hat{n}\times\left(\hat{n}\times\left\{(\hat{n}-\bar{\beta})\times\dot{\bar{\beta}}\right\}\right)\right] \tag{II-33}$$

To convert Eqs. (II-24,32,33), which are in CGS units to MKS units, replace $\bar{E}$ by

$\bar{E}\sqrt{4\pi\varepsilon_0}$, e by $e/\sqrt{4\pi\varepsilon_0}$, and $\bar{B}$ by $\bar{B}\sqrt{4\pi/\mu_0}$.

For the sake of completeness, these equations in MKS units are given below as they appear in a standard text (Ref. 2, p. 356):

$$\bar{B} = \frac{\bar{r}\times\bar{E}}{rc} \tag{II-34}$$

$$\bar{E} = \frac{e}{4\pi\varepsilon_0}\left[\frac{1}{s^3}\left(\bar{r}-\frac{r\bar{u}}{c}\right)\left(1-\frac{u^2}{c^2}\right) + \frac{1}{c^2s^3}\left\{\bar{r}\times\left[\left(\bar{r}-\frac{r\bar{u}}{c}\right)\times\dot{\bar{u}}\right]\right\}\right] \tag{II-35}$$

$$\bar{B} = \frac{e}{4\pi\varepsilon_0c^2}\left[\frac{\bar{u}\times\bar{r}}{s^3}\left(1-\frac{u^2}{c^2}\right) + \frac{1}{cs^3}\frac{\bar{r}}{r}\times\left\{\bar{r}\times\left[\left(\bar{r}-\frac{r\bar{u}}{c}\right)\times\dot{\bar{u}}\right]\right\}\right] \tag{II-36}$$

The following relationships hold between the symbols in Eqs. (II-34,35,36) taken from Ref. 2 and those used heretofore, taken from Ref. 1:

$$\begin{array}{ll} \underline{\text{Ref. 2}} & \underline{\text{Ref. 1}} \\ \bar{r} & = \bar{R} = R\hat{n} \\ \bar{u} & = \bar{v} \\ \bar{u}/c & = \bar{v}/c = \bar{\beta} \end{array} \tag{II-37}$$

$$s = r - \frac{\bar{u}}{c}\cdot\bar{r} = R - \bar{\beta}\cdot\bar{R} = R(1-\bar{\beta}\cdot\hat{n}) = RL$$

$$\bar{r} - r\frac{\bar{u}}{c} = \bar{R} - R\bar{\beta} = R(\hat{n}-\bar{\beta})$$

2. DISCUSSION OF THE FIELDS

The E field given by Eq. (II-36) has three terms which depend differently upon the particle velocity $\bar{\beta} = \bar{v}/c$. For a stationary charge $\bar{\beta} = \dot{\bar{\beta}} = 0$, $L = 1$, and the field reduces to the ordinary static field (MKS units)

$$\bar{E} = \frac{e\hat{n}}{4\pi\varepsilon_0 R^2} \tag{II-38}$$

For a charge moving at constant velocity, $\dot{\bar{\beta}} = 0$, and another term varying as $1/R^2$ appears, which is termed the quasi-static or induction field. For an accelerating charge, $\dot{\bar{\beta}} \neq 0$, and the third term in Eq. (II-32), which depends upon acceleration $\dot{\bar{\beta}}$ varies as $1/R$ and therefore represents radiation. Similar remarks apply to the $\bar{B}$ fields. Equation (II-33) shows there is an induction field varying as $1/R^2$ which depends upon velocity $\bar{\beta}$, and a radiation field varying as $1/R$ which depends upon acceleration $\dot{\bar{\beta}}$.

3. RADIATION FIELDS FOR THE LOW-VELOCITY CASE

Equations (II-32,33) apply to all possible velocities. The physics literature is replete with examples and applications to high velocity particles (relativistic case). However, the r. f. antenna engineer is concerned mostly with charges that move in or on conductors. While the field waveforms (also current and voltage waveforms) can move at essentially the speed of light c along antennas or transmission line conductors, the charges themselves move only at very low velocities compared to c. This is discussed in detail in Appendix IV. For such low-velocity particles, $\beta = v/c$ is very small compared to unity, and the following approximations hold:

$$\begin{aligned} &\beta \ll 1 \\ &L = 1 - \hat{n} \cdot \hat{\beta} \approx 1 \\ &1 - \beta^2 \approx 1 \\ &\hat{n} - \bar{\beta} \approx \hat{n} \end{aligned} \qquad \text{(II-39)}$$

The radiation terms in Eqs. (II-32,33), denoted by subscript "a" for acceleration, become

$$\bar{E}_a = \frac{e}{c^2}\left[\frac{\hat{n}\times(\hat{n}\times\bar{a})}{R}\right]_{ret} \qquad \text{(II-40)}$$

$$\bar{B}_a = \frac{e}{c^2}\left[\frac{\bar{a}\times\hat{n}}{R}\right]_{ret} \qquad \text{(II-41)}$$

where $\bar{a} = \dot{v} = c\dot{\bar{\beta}} =$ acceleration.

For the special case where $\bar{a}$ is perpendicular to $\bar{R}$ ("broadside" radiation),

$$\bar{E}_a = -\frac{e}{c^2}\left[\frac{\bar{a}}{R}\right]_{ret} \qquad \text{(II-42)}$$

$$\bar{B}_a = \frac{e}{c^2}\left[\frac{\bar{a}\times\hat{n}}{R}\right]_{ret} \qquad \text{(II-43)}$$

In MKS units, Eqs (II-42,43) are

$$\bar{E}_a = -\frac{e}{4\pi\varepsilon_0 c^2}\left[\frac{\bar{a}}{R}\right]_{ret} \qquad \text{(II-44)}$$

$$\bar{B}_a = -\frac{e}{4\pi\varepsilon_0 c^3}\left[\frac{\bar{a}\times\hat{n}}{R}\right]_{ret} \qquad \text{(II-45)}$$

which agree with Ref. 4 (pp. 376,387).

APPENDIX III

WAVE PROPAGATION ON TRANSMISSION LINES AND LINEAR ANTENNAS

1. TRAVELING WAVES ON LOSSLESS TRANSMISSION LINES

This section is intended to introduce traveling wave concepts. Voltage and current waves, which may be arbitrary functions of time, travel on the idealized, lossless, transmission line at a velocity given by

$$v = \frac{1}{\sqrt{LC}} \ \text{m/s} \qquad \text{(III-1)}$$

where L is the distributed inductance in henrys per meter and C is the distributed capacity in farads per meter of line (Ref. 5, p. 12). For an air medium, v = c = velocity of light = 3 x 10 m/s. The ratio of voltage to current is the characteristic impedance

$$Z_0 = \sqrt{L/C} \ \text{ohms} \qquad \text{(III-2)}$$

The argument of traveling-wave functions $i\ (z,t\ )$ on such lines is of the form $(\ t \pm z/v\ )$. A step-function traveling-wave current is given by

$$i(z,t) = I\,U(t - z/v) \qquad \text{(III-3)}$$

where $U(t-a)$ is the step function of unit amplitude for $t > a$, and of zero amplitude for $t < a$. A step function at $(z=0, t=0)$ will arrive at z at time $t = z/v$.

The above transmission line is a special case of the broader class of guided systems using the TEM mode of propagation (Ref. 6, p. 177). For such systems, assuming lossless conductors and dielectrics, the fields and their associated currents and voltages again may be arbitrary functions of time, and again travel undistorted at the velocity

$$v = \frac{1}{\sqrt{\mu \varepsilon}} \qquad \text{(III-4)}$$

For air media, v = c.

2. TRAVELING WAVES WITH SINUSOIDAL TIME VARIATION ON LOSSY LINES

A sinusoidally-time varying traveling-wave on a lossy line is of the form

$$i(z,t) = I e^{-\alpha z} \cos(\omega t - \beta z) \qquad \text{(III-5)}$$

where α is the attenuation constant (neps/m) and β is the propagation constant (rad/m). The propagation function γ is

$$\gamma = \alpha + j\beta \qquad \text{(III-6)}$$

and is given by

$$\gamma = \left[(R + j\omega L)(G + j\omega C) \right]^{1/2} \qquad \text{(III-7)}$$

where R,G are the series resistance and shunt conductance per meter, respectively. The phase velocity and characteristic impedance are now functions of frequency, whose equations are given in the literature (Ref. 5, Chap. 4). The various frequency components of any time waveform now travel at different velocities and also attenuate differently, resulting in distortion of any original waveform.

3. WAVE TRAVEL OF STEP-FUNCTIONS AND PULSES ON LOSSY LINES

Many of the characteristics of pulse waveforms traveling on linear antennas depend upon the propagation of such signals on linear transmission lines. The propagation of pulses or step-function wavefronts on lossy lines has been investigated (Ref. 5, Chap. 7). Such waveforms imply wide-band frequency components. There are at least two approaches to this problem. The first assumes that L, C, R, and G are frequency-independent. The second approach, which is claimed to be more realistic (Ref. 5, pp. 5 and 112), includes skin effects, and assumes that the resistance and the inductance arising from internal flux linkages vary as the square root of frequency, the same as the high-frequency asymptotes of these parameters. G is assumed to be ignorable, and C is assumed constant.

For the solutions (based upon Laplace transform methods) and graphs of the behaviour of step-function voltages and currents on such lossy lines, details are available (Ref. 5, Chap. 7). In this appendix, some conclusions will be reviewed. For both of the approaches mentioned above, a time delay

$$t_{delay} = \ell\sqrt{LC} \qquad \text{(III-8)}$$

elapses before the voltage (or current) at distance ℓ from an applied step function becomes non-zero. The velocity of propagation of a step-function may be said to be $v = 1/\sqrt{LC}$ only in the sense that this governs the elapsed time between switch-on time and the time when some effects begin to take place at distance ℓ away. The calculation of these effects (i.e., rise time) depends upon which of the two approaches mentioned above is taken.

For the variable-parameter approach, at the instant of arrival of the wavefront at distance ℓ from the source, the solution predicts a smoothly changing rise in voltage and current, with finite rates of rise inversely proportional to ℓ^2. Thus the practical result of skin effect is to produce finite slopes of rise and fall of applied square pulses.

4. VELOCITY OF PROPAGATION ALONG A THIN WIRE ANTENNA

The current produced on an antenna by a transmitter is a boundary value problem. Several methods have been used to solve this problem (Ref. 7, pp. 176-180). In this section, a method due to Pocklington (Ref. 8) will be reviewed briefly, following Jones (Ref. 7). The details give insight into the phenomenon of wave propagation along a wire antenna. Pocklington was able to show that the current on a thin wire is sinusoidally distributed for sinusoidal time excitation, and that the velocity of the wave $\approx$ the velocity of light c.

The mathematics involved will be described mostly in words. The field $\bar{E}$ is written as an integral of the current, which in turn is used to set up an integral equation for the current. Assume a perfectly conducting body S (antenna less feeder and receiver) in an external applied field $\bar{E}_0 e^{j\omega t}$. The resultant total field $\bar{E} e^{j\omega t}$ is the sum of $\bar{E}_0$ and an integral of the surface current linear density $\bar{J}_s$ over S. By using the boundary condition that the tangential component of $\bar{E} = 0$ on S, the integral equation for $\bar{J}_s$ is obtained.

Restriction to thin wires, with radius a small compared to antenna length and to the wavelength, reduces the integral equation to one dimension. The wire need not be straight, but sharp changes in curvature are not allowed. To find how a disturbance propagated along the wire, Pocklington set $\bar{E}_0 = 0$, and retained only the dominant terms in the integral equation for $\bar{J}_s$. To this approximation, the solution for the antenna current $I(\ell) = 2\pi a J_s$ at distance ℓ from the origin is found to be

$$I(\ell) = (Ae^{-jk\ell} + Be^{jk\ell})e^{j\omega t} \qquad \text{(III-9)}$$

where

$$k^2 = \omega^2 \mu \varepsilon \qquad \text{(III-10)}$$

Using

$$R_e\left[e^{-jk\ell} e^{j\omega t}\right] = \cos(\omega t - k\ell) \qquad \text{(III-11)}$$

the velocity of propagation is seen to be

$$v = \frac{\omega}{k} = \frac{1}{\sqrt{\mu\varepsilon}} \qquad \text{(III-12)}$$

Thus, for air, the propagation velocity along the wire is v = c.

5. SOME CHARACTERISTICS OF WAVE PROPAGATION ALONG A THIN-WIRE LINE

A traveling wave of current along a thin-wire line extending along the Z-azis may be represented by

$$I(z,t) = I(t - z/c) \qquad \text{(III-13)}$$

for propagation in the positive Z direction. The velocity of propagation has been taken as essentially equal to that of light c. The current I is related to the current density $\bar{J}$ (amps. per sq. m.) by

$$I(z,t) = \int_S \bar{J}(z,t) \cdot d\bar{S} \qquad \text{(III-14)}$$

where S is the cross-section of the wire. Determination of the variation of $\bar{J}$ with depth is a boundary-value problem which is not addressed here. The integral of J over the cross-section in Eq. (III-14) may be replaced by the product of a mean J taken as constant over some cross-section area A characteristic of the particular problem. Thus

$$I(z,t) \equiv J(z,t)\,A \qquad \text{(III-15)}$$

For example, for a round wire, A might be taken, as a first approximation, as the cross-section area of the layer of thickness δ beneath the wire's surface where δ is a mean skin depth. Then

$$J(z,t) = A^{-1}\,I(t-z/c) \qquad \text{(III-16)}$$

We now investigate the magnitude of the ratio of $(\rho\,\partial v/\partial t)$ to $(v\,\partial\rho/\partial t)$, where ρ is the electron charge density, and v is the electron drift velocity. These quantities arise when the time derivative of I(Z,t) is used in calculation of radiation. The term $(\rho\,\partial v/\partial t)$ represents charge acceleration in the Z-direction and will be shown to be much greater than the other term $(v\,\partial\rho/\partial t)$, which represents time-rate-of-change of charge density.

Using

$$\bar{J} = \rho\,\bar{v} \qquad \text{(III-17)}$$

there results

$$A^{-1}\frac{\partial I}{\partial t} = \frac{\partial J}{\partial t} = \rho\frac{\partial v}{\partial t} + v\frac{\partial \rho}{\partial t} \qquad \text{(III-18)}$$

The continuity equation $\nabla\cdot\bar{J} = -\partial\rho/\partial t$ reduces, in this one-dimensional case to

$$\frac{\partial J}{\partial z} = -\frac{\partial \rho}{\partial t} \qquad \text{(III-19)}$$

From Eq. (III-16)

$$\frac{\partial J}{\partial z} = -\frac{A^{-1}}{c}I' \qquad \text{(III-20)}$$

where I' is the derivative of I with respect to its argument (t-Z/c). Likewise

$$\frac{\partial J}{\partial t} = A^{-1}I' \qquad \text{(III-21)}$$

Combining Eqs. (III-20,21)

$$-c\frac{\partial J}{\partial z} = \frac{\partial J}{\partial t} \qquad \text{(III-22)}$$

Substituting Eqs. (III-19,22) into Eq. (III-18),

$$c\frac{\partial \rho}{\partial t} = \rho\frac{\partial v}{\partial t} + v\frac{\partial \rho}{\partial t}$$

$$\therefore \quad \frac{\rho(\partial v/\partial t)}{v(\partial \rho/\partial t)} = \frac{c}{v}\left(1-\frac{v}{c}\right) \qquad \text{(III-23)}$$

Since $v/c \ll 1$, as shown in Appendix IV, then

$$\frac{\rho(\partial v/\partial t)}{v(\partial \rho/\partial t)} \approx \frac{c}{v} \gg 1 \qquad \text{(III-24)}$$

Thus the "acceleration" term ($\rho\,\partial v/\partial t$) dominates the ($v\,\partial \rho/\partial t$) term in $\partial I/\partial t$ by many orders of magnitude (about 10^8). That is,

$$A^{-1}\frac{\partial I}{\partial t} \approx \rho\frac{\partial v}{\partial t} \qquad \text{(III-25)}$$

6. SURFACE CHARGES

From Eq. (III-19) it is seen that there is no change of charge density ρ wherever the current is uniform (i.e., constant) in Z. However, if the current is not uniform along Z (at fixed time t), then Eq. (III-19) shows that there must be a change in ρ with time. Such an antenna can be represented as a chain of small current elements or Hertzian dipoles each of length dl, with end charges which change differentially from element to element (Ref. 6, p. 322). These adjacent charges do not cancel, and the non-cancelled charges appear on the surface of the wire, where they produce an electric field normal to the wire's surface (Ref. 6, p. 322). This is illustrated in Fig. 40, based upon figures in Ref. 6 (p. 322). For a Hertzian dipole, discussed in Appendix V, the radiation fields can be obtained from the longitudinal (Z-direction) acceleration of the charges in the wire, or, equivalently, the time-derivative of the current.

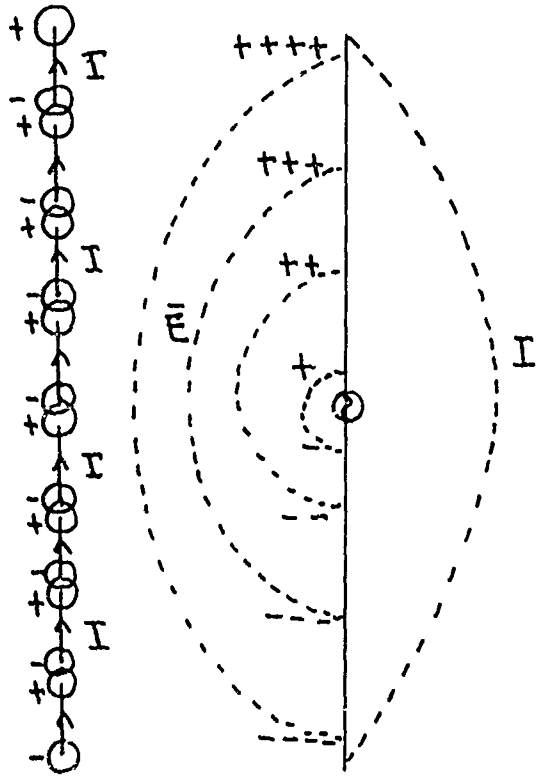

FIG. 40 Chain of dipoles and current, charge and local $\overline{E}$ field distributions.

The continuity equation automatically takes into account the net charges present at the dipole ends. This comment holds equally well for a finite-sized linear antenna with non-uniform current distribution, by superposition of the elementary dipoles.

Some comments are now made about surface charges on a bent thin-wire line. According to Torre and Longo (Ref. 9, p. 391) the current and current density $\bar{J}$ must follow the bends, and therefore the internal $\bar{E}$ field given by $\bar{J} = \sigma\bar{E}$ must also follow bends. Thus electric flux follows the bends with the current (Ref. 9, p. 391). In order for this to be possible, additional surface charges must appear at the bends, as shown in Fig. 41, (Ref. 9, p. 391). The net result of this, for the time-varying case, has not been investigated by this writer, except that it appears clear that the centripetal acceleration experienced by charges moving in the wire around bends must be due to the fields produced by these surface charges. These remarks apply strictly to a generator-driven loop, and not a loop being driven by an externally-applied changing magnetic flux. In the latter case the induced $\bar{E}$ field has nonzero curl, and forms closed loops without requiring any charges.

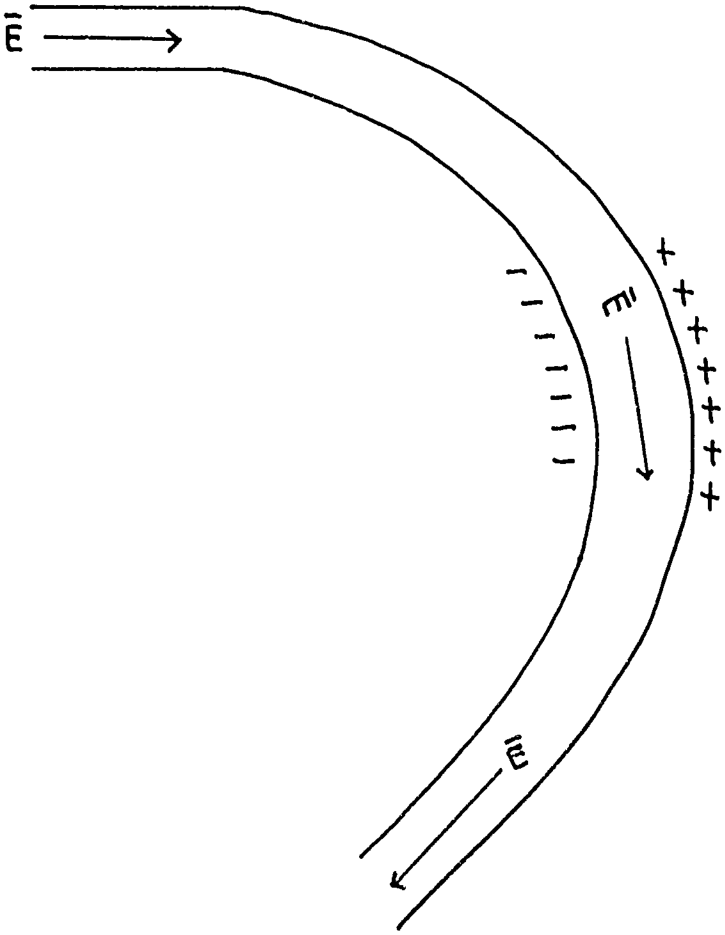

FIG. 41 Surface charges at a bend in a conductor carrying current.

APPENDIX IV

DRIFT VELOCITY OF ELECTRONS IN CONDUCTORS

1. FREE ELECTRON THEORY OF METALS

According to the free electron theory of metals, a conductor is a lattice of positive ions among which some electrons are free to move under the influence of external fields. In monovalent metals such as copper, silver, and gold, the number of electrons averages about one per atom (Ref. 9, p. 144). For copper this constitutes a free electron density $N \approx 10^{25}$ per m^3 (Ref. 9, p. 147)

2. RELAXATION TIMES

A net (nonzero) charge density ρ (coulombs per m^3) cannot exist permanently inside a conductor (Ref. 10, p. 15, also Ref. 11, p. 78). In the absence of an external time-varying field, any pre-existing charge inside a conductor decays exponentially and flows to the surface. The transient decay equation may be derived as follows (Ref. 10, p. 15):

$$\bar{J} = \sigma \bar{E} \qquad \text{(IV-1)}$$

$$\nabla \cdot \bar{J} = -\frac{\partial \rho}{\partial t} \qquad \text{(IV-2)}$$

Equation (IV-1) is Ohm's law, which will be modified subsequently, and Eq. (IV-2) is the continuity equation.

Hence

$$-\frac{\partial \rho}{\partial t} = \sigma \nabla \cdot \bar{E} = \frac{\sigma}{\varepsilon} \nabla \cdot \bar{D} = \frac{\sigma}{\varepsilon} \rho$$

Thus the differential equation for ρ is

$$\frac{\partial \rho}{\partial t} - \frac{\sigma}{\varepsilon} \rho = 0 \qquad \text{(IV-3)}$$

The solution of Eq. (IV-3) is

$$\rho(t) = \rho(0) \exp.\left(-\frac{t}{\varepsilon/\sigma}\right) \qquad \text{(IV-4)}$$

The decay time (ε/σ) is called the relaxation time constant (Ref. 11, p. 78) τ_1 , so

$$\tau_1 = \varepsilon/\sigma \qquad \text{(IV-5)}$$

For copper $\tau_1 \approx 10^{-19}$ sec., which is far less than any characteristic times in microwaves or radio impulse systems. This decay process is entirely independent of an applied field, if present (Ref. 11, p. 78).

There is another time constant referred to as the electron "relaxation time" of a metal (Ref. 9, p. 358; Ref. 12, p. 292), which is the mean free time t_f between collisions of an average electron and the lattice ions, and is on the order of 10^{-14} secs. for copper (Ref. 13, p. 481). This is the time constant of the exponential decay of the electron drift velocity after all excitation is removed, as shown below. Again, this time constant [illegible] is much less than typical characteristic [illegible]

[illegible]. The significance of this [illegible] the equations governing the [illegible]

[illegible] VELOCITY OF ELECTRONS

[illegible] drift velocity [illegible] derived [illegible], p. 635.)

[illegible] due to field E is much less than the [illegible] free time is unaffected by the [illegible] is small enough so that the electron [illegible]

[illegible] velocity $\bar{V}_d$ of N electrons [illegible]

$$[illegible]$$

[illegible]

$$[illegible]$$

[illegible]

$$m\bar{V}_d/\tau = -e[illegible]$$

From Eqs. (II-7.8),

[illegible]

Assuming conductivity [illegible]

[illegible]

then

[illegible]

Since N, e, m are known, [illegible] measured σ. For copper [illegible] mho/m, and using $e = -1.6 \times 10^{-19}$ coulomb [illegible] $\times 10^{-14}$ sec.

Now suppose [illegible] compared to [illegible] the force Eq. [illegible]

[illegible]

The terms [illegible]

[illegible]

is

[illegible]

Thus the drift velocity $\bar{V}_d$ decays exponentially with time constant t_f, if an applied field is removed suddenly, as previously stated.

The $\bar{V}_d$ which results from a sinusoidally time-varying $\bar{E}(t) = \bar{E}_o e^{j\omega t}$ is (Ref. 13, p. 485)

$$m\left(j\omega + \frac{1}{t_f}\right)\bar{V}_d = -e\bar{E} \qquad \text{(IV-15)}$$

which is obtained from Eq. (IV-12) by replacing $\frac{d}{dt}$ by $j\omega$. Since $1/t_f >> \omega$, Eq. (IV-15) becomes

$$\frac{m\bar{V}_d}{t_f} \approx -e\bar{E} \qquad \text{(IV-16)}$$

which is the same as Eq. (IV-8) for a constant field E. Therefore, even up to frequencies on the order of 10^{13} Hertz, $\bar{V}_d$ and $\bar{J}$ remain in phase with $\bar{E}$, and Eqs. (IV-10,11) remain valid. This has been verified by experiments at K-band using $\omega = 2 \times 10^{11}$ rad/sec (Ref. 13, p. 481). Thus Ohm's law $\bar{J} = \sigma \bar{E}$ remains valid up to frequencies on the order of 10^{12} Hertz, where σ is the d.c. value. In turn, this implies that $\bar{V}_d$ is given correctly by Eqs. (IV-7,8).

An alternative approach to the behaviour of conductors at high frequencies is through the concept of the dynamic conductivity (Ref. 14, p. 237). The force equation on the

i^{th} electron is written in the standard form

$$m \frac{d\bar{V}_i}{dt} + b\bar{V}_i = -e\bar{E} \qquad \text{(IV-17)}$$

where

$\bar{V}_i$ = velocity of i^{th} electron

b = a constant to account for the frictional resistance encountered by an electron, proportional to velocity.

Ref. 14 defines

$$\bar{g} = -\sum_{i=1}^{N} e\bar{V}_i = -e\sum_{i=1}^{N} \bar{V}_i \qquad \text{(IV-18)}$$

From Eqs. (IV-6,7) it is seen that

$$\bar{g} = \bar{J} = -Ne\bar{V}_d \qquad \text{(IV-19)}$$

Multiplying Eq. (IV-17) by $-e$, and summing over N electrons,

$$m \frac{\partial\bar{J}}{\partial t} + b\bar{J} = Ne^2\bar{E} \qquad \text{(IV-20)}$$

For the stationary (d.c.) case, $\bar{J} =$ constant and Eq. (IV-20) reduces to

$$\bar{J} = \frac{Ne^2}{b}\bar{E} \qquad \text{(IV-21)}$$

For the stationary case, write Ohm's law as

$$\bar{J} = \sigma_0 \bar{E} \qquad \text{(IV-22)}$$

where σ_0 is defined as the stationary value (zero frequency) of the conductivity. Hence

$$\sigma_0 = \frac{Ne^2}{b} \tag{IV-23}$$

Equation (IV-20) becomes

$$\frac{\partial \bar{J}}{\partial t} + \frac{\bar{J}}{\tau} = \frac{Ne^2}{m}\bar{E} \tag{IV-24}$$

where

$$\tau = \frac{m}{b} = \frac{m\sigma_0}{Ne^2} \tag{IV-25}$$

For copper $\tau = 2.4 \times 10^{-14}$ sec. $\approx 10^{-14}$ sec. (Ref. 14, p. 238). From Eqs. (IV-11,25) it is seen that $\tau = t_f$, provided it is understood that the σ in Eq. (IV-11) is the stationary conductivity σ_0. In other words, the derivation leading to Eq. (IV-11), (Ref. 13), assumes that $\sigma = \sigma_0$. This assumption is valid for frequencies up to about 10^{12} Hertz, as will now be shown.

Write Eq. (IV-24) as

$$\tau \frac{\partial \bar{J}}{\partial t} + \bar{J} = \sigma_0 \bar{E} \tag{IV-26}$$

which is recognized as the dynamic generalization of Ohm's law Eq. (IV-22). For harmonic fields, $\bar{E}$ and $\bar{J}$ vary as $e^{j\omega t}$ and

Eq. (IV-26) becomes

$$(j\omega\tau+1)\bar{J}=\sigma_0\bar{E} \qquad \text{(IV-27)}$$

Defining the dynamic conductivity σ by

$$\bar{J}=\sigma\bar{E} \qquad \text{(IV-28)}$$

it is seen that

$$\sigma=\frac{\sigma}{j\omega\tau+1} \qquad \text{(IV-29)}$$

which is analogous to Eq. (IV-15). For frequencies less than 10^{12} Hertz, $\omega\tau \ll 1$, and $\sigma \approx \sigma_0$, so the dynamic Eq. (IV-26) reduces to the static version

$$\bar{J}=\sigma_0\bar{E} \qquad \text{(IV-30)}$$

Hence $\bar{V}_d$ may be calculated from

$$\bar{J}=-Ne\bar{V}_d=\sigma_0\bar{E} \qquad \text{(IV-31)}$$

4. ESTIMATION OF ELECTRON DRIFT VELOCITIES IN CONDUCTORS

The drift velocity V_d will be calculated first for several limiting stationary (d.c.) cases, and then estimated for the time-varying case.

As a first example consider a pair of parallel wires in air, each $1\ \text{mm.}^2$ in area (AWG No. 17), spaced 1 cm. center-to-center (Ref. 15, p. 126). Let the current be 6 amps, which is the maximum permissable for air-cooling, and the voltage be 2,200 volts, which is almost equal to the voltage breakdown limit in air. The excess (surface) charge on each wire, resulting from the capacity and impressed voltage, is 0.04 microcoulombs per meter, which is completely insignificant compared to the free electron charge transported by the current. For copper, with $N \approx 10^{29}$ electrons $/m^3$, the number of free electrons per meter is $10^{29} \times 10^{-6} = 10^{23}$. Hence the conduction electron charge is $10^{23} \times 1.6 \times 10^{-19} \approx 16$ kilocoulombs per meter, as compared to the surface charge of 0.04 microcoulombs per meter. The electron drift velocity follows from Eq. (IV-31):

$$J = \frac{\text{current } I}{\text{area } A} = N e V_d$$

$$V_d = \frac{I}{NeA} = \frac{6}{10^{29} \times 1.6 \times 10^{-19} \times 10^{-6}} \approx 4 \times 10^{-4}\, m/s$$

It is seen that this value of V_d is negligible compared to the velocity of light $c = 3 \times 10^{8}\, m/s$.

As a second example, consider the discussion of electric current and an example of the calculation of V_d by Sherwin (Ref. 16, p. 162-165). At any time t the free charges in all parts of a conducting loop have the same velocity V_d, the same magnitude of acceleration a, the same da/dt, etc., that is, the charges move in unison. Then if $n_0 =$ number of charged particles per meter whose flow is the current, and V_d is their average velocity, then the current i = coulombs/sec passing a point is given by

$$i = n_0 e V_d \qquad \text{(IV-32)}$$

Since n_0 and e are assumed constant, then the linear charge density $\rho_0 = n_0 e$ is constant. Then

$$\frac{di}{dt} = n_0 e \frac{dV_d}{dt} = n_0 e a \qquad \text{(IV-33)}$$

$$\frac{d^2 i}{dt^2} = n_0 e \frac{da}{dt} \qquad \text{(IV-34)}$$

Sherwin (Ref. 16) gives an example of a wire of diameter 1 mm, carrying current i = 100 amp., which is a large current for this size wire. Then $n_0 = N \times \text{area} \approx 10^{29} \times 10^{-6} = 10^{23}$ electrons per meter, and

$$V_d = \frac{i}{n_0 e} = \frac{100}{10^{23} \times 1.6 \times 10^{-19}} \approx 6 \times 10^{-3} \text{ m/s}$$

Sherwin (Ref. 16, p. 164-165) states that 100 amp. would cause serious heating in this wire, as a practical matter conduction electron velocities are rarely above 10^{-2} m/s.

Summarizing the above two examples, for currents which are uniformly distributed across the cross-section of a wire (d.c. and low frequency for small wires), the order of magnitude of the electron drift velocity is not more than 0.01 m/s.

The high frequency or short pulse case is now considered. Due to the skin effect, currents are not uniformly distributed across a conductor's cross-section. From Eq. (IV-7), the drift velocity V_d will vary with the distribution of the current density J across the cross-section. This also follows from Eq. (IV-8), since the field E varies similarly with the depth of penetration in the conductor. Hence calculation of V_d requires knowledge of either $\bar{J}$ or $\bar{E}$, per Eq. (IV 31). An estimate of V_d can be obtained by following the well-known assumption that a given wire at a given frequency carries its entire current uniformly distributed within the skin depth. Since the skin depth varies inversely with the square root of the frequency, the solution for a given exciting waveform will depend upon the frequency content of the waveform. Hence if we assume that a given total current I is confined uniformly with a skin depth determined by one of the higher frequency components of the waveform, the calculated $\bar{J}$ and V_d will be larger than the actual average $\bar{J}$ and V_d respectively. Since the V_d calculated in this manner is a high estimate of V_d, and since the resultant V_d is still many orders of magnitude less than c, as shown below, more accurate calculations for V_d, involving averaging, are not required.

As an example consider a pulse shaped as a symmetrical trapezoid, with rise and fall times = t_r sec. and with duration of the flat portion = T sec. The amplitude spectrum is (Ref. 17)

$$|A(f)| = (T+t_r)\left|\operatorname{sinc}(ft_r)\operatorname{sinc} f(T+t_r)\right| \tag{IV-35}$$

where sinc χ = sin ($\pi\chi$) / ($\pi\chi$). For $T=0$, the shape is that of an isosceles triangle, with base width = $2t_r$ sec, and spectrum given by

$$|A(f)| = t_r \operatorname{sinc}^2(ft_r) \tag{IV-36}$$

The first zero in $|A(f)|$ as given by Eq. (IV-36) occurs at frequency $f_0 = 1/t_r$ Hertz. For a relatively short pulse specified by $T=0$, $t_r = 10$ picoseconds, $f_0 = 100{,}000$ MHz. For copper, the skin depth δ millimeters) at frequency f (Hertz) is

$$\delta = 66/\sqrt{f} \tag{IV-37}$$

Hence for this example, $\delta \approx 2\times10^{-4}$ mm. Let us apply this to the case considered previously (Ref. 15) of a circular wire of diameter $\approx$ 1 mm., carrying I = 6 amps. of current. For the short pulse, assume that this current is crowded uniformly into a cross-section consisting of a layer just beneath the wire's surface of thickness δ . Without external cooling, this would be impossible, due to the increased heating compared to the already-marginal d.c. case. For the d.c. case, I is spread uniformly over the cross-section = $\pi d^2/4$. For the pulse case, I is assumed to be distributed over the layer cross-section = $\pi d \delta$. It then follows that

$$\frac{V_d}{(V_d)_{dc}} = \frac{J}{J_{dc}} = \frac{R}{R_{dc}} = \frac{d}{4\delta} \qquad \text{(IV-38)}$$

where R is the resistance per unit length. Equation (IV-38), as far as the resistance is concerned, is a well-known result (Ref. 18, p. 176). It is based upon the assumption that the dynamic conductivity $\sigma = \sigma_{dc}$, which is valid up to $f = 10^{12}$ Hertz, as discussed previously. For d = 1 mm. and $\delta = 2 \times 10^{-14}$ mm., the ratio $d/(4\delta)$ is approximately = 10^3 . Using $(V_d)_{dc} = 4 \times 10^{-4}$ m/s, as previously obtained, it is seen that V_d for even this extreme case is 0.4 m/s, which is still negligible compared to c = 3×10^8 m/s.

It is concluded, therefore, that even for extremely short pulses of relatively large current amplitudes, an upper-bound estimate of V_d is about 1 m/s.

APPENDIX V

DERIVATION OF THE RADIATION FIELDS OF AN ELECTRIC DIPOLE USING MOVING CHARGES

The term "Hertzian dipole" is used to describe the following configuration (Ref. 19, p. 148): A charge $+e$ moves along a straight line about a stationary charge $-e$ to form an electric dipole moment $\bar{p}(t)$ given by

$$\bar{p}(t) = e\,\bar{\ell} \tag{V-1}$$

where $\bar{\ell}$ is the vector denoting the separation of the charges, drawn from $-e$ to $+e$. For convenience, take $\bar{\ell}$ along the z-axis of a spherical coordinate system (r, θ, ϕ). The radiation fields of this dipole, in MKS units, derived from a Hertzian vector, are given by Sommerfeld as follows (Ref. 19, p. 150):

$$H_\phi = \frac{\sin\theta}{4\pi c r}\,\ddot{p}(t - r/c) \tag{V-2}$$

$$E_\theta = \frac{\sin\theta}{4\pi \varepsilon_0 c^2 r}\,\ddot{p}(t - r/c) \tag{V-3}$$

Here $(\dot{\ })$ denotes differentiation with respect to time t, and p is the time-varying amplitude of $\bar{p}(t)$.

For a periodically oscillating dipole,

$$p(t) = e\,l(t) \equiv p_0 \cos\omega t = \ldots (e^{i\omega t}) \quad \text{[illegible]}$$

[illegible] (II-3) become

$$H_\phi = -\frac{k\omega^2 \sin\theta}{4\pi c\,r}\, e^{-ikr}\, e^{i\omega t}$$

$$E_\theta = -\frac{k\omega^2 \sin\theta}{4\pi \epsilon_0 c^2 r}\, e^{-ikr}\, e^{i\omega t}$$

where $k = \omega/c$. For consistency with the rest of this [illegible] $e^{i\omega t}$ is used above, instead of $e^{-i\omega t}$ as in Ref. [illegible]

These radiation fields are easily derived from the radiation fields due to a charge moving at low relative velocities. Equations (II-40,41), in MKS units, [illegible]

[illegible]

$$[illegible]$$

$$[illegible]$$

The dipole moment is, in local [illegible]

[illegible]

where [illegible] is the unit vector along [illegible] tion [illegible] is

[illegible]

Hence

[illegible]

Equations [illegible]

[illegible]

[illegible]

Since [illegible] is the [illegible]

[illegible]

[illegible]

where [illegible]

[illegible] system. Hence

[illegible]

[illegible]

[illegible] (2-6, [illegible]).

[illegible] literature, the term 'Hortzian [illegible] [illegible] to describe a center-driven symmetrical [illegible] [illegible] whose arms (length) are very short [illegible] [illegible] 22, p. 198), or a very small [illegible] element 3 which is part of a larger [illegible] [illegible] (22, p. 221). To isolate this [illegible] [illegible] be [illegible] in small spheres or [illegible] [illegible] so as to satisfy the equation of [illegible]

[illegible] compared [illegible]

[illegible]

[illegible]

[illegible]

[illegible] is shown. [illegible] current element [illegible]

from 0 to [illegible]. The coupling [illegible]

[illegible]

For [illegible]

density [illegible]

[illegible]

where [illegible] the [illegible]

current distribution. By definition [illegible]

in Z, hence [illegible]

[illegible]

Then, integrating over the interval $(h-\Delta z, h)$

$$\int_{h-\Delta z}^{h} -\frac{J}{\Delta z}\, dz = -J = -\frac{\partial}{\partial t}\int_{h-\Delta z}^{h} \rho\, dz$$

Multiplying by A, the desired equation is obtained,

$$I = JA = \frac{\partial}{\partial t}\int_{h-\Delta z}^{h} \rho A\, dz = \frac{\partial}{\partial t} q_{end} \qquad \text{(V-19)}$$

where

$$q_{end} \equiv \lim_{\Delta z \to 0} \int_{h-\Delta z}^{h} \rho A\, dz \qquad \text{(V-20)}$$

The dipole moment of the above isolated current element dipole is then

$$p(t) = q(t)\, h = \left(\int I\, dt\right) h \qquad \text{(V-21)}$$

Thus

$$\ddot{p}(t-r/c) = \dot{I}(t-r/c)\, h \qquad \text{(V-22)}$$

and the radiation field, from Eq. (V-2) is

$$H_\phi = \frac{\sin\theta}{4\pi c r}\, \ddot{p}(t-r/c) = \frac{\sin\theta}{4\pi c r}\, \frac{\partial}{\partial t} I(t-r/c)\, h \qquad \text{(V-23)}$$

For the harmonic oscillation case, it is assumed that

$$I(t) = I_0\, e^{j\omega t} \qquad \text{(V-24)}$$

From Eq. (V-23) the radiation field is

$$H_\phi = \frac{\sin\theta}{4\pi c r} j\omega I_o h e^{j\omega t} e^{-jkr} \qquad \text{(V-25)}$$

which is a well-known result (Ref. 20, p. 498). To obtain this from Sommerfeld's results, note that the complex $p(t)$ is

$$p(t) = q(t) h = \frac{I_o h}{j\omega} e^{j\omega t} \qquad \text{(V-26)}$$

Since

$$p(t) \equiv A_o \cos\omega t = R_e \left[\frac{I_o h}{j\omega} e^{j\omega t} \right] \qquad \text{(V-27)}$$

it follows that

$$A_o = \frac{I_o h}{j\omega} \qquad \text{(V-28)}$$

Then the Sommerfeld result Eq. (V-5) reduces immediately to Eq. (V-25).

Equation (V-25) will now be derived directly from the fields due to moving charges for the sinusoidally time-varying current element dipole of length h described above. Consider a differential length dz at position $(0, 0, z)$ along the dipole. The charge dq in this length is

$$dq = \rho A dz \qquad (A = \text{area}) \qquad \text{(V-29)}$$

which is taken as the term e in Eqs. (V-7,8). The acceleration of this charge is found from differentiating $\bar{J} = \rho\bar{v}$. Thus

$$\dot{I} = \frac{d\bar{I}}{dt'} = A\frac{d\bar{J}}{dt'} = A\rho\frac{d\bar{v}}{dt'} = A\rho\bar{a} \qquad \text{(V-30)}$$

Then

$$e\bar{a} = \rho A\,dz\,\frac{\dot{\bar{I}}}{\rho A} = \dot{\bar{I}}\,dz \qquad \text{(V-31)}$$

Thus Eq. (V-7) becomes

$$d\bar{H}_a = \frac{1}{4\pi c}\left[\frac{\dot{\bar{I}}\,dz \times \hat{n}}{R}\right]_{ret} \qquad \text{(V-32)}$$

where R is the magnitude of the vector $\bar{R}$ from element dz to observation point $P(r,\theta,\phi)$. The total $\bar{H}_a$ field is found by integrating Eq. (V-32) over the dipole length h. Since $\bar{I}$ is in the z direction, then for this time-harmonic case it is

$$\bar{I} = I_0 e^{j\omega t'}\hat{a}_z \qquad \text{(V-33)}$$

and

$$\left[\dot{\bar{I}} \times \hat{n}\right]_{ret} = j\omega I_0 e^{j\omega(t-R/c)}\hat{a}_z \times \hat{a}_R$$

$$= I_0 e^{-jkR}\sin\theta\,\hat{a}_\phi\,e^{j\omega t} \qquad \text{(V-34)}$$

By definition the dipole length h is small enough so that the integral

$$\bar{H}_a = \frac{j\omega I_0}{4\pi c}\int_0^h \frac{e^{-jkR}\sin\theta\,\hat{a}_\phi}{R}\,e^{j\omega t}\,dz \tag{V-35}$$

may be replaced by

$$H_\phi(\bar{r},t) = \frac{\sin\theta}{4\pi c r}\,j\omega I_0 h\, e^{-jkr} e^{j\omega t} \tag{V-36}$$

Equation (V-36) is identical to Eq. (V-25).

The $\bar{E}$ field of the dipole may be found from Eq. (V-36) and the far-field Equation (II-34), which in MKS units is

$$\bar{E} = \sqrt{\mu_0/\varepsilon_0}\;(\bar{H} \times \hat{n}) \tag{V-37}$$

This gives

$$\bar{E} = \frac{j\omega I_0 h \sin\theta\,\hat{a}_\theta\, e^{-jkr}}{4\pi\varepsilon_0 c^2 r}\,e^{j\omega t} \tag{V-38}$$

Equation (V-38) can also be derived from the generalized Lienard-Wiechert potentials (see Eqs. (I-45,46)) and the differential operations described in Appendix I, or from the integral formulations for ϕ and A given by Eqs. (I-30,31). These derivations will not be reproduced here; for details see Maddocks (Ref. 3).

APPENDIX VI

SOME RESULTS OF DELTA FUNCTION INTEGRALS

An integral which appears at several places in this report (e.g., Eqs. (102, I-33)), is of the following type:

$$I = \int g(x)\,\delta\left(f(x)-d\right)dx \qquad \text{(VI-1)}$$

In Ref. 1 (p. 465) this appears as

$$I = \left.\frac{g(x)}{df/dx}\right|_{f(x)=d} \qquad \text{(VI-2)}$$

This is not quite correct. From Ref. 1 (p. 4, example (5)),

$$\delta\left(f(x)\right) = \left.\frac{\delta(x-x_0)}{|df/dx|}\right|_{f(x_0)=0} \qquad \text{(VI-3)}$$

the correct result is

$$I = \left.\frac{g(x)}{|df/dx|}\right|_{f(x)=d} \qquad \text{(VI-4)}$$

This can also be shown starting from the basic equation (Ref. 36, p. 76)

$$\delta(ax) = \frac{\delta(x)}{|a|} \qquad \text{(VI-5)}$$

In Eq. (I-33), the variable is t' instead of x. Since $df(t')/dt' \geq 0$ (see Eq. (I-40)), no error results in omitting the $|\ |$ symbol.

Eq. (102) is of the same form as Eq. (VI-1), the variable being z, and $g(z)=1$. Let

$$f(z) \equiv -z(1-\cos\theta)/c$$

$$\therefore \left|\frac{df(z)}{dz}\right| = \frac{|1-\cos\theta|}{c}$$

$$\alpha \equiv -(t-r/c)$$

Using $g(z)=1$ in Eq. (VI-4), Eq. (102) becomes

$$H_\phi = \frac{I_o \sin\theta}{4\pi r c} \frac{c}{|1-\cos\theta|} \qquad \text{(VI-6)}$$

at

$$-z(1-\cos\theta)/c = -(t-r/c)$$

or,

$$t = \frac{r}{c} + \frac{z}{c}(1-\cos\theta) \qquad \text{(VI-7)}$$

Since $(1\pm\cos\theta)\geq 0$, $|1\pm\cos\theta|$ may be replaced by $(1\pm\cos\theta)$. For $0\leq z\leq h$, Eqs. (VI-6,7) yield

$$H_\phi = \frac{I_o U(t-r/c)}{4\pi r} \frac{1+\cos\theta}{\sin\theta} \qquad \text{(VI-8)}$$

$$\frac{r}{c} \leq t \leq \frac{r}{c} + \frac{h}{c}(1-\cos\theta) \qquad \text{(VI-9)}$$

which is the same as Eq. (107).

APPENDIX VII

ILLUSTRATIONS OF USE OF EQUATION (74) FOR SOME STANDARD ANTENNAS WITH SINUSOIDAL TIME-VARYING EXCITATION

1. TRAVELING-WAVE ANTENNA

The traveling-wave current distribution on a terminated wire antenna of length L placed along the Z-axis from -L/2 to L/2 is (Ref. 6, p. 342)

$$I(z,t) = I_m e^{-jkz} e^{j\omega t} \tag{VII-1}$$

Eq. (74) yields

$$H_\phi(r,t) = \frac{\sin\theta}{4\pi c} j\omega I_m e^{j\omega t} \int_{-L/2}^{L/2} \frac{e^{-jkz} e^{-jkR}}{R}\, dz \tag{VII-2}$$

The usual far-field approximation, $r \gg z$,

$$R \approx r - z\cos\theta \tag{VII-3}$$

substituted into Eq. (VII-2) yields

$$H_\phi = \frac{\sin\theta}{4\pi rc} j\omega T_m e^{j\omega t} e^{-jkr} \int_{-L/2}^{L/2} e^{-jkz(1-\cos\theta)}\, dz$$

$$= \frac{I_m e^{-jkr} e^{j\omega t}}{2\pi r} \; \frac{\sin\theta}{1-\cos\theta} \sin\left[\frac{kL}{2}(1-\cos\theta)\right]$$

$$H_\phi = \frac{I_m}{4\pi r} e^{-jkr} e^{j\omega t} \frac{\sin\theta}{1-\cos\theta} \left[2 - 2\cos k(1-\cos\theta)L\right]^{1/2} \tag{VII-4}$$

$$E_\theta = H_\phi \sqrt{\mu_0/\varepsilon_0} \tag{VII-5}$$

Eq. (VII-5) agrees with (Ref. 6, p. 342).

2. HALF-WAVE LENGTH DIPOLE

Consider a dipole along the Z-axis, centered at the origin, of total length $2h = \lambda/2$. See Fig. 24. For sinusoidal time-variation, the currents on the antenna are known to be closely approximated by (Ref. 6, p. 328)

$$I(z,t) = I_m \sin k(h-z)\, e^{j\omega t} \qquad (z>0) \tag{VII-6}$$

$$I(z,t) = I_m \sin k(h+z)\, e^{j\omega t} \qquad (z<0) \tag{VII-7}$$

Then

$$\begin{aligned} I(z,t-R/c) &= I_m \sin k(h \mp z)\, e^{j\omega(t-R/c)} \\ &= I_m \sin k(h \mp z)\, e^{-jkR} e^{j\omega t} \end{aligned}$$

$$\therefore \frac{\partial}{\partial t} I(z,t-R/c) = j\omega I_m \sin k(h \mp z)\, e^{-jkR} e^{j\omega t} \tag{VII-8}$$

Using Eq. VII-8,

$$\frac{\partial}{\partial t} I(z, t - R/c) = j\omega I_m \sin k(h \mp z) e^{jkz\cos\theta} e^{-jkr} e^{j\omega t} \qquad \text{(VII-9)}$$

Introducing Eq. (74), and integrating, there is obtained

$$H_\phi = f\left[\int_{-h}^{0} \sin k(h+z) e^{jkz\cos\theta} dz + \int_{0}^{h} \sin k(h-z) e^{jkz\cos\theta} dz\right] \qquad \text{(VII-10)}$$

$$f \equiv \frac{\sin\theta}{4\pi c r} j\omega I_m e^{j(\omega t - kr)} \qquad \text{(VII-11)}$$

The integral in Eq. (VII-10) is (Ref. 6, p. 329)

$$\frac{2}{k} \frac{\cos\left(\frac{\pi}{2}\cos\theta\right)}{\sin^2\theta}$$

Hence, using $k = \omega/c$,

$$H_\phi = \frac{j I_m}{2\pi r} \frac{\cos\left(\frac{\pi}{2}\cos\theta\right)}{\sin\theta} e^{j(\omega t - kr)} \qquad \text{(VII-12)}$$

which is a well-known result (Ref. 6, Eq. (10-59)).

3. LINEAR ANTENNA WITH ARBITRARY CURRENT DISTRIBUTION I(Z,t)

For sinusoidal time-varying current distributions such as discussed in subsections 1 and 2 above, the current can be represented as the product of two separate functions

$$I(z,t) = I_1(z) e^{j\omega t} \qquad \text{(VII-13)}$$

Then

$$\frac{\partial}{\partial t} I(z, t-R/c) = j\omega e^{j(\omega t-kr)} I_1(z) e^{jkz\cos\theta} \qquad \text{(VII-14)}$$

Using Eq. (74), in the far field

$$H_\phi = \frac{\sin\theta}{4\pi c r} j\omega e^{j(\omega t-kr)} \int_{\text{antenna}} I_1(z) e^{jkz\cos\theta} dz \qquad \text{(VII-15)}$$

Eq. (VII-15) is a general result for sinusoidal time variation.

It can also be shown that for a more general case, where I(Z,t) is not necessarily separable, and represents a general (non-sinusoidal in time) variation, that Eq. (74) gives the same result as obtained from the usual vector potential $\bar{A}$ formulation. Thus, the standard $\bar{A}$ formulation proceeds from (Ref. 6, p. 315)

$$\bar{A}(\bar{r}, t) = \frac{\mu}{4\pi} \int_{V'} \frac{\bar{J}(\bar{r}', t-R/c)}{R} dV' \qquad \text{(VII-16)}$$

For the linear antenna $\bar{J}dV' = I\, dz' \hat{a}_z$, and using Eq. (VII-8) for the far-field, Eq. (VII-16) states that

$$d\bar{A} = \frac{\mu}{4\pi r} I(z', t - \frac{r}{c} + \frac{z'}{c}\cos\theta) dz' \hat{a}_z \qquad \text{(VII-17)}$$

Hence, using $\bar{B} = \nabla \times \bar{A}$,

$$d\bar{H} = \frac{dz'}{4\pi} \nabla \times \left[\frac{I(z', t - \frac{r}{c} + \frac{z'}{c}\cos\theta)}{r} \hat{a}_z \right] \tag{VII-18}$$

The curl operation is with respect to the coordinates (r, θ, ϕ) of field point P. The function in the brackets of Eq. (VII-18) is not a function of ϕ, hence $\partial / \partial\phi = 0$. Further, since $\hat{a}_z = \hat{a}_r \cos\theta - \hat{a}_\theta \sin\theta$, the function has no ϕ-component. Then the curl operation yields

$$d\bar{H} = \frac{dz'}{4\pi} \frac{\hat{a}_\phi}{r} \left[-\frac{\partial}{\partial r}\left(r\sin\theta \frac{I}{r} \right) - \frac{\partial}{\partial \theta}\left(\cos\theta \frac{I}{r} \right) \right] \tag{VII-19}$$

where I has the argument $arg \equiv (z', t - r/c + z'\cos\theta/c)$. Retaining only the radiation term$\sim(1/r)$, then

$$dH_\phi = -\frac{\sin\theta}{4\pi r} dz' \frac{\partial}{\partial r} I(z', t - \frac{r}{c} + \frac{z'}{c}\cos\theta) \tag{VII-20}$$

Using $\partial I/\partial r = -(\partial I/\partial t)/c$, and $r \simeq R$ in the denominator,

$$dH_\phi = \frac{\sin\theta}{4\pi c R} \frac{\partial}{\partial t} I(z', t - R/c) dz' \tag{VII-21}$$

which is the same as Eq. (74), derived from the accelerated charge viewpoint.